A STUDY OF FACTORS AFFECTING PRECISION IN ATOMIC ABSORPTION SPECTROMETRY

by

Johannes Tielman Hofmeyr Roos

A thesis submitted in fulfilment of the requirements for the degree of Doctor of Philosophy of Rhodes University

Department of Chemistry,
University of Rhodesia,
Salisbury.
Rhodesia.

November, 1975

TO

W. JOHN PRICE, PH.D.,

Spectroscopist, mentor, and friend

CONTENTS

ACKNOWLEDGEMENTS

The author wishes to express his gratitude and appreciation to the following:

Dr. W.J. Price, Chief Chemist, Pye Unicam Limited, for making it possible for the author to commence his research into atomic absorption spectrometry, and for his continued assistance, advice and encouragement; to whom this thesis is respectfully dedicated;

Dr. N. Agnew of the Department of Chemistry, Rhodes University, who acted as internal supervisor, for the interest he has shown and the ready advice he has given during every stage of the work;

The author's colleagues in the Department of Chemistry, University of Rhodesia, especially Dr. D.J. Eve, Dr. R.J. Decker, and Mrs. P. McFadden, for their interest, advice and help;

Mrs. A.McCabe of the Computer Centre at the University of Rhodesia, for her assistance with computing problems;

The management of Pye Unicam Limited for providing atomic absorption equipment, and to Messrs. P.A. Cooke, A. P. Husbands and R. Manning, for helpful discussions during the early stages of the work.

Mrs. M.I. Talbot, for typing, and re-typing, parts of the draft of this thesis;

Mrs. E. Gascoigne, for undertaking the exacting task of typing this thesis in its final form;

And to his wife, for her help and encouragement throughout the course of this work.

SUMMARY

1. The effect of deviations from Beer's law on the precision of atomic absorption analysis has been examined from a theoretical point of view, and a function has been derived which makes it possible to evaluate quantitatively the effect of calibration curvature on the precision of analysis. The influence of incomplete sample volatilization on calibration curvature has been briefly investigated.

2. Possible error sources in atomic absorption spectrometry have been classified according to the "error function" (i.e., the dependence, upon transmittance T, of the uncertainty dT in a given transmittance measurement) with which they are associated. The magnitude of the contribution from each component function to the overall error function has been evaluated quantitatively, and it has been shown that the major component in nearly every case examined is that associated with the dynamic nature of the flame. Concentration ranges for optimum precision are suggested.

3. The effect of varying instrumental parameters on precision has been investigated, and generalized conditions for best precision have been ascertained.

4. The effect of an initial solvent extraction step on the precision of atomic absorption has been investigated for the elements copper and lead. It is shown that solvent extraction may be used to improve both the analytical sensitivity and the precision of analysis when very low concentrations of metal are determined.

5. The precision of analytical methods involving atomic absorption spectrometry has been studied, and the standard deviations compared with those obtained for the analysis of similar samples by means of a variety of other methods of analysis, both instrumental and classical.

Chapter 1

INTRODUCTION

Few analytical techniques have risen as rapidly to prominence and general acceptance as has atomic absorption spectrometry. The development of this technique as a versatile and efficient method of analysis stems from the studies of Walsh and co-workers [1, 2] in Melbourne, and Alkemade and Milatz [3, 4] in Utrecht, who showed, independently, that atomic absorption measurements could be applied to a wide variety of analytical problems. Since the publication of their work in 1955-57, approximately three thousand papers have appeared which deal with this method of analysis.

Considering the vast literature which has grown up around atomic absorption spectrometry, it is surprising how little work appears to have been done on the question of precision in atomic absorption analysis. Indeed, the author of a recent paper in this field [5] has commented: "It is unfortunate that, of the great majority of abundant papers which deal with atomic absorption spectrometric analysis, only a small fraction present or discuss precision (i.e., report standard deviations)". In addition to a dearth of published information on analytical precision in day-to-day atomic absorption analysis, however, there has also been a conspicuous lack of fundamental investigations into the underlying causes of non-reproducibility of results, means by which precision may be improved, and the nature of the error function or functions associated with atomic absorption spectrometry. Furthermore, much of the precision data that has been published refers to the detection limit rather than

to working concentration ranges, whereas many sources of noise which are unimportant at or near the limit of detection assume considerable significance at higher concentrations, and vice versa; hence, optimization of instrumental parameters at the detection limit may not necessarily provide optimal conditions at higher concentrations.

A number of workers [6-12] have dealt extensively with the types of noise and signal-to-noise ratio near the detection limit, and with the dependence of the noise sources on various instrumental and chemical parameters. Lang and Herrmann [6] derived an equation for the signal-to-noise ratio in atomic absorption spectrometry, and used it in their study of detection limits. These workers were able to suppress flame noise by using an additional mirror arrangement which gave a longer absorption path, but showed that this did not lead to any significant improvement in the limit of detection.

The majority of the published work on noise sources in flame spectrometry has come from Winefordner and his co-workers. Winefordner and Vickers derived equations for the minimum detectable atomic concentrations (in atoms per cm^3 of flame gases) and solution concentrations in both flame emission [7] and atomic absorption analysis [8]. They demonstrated that, if a monochromator of high resolving power was employed in conjunction with a photomultiplier detector, the stability of the resonance radiation line source (e.g. a hollow cathode lamp) was of primary importance in determining the limit of detection, and that a significant improvement in detection limit could be obtained only (i) by improving the stability of the source or,

(ii) by an increase in the absorption path length. Provided that the emission line of the source and the absorption line of the atom in the flame were single and spectrally isolated, the detection limit would be independent of the instrumental parameters over a broad range of experimental conditions. This would not be the case if the absorption lines were not resolved, since then both the monochromator setting and the monochromator slit width could have a considerable effect on the detection limit. In a later paper, Winefordner and Veillon [9] discussed the influence, previously omitted, of electrometer noise on detection limit and concluded that, although the total noise signal at low concentrations would consist, in many instances, chiefly of electrometer noise, which would thus profoundly affect the absolute value of the minimum detectable concentration, nevertheless changes in instrumental settings would still not influence the detection limit significantly.

In a further series of papers [10-12], Winefordner *et al.* have outlined the application of signal-to-noise ratio theory in selecting the optimum conditions for spectrochemical methods of analysis, with particular reference to atomic absorption, atomic emission, and atomic fluorescence flame spectrometry. Their discussion has included the effects of fluctuations in source intensity and flame dimensions (i.e., absorption path length), and the influence of parameters such as flame temperature and monochromator slit width, but always with reference only to analyte concentrations at or near the limit of detection. Nevertheless from the atomic absorption point of view, it is of interest to note that (i) beyond a critical, minimum value of

about 0,05 mm, slit width is always "optimum" provided only that the monochromator retains sufficient resolution to isolate the source resonance line, and (ii) that a line source always leads to a lower (i.e. better) limit of detection than does a continuous source.

The little work [13-15] that has been done to predict how the relative standard deviation in absorbance (dA/A) varies with absorbance (A) or transmittance (T) has referred for the most part to the older theories developed for molecular absorption measurements in solution in which only scale reading errors or other errors independent of transmittance are considered, so that a minimum is predicted for dA/A at a transmittance of about 0,37 (or at an absorbance of 0,434). However, significant differences exist between ultraviolet/visible molecular absorption spectrometry and atomic absorption spectrometry, so that even if the older approach was found to be valid for the former, it would not be likely to hold for the latter. In fact, published dA/A vs A data [5, 16-20] for atomic absorption analysis indicate that both the magnitude of dA/A and the shape of the dA/A vs A curve depend on the element being determined (even with the same instrument) and on the instrumental settings chosen for a particular analysis. Such evidence suggests that the simple approach borrowed from solution spectrophotometry is not valid and that a thorough reassessment of the causes of imprecision in atomic absorption spectrometry, and the type of dA/A vs A behaviour to which they give rise, is called for. This has recently been done in part by Ingle [5] who, adopting an approach similar to that outlined in three publications by the

present author [21-23] and based on the work reported in chapters 3 and 4 of this thesis, has presented a detailed theoretical study of the major sources of noise that might be significant in atomic absorption measurements. He has developed equations which predict the nature of the dependence of dA/A on absorbance or transmittance, and has discussed particular cases in which the noise from one or other component is the dominant factor.

Several workers in this field have approached the question of precision from a practical point of view, and have experimentally ascertained those instrumental settings which, for a given element, give rise to best analytical precision. Thus Erdey et al. used precision (i.e. relative standard deviations, dA/A) as a criterion for optimizing conditions for the determination of zinc [16] silver [17] and copper and gold [18]. These authors recommended working concentration ranges of 30-120 $\mu g/cm^3$ for zinc, 60-400 $\mu g/cm^3$ for copper, and 100-500 $\mu g/cm^3$ for gold. In terms of multiples of the analytical sensitivity (expressed as $\mu g/cm^3$ per 1% absorption) of these elements as measured by the authors, these figures correspond to 39-160x, 55-370x, and 36-180x, respectively. In the case of silver, best precision was obtained over the range 200-1300 $\mu g/cm^3$, corresponding to 140-900x (!) the analytical sensitivity. No allowance appears to have been made for the effect of deviations from Beer's law, although these were very much in evidence in the published results of their investigations. Herrmann and Lang [24] considered several factors affecting precision and sensitivity of atomic absorption determinations, such as air pressure and atomizer performance, fuel-to-air ratio, hollow

cathode lamp current, and monochromator band-pass, and quoted measured sensitivities for cobalt, copper, magnesium, manganese and lead.

These investigations by Erdey *et al.* and Herrmann were performed with early atomic absorption equipment utilizing d.c. amplification and an air-propane flame. The recent trend has been to equate "optimum conditions" for an analysis with those affording best sensitivity rather than best precision (or greatest signal-to-noise ratio), with the result that very little published information is available on how changes in instrumental settings are likely to affect precision in later-model atomic absorption spectrometers. Such an investigation has therefore formed an important part of the work reported in this thesis.

The theoretically linear relationship between concentration and absorbance, the Beer-Lambert law, is followed only approximately in atomic absorption spectrometry, and analytical curves in general tend to approach an asymptote drawn parallel to the concentration axis. This fact is now widely recognized by workers in this field [25, 26], and the literature contains many discussions on the causes of line curvature in atomic absorption analysis [25, 27-32]. It is surprising, therefore, that virtually none of the published papers on precision in atomic absorption spectrometry discusses the question of deviations from the absorption law and their effect both on precision of analysis and on the elucidation of the most precise analytical working range. To the present author's knowledge, the only exceptions to this statement are his own work on this topic [22, 23], and a section in a recent text which was based largely on this work [26]. In much of the published work the standard deviation in terms of absorbance, dA/A, is equated

directly with the standard deviation in terms of concentration, dc/c, without considering the changes which occur in the slope of the analytical curve due to deviation from Beer's law. Thus Erdey and co-workers [16] expressly state that "the relative error of the concentration determination can be deduced from Beer's law" and proceed to apply the equation, developed by Hiskey [33] on the assumption of the validity of Beer's law, to their own results for zinc; however, an examination of their published analytical curve shows that the slope decreases by a factor of approximately 2,5 from the lower limit of their recommended working range to the upper limit, so that their calculated values of dc/c (in reality, dA/A) cannot be compared directly.

It can be seen qualitatively from this brief discussion that one of the effects of working with a system which deviates from Beer's law is a shortening of the predicted optimum absorbance range by curtailing the upper limit of reproducible measurement, due to the decreasing slope of the analytical curve. Attempts have been made [34, 35] to express the shapes of analytical curves by means of polynomials, but these had in view the possibility of dispensing with the need to plot analytical curves rather than an evaluation of the tangential slope of the curves over the entire working range. There is thus a considerable need to express deviation from Beer's law in a quantitative fashion in order to evaluate its effect on analytical precision.

In two elegant papers, Weir and Kofluk [19] and Meddings and Kaiser [20] have reported the results of comprehensive investigations into overall atomic absorption precision,

and compared this with the expected [19] and experimentally determined [20] reproducibility of "wet" chemical methods. These results have shown that, although indeterminate errors are more serious in atomic absorption analysis than in classical analysis, the precision attainable with the former is quite acceptable (generally giving coefficients of variation of between 0,3% and 0,9%) and is able to compete very favourably with that normally obtainable during classical methods of analysis when used on a routine basis. The overall coefficient of variation of the most carefully performed "wet" analysis was shown to be about 0,1%. During the course of that work it was demonstrated, inter alia, that the coefficient of variation for manipulations involving pipettes and volumetric flasks was extremely small, being of the order of 0,1%. In addition, calculations based on the results which they obtained have shown [35] that flame fluctuations contributed significantly more than any other noise source to the overall standard deviation.

Langmyhr and Paus [36] have published data on intra-laboratory precision for silicate rock analysis involving atomic absorption spectrometry, X-ray spectrography, classical analysis, and emission spectrographic analysis. The data for atomic absorption spectrometry were found to compare favourably with those for the other methods.

The investigations described in this thesis were undertaken with a view to obtaining a more complete understanding of some of the factors affecting precision in atomic absorption spectrometry, and were particularly aimed at

(i) obtaining a quantitative expression for the effect, on precision, of deviations from the Beer-Lambert law;

(ii) establishing the most common type of error function (or functions) exhibited by atomic absorption spectrometry, and hence evaluating concentration range(s) for optimum analytical precision;

(iii) studying the relative importance, with respect to precision, of various instrumental parameters;

(iv) assessing the effect which a solvent extraction step has on the precision of analysis vis-à-vis direct analysis of the aqueous solution itself; and

(v) evaluating the reproducibility of the atomic absorption technique as applied to the analysis of chemical samples of differing characteristics and complexity.

Throughout this thesis the terms "precision" and "reproducibility" have been used interchangeably; the standard deviation, calculated from at least ten, and in many instances from between 20 and 50, replicate readings or determinations, has been taken as a quantitative measure of precision. Due to problems in typing, standard deviations have been represented by the exact differentials dA, dT, dc and not by the more usual 's' or 'sigma' forms, viz. s_A, σ_A, s_T, etc. Relative standard deviations (or coefficients of variation, dA/A, dT/T, dc/c) have been used to express precision relative to the magnitude of the quantity determined, and have normally been written in percentual form. Standard deviations have been calculated in the usual manner, viz.

$$dx = \sqrt{\sum_{i=1}^{i=n} \frac{(x_i - \bar{x})^2}{n - 1}}$$

The term "sensitivity" is used in its accepted atomic

absorption sense throughout, i.e. "the concentration, quoted in parts per million* in aqueous solution, which will absorb 1% of the incident resonance radiation of that element" [37]. This is equivalent to the concentration, expressed in the same units, which will give an absorbance of 0,00436. Some confusion is apt to arise over the question of sensitivity since, as defined above, it is proportional to the reciprocal of the slope of the analytical curve in the vicinity of the origin, whereas a modern textbook on instrumental analysis [38] defines sensitivity as the "ratio of the change in the response R to the change of the quantity (i.e., concentration) C which is measured". Thus sensitivity, $\triangle R/\triangle C$, is equated with the slope of the analytical curve, and is the way in which "sensitivity" is generally understood. For this reason it has been suggested that the term "characteristic concentration" be substituted for "sensitivity" in its current atomic absorption usage, and that "sensitivity" be employed only as a measure of the slope of the analytical curve [39]. This suggestion does not appear to have gained wide acceptance, and sensitivity in atomic absorption terminology has retained its original meaning. Because this connotation is so widespread, it is used in this sense here.

The meaning of the term "detection limit" has been discussed at great length by many authors, and a number of different

---

* Although the term "part per million" is still employed widely as a unit of aqueous solution concentration, it may readily be confused with the same term used as a measure of composition with particular reference to solid samples. Therefore the equivalent but more satisfactory unit of concentration, $\mu g/cm^3$, will normally be used here.

definitions have been proposed [40], such as "the concentration of an element which will shift the absorbance signal an amount equal to the peak-to-peak noise of the baseline", or "the concentration to give a signal-to-noise ratio of 2". The most satisfactory definition appears to be that finally accepted by the Society for Analytical Chemistry : "the detection limit in atomic absorption spectrometry is the concentration corresponding to twice the standard deviation of a series of not less than ten readings taken close to the blank level" [37]. This definition, although more stringent than many others that have been proposed from time to time, elevates the concept of detection to a 95% confidence level. It requires more attention to detail, such as a quantitative evaluation of the fluctuations in instrument response at the level of the blank, and as a consequence provides a more rigorous measure of instrumental performance at this level; at the same time, as it does not depend directly on the instrumental noise level, but rather on a calculated standard deviation, this definition may be used in respect of all types of instruments, including those with integrating read-out systems. (In this thesis the terms "detection limit" and"limit of detection" are used interchangeably).

Following Crawford [41, 42] and Pollard [43], the term "analyte" is used always to denote the element which is being determined, and never refers to the solution to be analysed.

Chapter 2

EQUIPMENT

2.1 Atomic absorption instrumentation

2.1.1 Pye Unicam SP90 atomic absorption spectrometer

The work described in this thesis was performed largely with a Pye Unicam SP90 series II atomic absorption spectrometer. This is a single beam instrument employing a 30^{o} silica Littrow prism monochromator, and permits measurements of absorption or emission to be made in the range 190 - 852 nm. The optical diagram is shown in figure 2.1, while figure 2.2 shows the spectral band-pass of the monochromator (for a 0,1 mm slit) as a function of wavelength.

Sample is taken up into the instrument through a concentric nebulizer (normally constructed of steel) at a rate of about 3,5 cm^3/min, to produce a fine spray which mixes with the fuel and support gases. Because of the corrosive nature of some of the solutions aspirated during the course of this work, the steel nebulizer was replaced by one constructed from platinum-iridium and PTFE components, supplied by the manufacturers. A rack and pinion mechanism controls the vertical distance between the burner top and the optical axis ("observation height"), which may be varied readily from 0 to 2,0 cm. Interchangeable burner heads were of the laminar flow type and included a Meker burner head for use with air-acetylene mixtures. This burner head was the one intended for use in flame emission work; nevertheless it was found to operate perfectly satisfactorily in the absorption mode as well. During operation, the burner compartment could be fully enclosed in order to protect slow-burning flames from draughts.

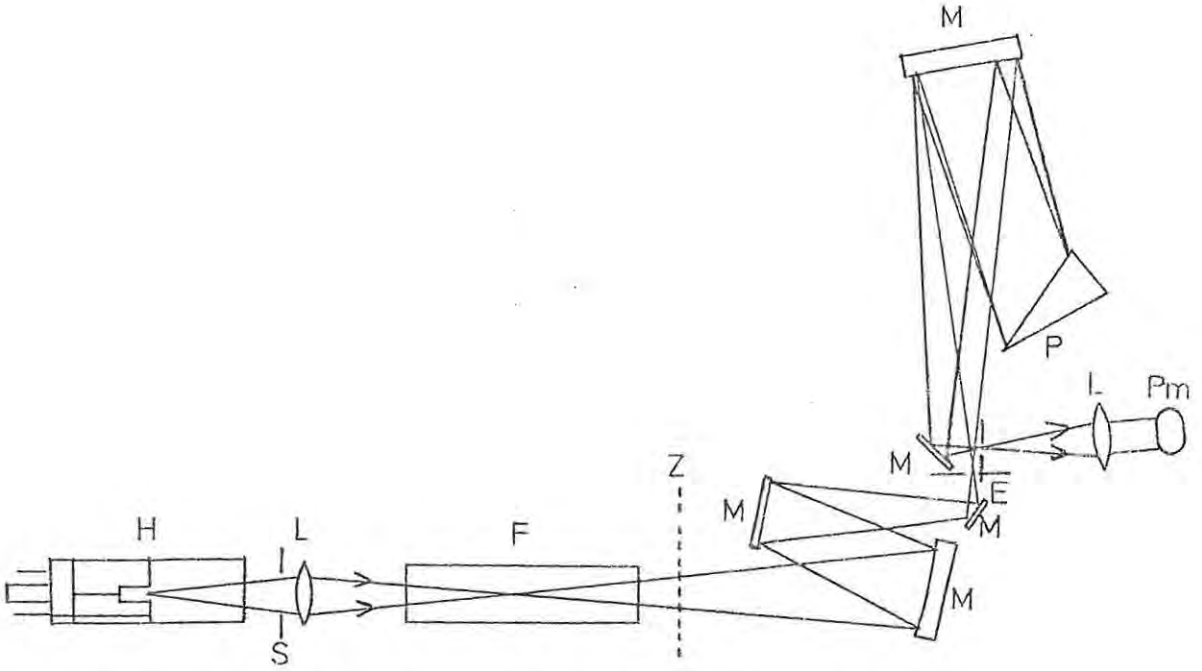

Figure 2.1. Optical diagram for Pye Unicam SP90.

E, entrance & exit slits; F, flame & burner; H, hollow cathode lamp; L, lenses; M, mirrors; P, 30° silica prism; Pm, photomultiplier tube; S, light stop; Z, zero light shutter.

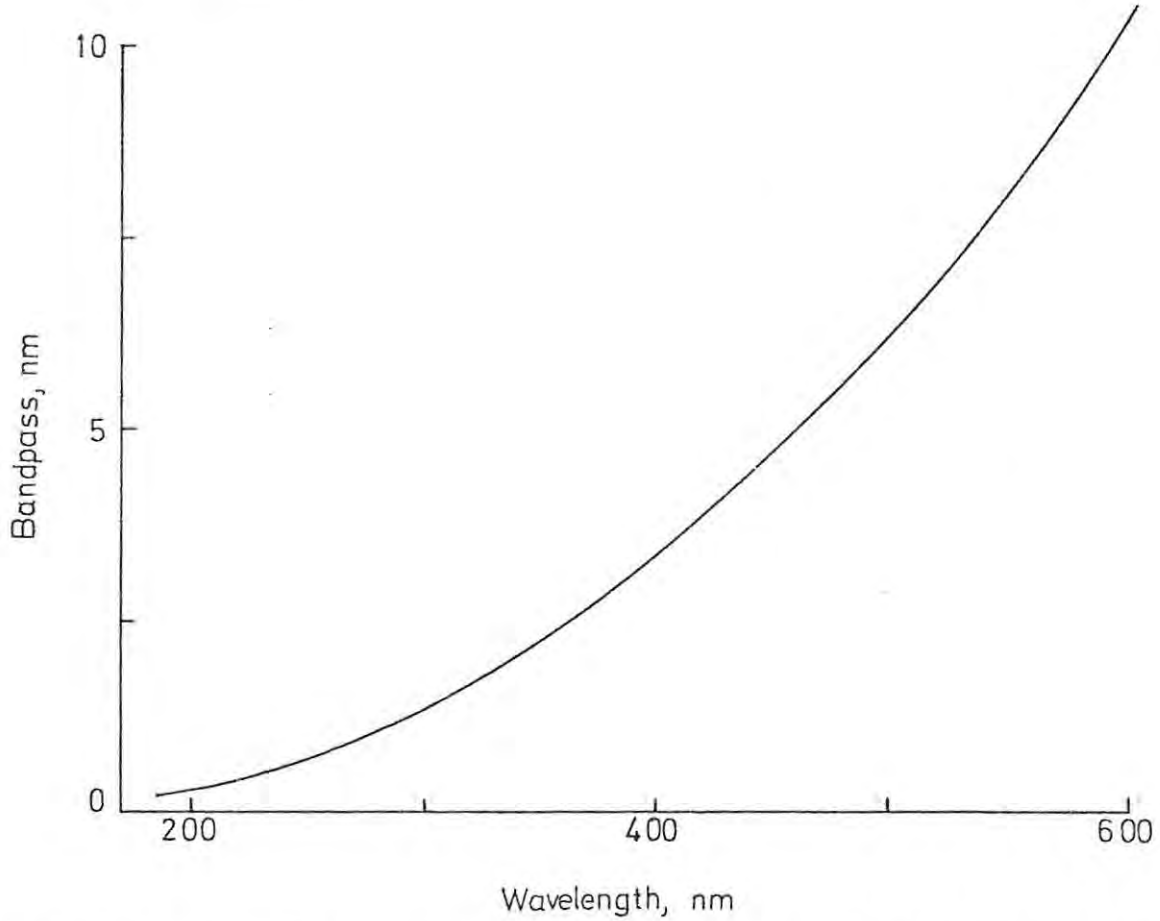

Figure 2.2. Monochromator bandpass (0,1 mm slit) as a function of wavelength for the Pye Unicam SP90.

Spectral sources used in the work described in this thesis were invariably hollow cathode lamps, and were normally obtained from Pye Unicam Limited. It was found convenient to use them in conjunction with a Unicam SP91 lamp turret accessory - a turret accommodating a maximum of three hollow cathode lamps which could be run independently at their correct operating currents. Rotation of the turret brought any chosen lamp into the operating position without requiring further adjustment in lamp current or focussing. Modulation of the hollow cathode lamp radiation was achieved by means of an interrupted d.c. supply to the lamps. The detector unit was an EMI9663B photomultiplier tube, and was used in conjunction with an a.c. amplifier.

The read-out from the basic instrument was a taut suspension meter with a scale calibrated linearly from 0 - 100. A built-in linear-logarithmic converter enabled the calibrated scale to be used directly for either absorbance or transmittance (energy) measurements as selected by the operator. In addition, both a 10 mV recorder output plug and a 1 V digital voltmeter/printer output plug were provided; such accessories could be used in place of the meter, if desired. Built-in scale expansion facilities enabled scale expansion, up to a maximum of about five times, to be used with either the meter or the recorder/digital outputs.

The standard Pye Unicam SP94 nitrous oxide control unit was used for determinations involving the nitrous oxide-acetylene flame. This control unit makes possible a smooth change-over from air to nitrous oxide and vice-versa through the operation of a solenoid valve. This virtually eliminates

the possibility of flash-back when the correct burner head is used.

Most burners were found to clog fairly rapidly when solutions containing more than 2 - 3% of dissolved solids were aspirated. This problem was overcome by using a multislot burner in such cases. Such a burner head is able to accept solutions containing up to approximately 12% of total dissolved solids without clogging, but must be used in conjunction with an increased air flow rate to prevent flash-back into the cloud-chamber. This is made possible by the Pye Unicam auxiliary air system which provides a secondary supply of air directly into the cloud-chamber without passing through the nebulizer. Such a system therefore enables a higher overall flow rate of air to be used without affecting either the rate or the efficiency of nebulization.

2.1.2 Pye Unicam SP1900 atomic absorption spectrometer

A Pye Unicam SP1900 atomic absorption spectrometer, supplied by Pye Unicam Limited, Cambridge, England, was used to investigate the form of the error function occurring during double-beam operation. This instrument employs an Ebert type monochromator incorporating a diffraction grating ruled at 18 000 lines/cm, producing a linear dispersion at the exit slit of 2,2 nm per mm in the first order. The instrument incorporates double-beam optics, giving improved optical stability over the operating wavelength range (190 - 852 nm). A photomultiplier tube with S20 spectral response characteristics serves as the detector, and readings linear in either energy or absorbance are digitally displayed. The built-in intergration facility offers a choice of four integration times (0,2; 1; 4; 20 seconds) at a sampling rate of ten signals per second.

As with the SP90 spectrometer, sample is taken up through a conventional pneumatic nebulizer at a rate of 3,5 - 4,5 cm^3/min. The mixing chamber is fitted with titanium flow spoilers and an impact bead positioned directly in front of the nebulizer orifice. A schematic diagram of the instrument is shown in figure 2.3.

2.1.3 Hollow cathode lamps

Hollow cathode lamps used during the present work were of two different types. These were (i) the normal hollow cathode lamps containing a cathode of the required metal or suitable alloy, and having a cathode diameter of about 5 mm, and (ii) hollow cathode lamps of the "high spectral output" variety*. The latter were characterised by smaller cathode cups (internal diameter ca. 1,5 mm), and were designed in such a way as to produce much more intense emission. High spectral output lamps were used for cobalt, chromium, iron, molybdenum, and nickel, and were fitted into lamp-holders specially designed to facilitate lining up of the smaller cathode, characteristic of this type of lamp.

Dual element lamps containing calcium/magnesium or copper/zinc alloy cathodes were used for the determination of these elements.

2.1.4 Recorder and digital readouts

Both atomic absorption instruments employed during this investigation were provided with recorder outputs which could be connected to any suitable 10-millivolt recorder. A Philips

---

* These lamps are not the same as the so-called "high-brightness" lamps containing a set of secondary electrodes and requiring an additional power supply.

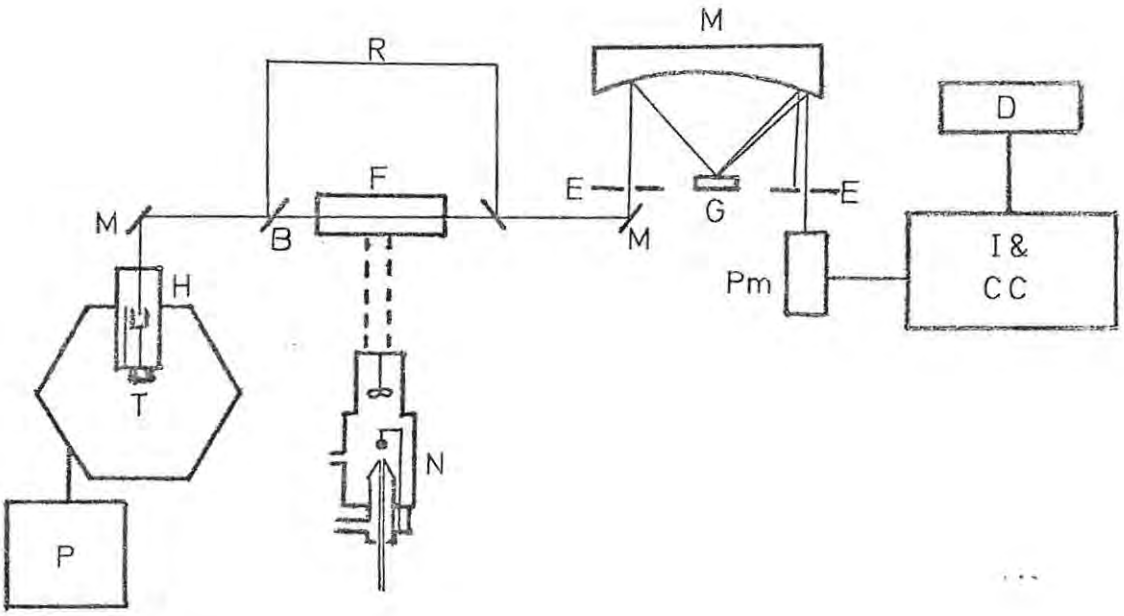

Figure 2.3. Schematic diagram of Pye Unicam SP1900.

B, beam splitter; D, digital display; E, entrance & exit slits; F, flame; G, diffraction grating; H, hollow cathode lamp; I & CC, integrator and concentration computer; M, mirrors; N, nebulizer & cloud chamber; P, lamp power supply; Pm, photo-multiplier; R, reference beam; T, lamp turret.

Universal flatbed recorder was used when required during the course of this work. The Pye Unicam SP90, in addition to the recorder plug, was also fitted with a 0 - 1 V output for a digital voltmeter. A Philips PM2422 digital voltmeter, supplied by Philips (Rhodesia) Limited and giving a non-integrated sampling rate of one reading per sec, was used during the statistical studies described in chapters 4 - 7. The results were analysed, and standard deviations calculated, by an IBM 1901 computer.

2.2 Miscellaneous equipment

All pH measurements were made with a Metrohm pH meter. A Griffin-Christ "Universal Junior III" centrifuge, supplied by Griffin and George Limited, was used for the removal of suspended matter from sample solutions, or to hasten the separation of organic and aqueous phases during extractions.

Water used during this investigation was either distilled or deionized (by passage through an Elgastat water deionizer, supplied by Elga Products Limited); in either case the purity of the water was ascertained by atomic absorption analysis prior to its use.

Unless otherwise stated, all reagents were of either specpure or analytical reagent grade purity. Precautions were taken to avoid anionic interferences by preparing metal-ion solutions as chlorides except in those instances where anions other than chloride were specifically required; these are indicated in the appropriate places in the text.

Where possible, the elemental metal was used in the preparation of standard solutions. Specpure metals were used for the preparation of aluminium, cobalt, iron and manganese

stock solutions, while chromium, lead, magnesium and zinc solutions were prepared from the analytical reagent grade metals. Hydrochloric acid, either alone or in combination with hydrogen peroxide, was used for dissolution of the metals. Calcium and strontium were used in the form of their carbonates and copper and molybdenum as oxides. After accurate weighing, the substances were dissolved in the minimum volume of hydrochloric acid necessary to afford complete dissolution and to prevent hydrolysis of the resultant metal-ion solution; where required, hydrogen peroxide was added to assist in the dissolution process, and the excess of peroxide destroyed by boiling. Concentrated stock solutions (generally 1000 $\mu g/cm^3$ with respect to the metal ion concerned) were further diluted as convenient. All such aqueous stock solutions were stored in polythene bottles.

Chapter 3

CALIBRATION CURVATURE AND PRECISION

As in most analytical techniques employing the absorption of electromagnetic radiation as the basis of measurement, atomic absorption spectrometry makes use of the Beer-Lambert (or, Beer) law in the quantitative evaluation of concentration. This law, which may be summarised [44] by saying that the absorption of radiation by molecules or atoms depends only on their total number, has been discussed fully by Pfeiffer and Liebhafsky [45] and, more recently, by Hughes [46]. Mathematically, Beer's law may be formulated as

$$A = \log I_o/I = -\log T = abc \qquad (3.1)$$

where A is the absorbance;
I_o is the incident intensity;
I is the transmitted intensity;
T is the transmittance;
a is a constant, the absorptivity, and depends on the nature of the absorbing species;
b is the thickness of the absorbing medium; and
c is the concentration of the absorbing species.

Since, theoretically, concentration is directly proportional to absorbance, atomic absorption working curves are normally plotted as the logarithmic function (absorbance) against concentration, rather than the non-logarithmic transmittance (or, more conveniently, absorption = 1-T) against concentration.

The basic measurement performed by all spectrometers, including atomic absorption spectrometers, is that of transmittance or per cent transmittance (100.T) - hence, by

implication, absorption or per cent absorption - rather than absorbance. It is necessary, therefore, to convert from transmittance to absorbance by means of one or other of the following techniques:

(i) By reading the absorbance on a logarithmically-calibrated (hence non-linear) meter scale;

(ii) By using standard conversion tables;

(iii) By employing an electronic logarithmic converter, such as a logarithmic recorder.

The problem of deviations from Beer's law has been discussed, with reference to UV-visible spectrophotometry, by Hiskey and Young [47], Lothian [48], and McBryde [49]. Lothian has outlined some of the causes of deviation from the Beer-Lambert law in spectrophotometry, and has shown that the validity of the law depends upon several factors, including the use of monochromatic radiation and the absence of stray (non-absorbable) radiation. In atomic absorption spectrometry the radiation employed is very nearly truly monochromatic; however, the extremely narrow absorption line-widths involved may cause deviations from linearity [50]. Various other factors are known to contribute to calibration curvature in atomic absorption analysis [27-32], with the result that deviations from Beer's law are more prevalent in this technique than in classical spectrophotometry; these factors include the profiles of source emission lines and self-absorption effects, the hyperfine structure of spectral lines, unequal absorption of closely-spaced emission lines from the lamp, and non-absorbable radiation from the light source impinging upon the detector.

3.1 The effect of calibration curvature on photometric precision

In general, the relationship between absorbance and analyte concentration may be expressed as

$$A = f(c).c \qquad (3.2)$$

where f(c) is a function which changes in some way with c and replaces the (constant) combined factor ab in the formulation of Beer's law (equation 3.1).

Differentiation of equation (3.2) gives

$$dA/dc = c.f'(c) + f(c) \qquad (3.3)$$

where
$$f'(c) = d[f(c)]/dc \qquad (3.4)$$

$\therefore$
$$dc/c = dA/[c^2.f'(c) + c.f(c)] \qquad (3.5)$$

$$= \frac{dA}{A}\left\{\frac{1}{\frac{c^2.f'(c)}{A} + 1}\right\} \qquad (3.6)$$

For negative deviations from Beer's law f'(c) will be a negative quantity, so that dc/c will be greater than dA/A at a given concentration or absorbance. In the limit, when the system obeys Beer's law, f(c) will be a constant; f'(c) will be equal to zero so that dc/c = dA/A. The extent to which calibration curvature affects the relative standard deviation (dc/c) of a particular analysis will depend on the form of f(c). This, in turn, will depend upon the actual causes of the observed deviation from Beer's law, and is dealt with more fully in the sections which follow.

In many instances of deviation from Beer's law it is possible, by means of scale expansion procedures, to introduce a correction and to obtain linear calibration graphs over a considerable range of concentration. This fact makes it possible

to derive a general expression for the transmittance in terms of the concentration, an expression which is valid whether or not Beer's law is followed. If Beer's law is obeyed,

$$T = 10^{-abc}, \tag{3.7}$$

and

$$1-T = 1 - 10^{-abc}. \tag{3.8}$$

If the Beer-Lambert law is not obeyed,

$$T > 10^{-abc}, \tag{3.9}$$

and

$$1-T < 1 - 10^{-abc}. \tag{3.10}$$

If scale expansion (of the linear T scale) by a factor 1/h ($h < 1$) restores linearity when "transmittance" is now converted to absorbance,

$$\frac{1 - T}{h} = 1 - 10^{-abc} \tag{3.11}$$

and

$$1 - T = h(1 - 10^{-abc}) \tag{3.12}$$

The value of h, which is unity for a system obeying Beer's law and decreases with increasing deviation therefrom, is equal to the reciprocal of the degree of scale expansion (of the transmittance scale) required to correct for calibration curvature when the apparent transmittance values, obtained after scale expansion, are converted to absorbances and plotted against concentration. The correction factor h is thus directly related to the extent to which the system conforms to Beer's law. Physically, h is equal to the absorption (1 - T) shown by an "infinitely concentrated" solution of the analyte in question measured under given conditions; (1 - h) is the relative intensity of non-absorbable radiation falling on the detector.

The validity of equation (3.12) was tested by preparing calibration graphs for cobalt, iron and nickel, all elements

which normally exhibit large deviations from the absorption law. Suitable standard solutions of these elements were aspirated, and the response measured at 240,7nm (cobalt), 248,3nm (iron), and 232,0nm (nickel). The instrumental conditions employed are shown in Table 3.1. Measurement of the calibration standards was repeated after introducing the required degree of scale expansion. In this way corrected absorbances were obtained, and the working curves re-plotted.

T A B L E 3.1.

Instrumental conditions for cobalt, iron and nickel

Element	Cobalt	Iron	Nickel
Wavelength (nm)	240,7	248,3	232,0
Slit width (mm)	0,10	0,10	0,10
Acetylene flow (cm^3/min)	1400	1400	1400
Observation height (cm)	1,0	1,0	1,0
Lamp current (mA)	12	7	7

Since the corrected graphs are linear it follows, at least in these cases, that equation (3.12) is valid and the factor h represents an accurate quantitative expression for the extent of deviation from Beer's law. Both corrected and uncorrected curves are shown in figure 3.1.

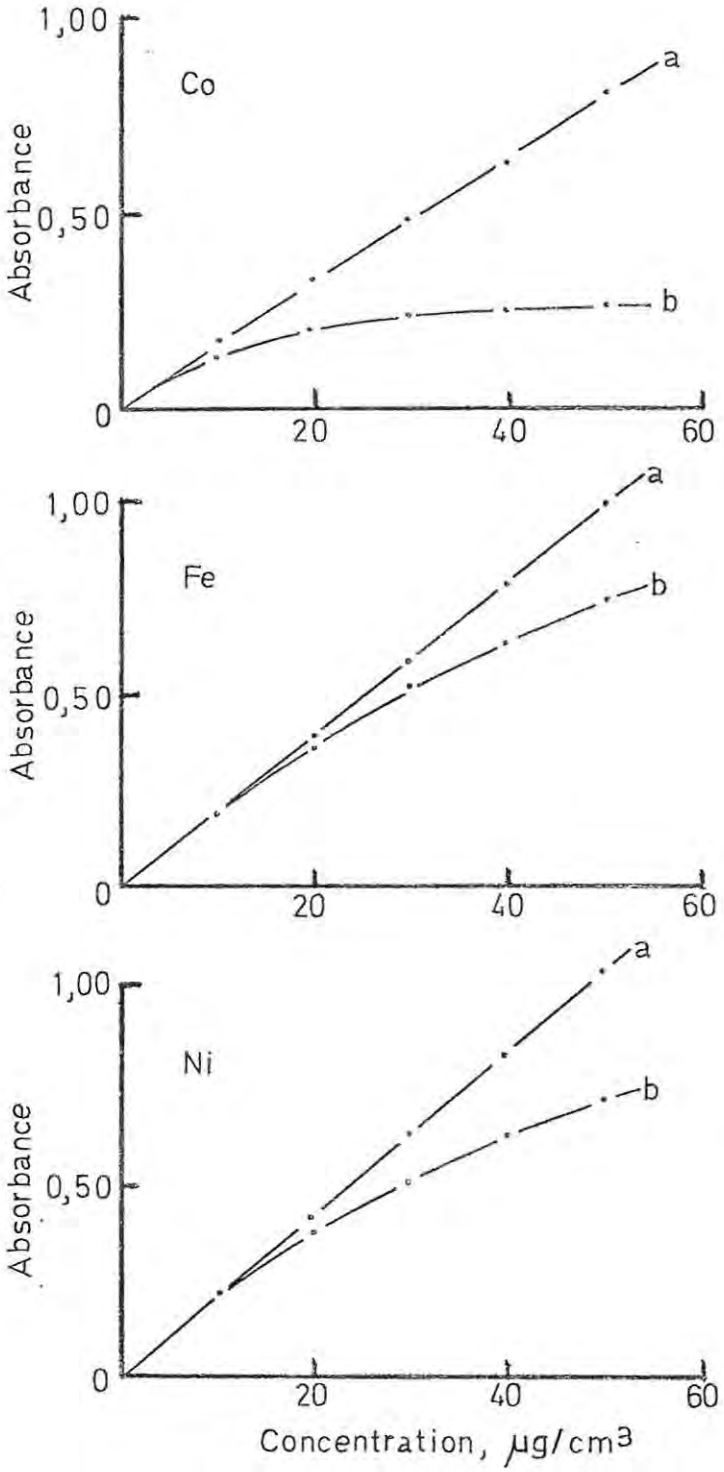

Figure 3.1. Corrected and uncorrected analytical curves for cobalt, iron and nickel.

a - corrected curves

b - uncorrected curves.

It is possible to express the effect of deviation from Beer's law on precision by means of the "relative error ratio", $\frac{(dc/c)}{(dA/A)}$.

$$1 - T = h(1-10^{-abc}) \qquad (3.12)$$

Differentiating, $$-dT = 2{,}303hab.10^{-abc}dc \qquad (3.13)$$

Therefore $$dc = -10^{abc}.dT/2{,}303hab \qquad (3.14)$$

But $$1 - T = h - h.10^{-abc} \qquad \text{(from 3.12)}$$

Therefore $$T + h - 1 = h.10^{-abc} \qquad (3.15)$$

and $$\log(T + h - 1) = \log h - abc \qquad (3.16)$$

Rearranging, $$c = \frac{1}{ab} \log \frac{h}{T+h-1} \qquad (3.17)$$

Therefore the relative error, dc/c, is given by

$$\frac{dc}{c} = \frac{-10^{abc}.dT}{2{,}303h.\log \frac{h}{T+h-1}} \qquad (3.18)$$

But $$10^{abc} = \frac{h}{T+h-1} \qquad \text{(from 3.15)}$$

Therefore $$\frac{dc}{c} = \frac{-dT}{2{,}303(T+h-1).\log \frac{h}{T+h-1}} \qquad (3.19)$$

$$A = -\log T \qquad \text{(by definition)}$$

Differentiating $$dA = -dT/2{,}303T \qquad (3.20)$$

Therefore $$dA/A = \frac{-dT}{2{,}303T.\log \frac{1}{T}} \qquad (3.21)$$

Combining equations (3.19) and (3.21) we obtain the relative error ratio

$$\frac{(dc/c)}{(dA/A)} = \frac{-T\log T}{(T+h-1).\log \frac{h}{T+h-1}} \qquad (3.22)$$

Figure 3.2 shows the variation in the relative error ratio, for different values of h, as a function of absorption (1-T). In figure 3.3 this is shown as a function of absorbance. The figures show that the relative error ratio increases with absorption or absorbance, and also with increasing deviation from Beer's law (smaller values of h).

In the pages which follow, the suitability of equation (3.12) for describing the shapes of analytical curves in atomic absorption spectrometry - and hence, by implication, the validity of equations (3.19) and (3.22) - is examined more fully.

3.2 Atomic absorption growth curves

It is convenient to distinguish between the growth curve (a log - log plot of the integrated intensity of absorption, 1-T, against the atomic concentration in the flame, or some related function) and the analytical curve (some function related to absorption - normally absorbance, -logT - against solution concentration). The former is determined largely by the spectral properties and light absorption characteristics of the system under study, viz. the emission and absorption line widths and line profiles, hyperfine structure, resonance broadening and line shift [27]. The analytical curve, on the other hand, since it is a function not of flame atomic concentration but of solution concentration, is affected also by considerations such as the efficiency of aspiration/nebulization, the degree of volatilization of the sample material, and the extent to which dissociation and ionization occur in the flame.

In their excellent paper [25], Zeegers, Smith and Winefordner have pointed out that the shape of the growth curve is the major factor in determining the shape of the analytical

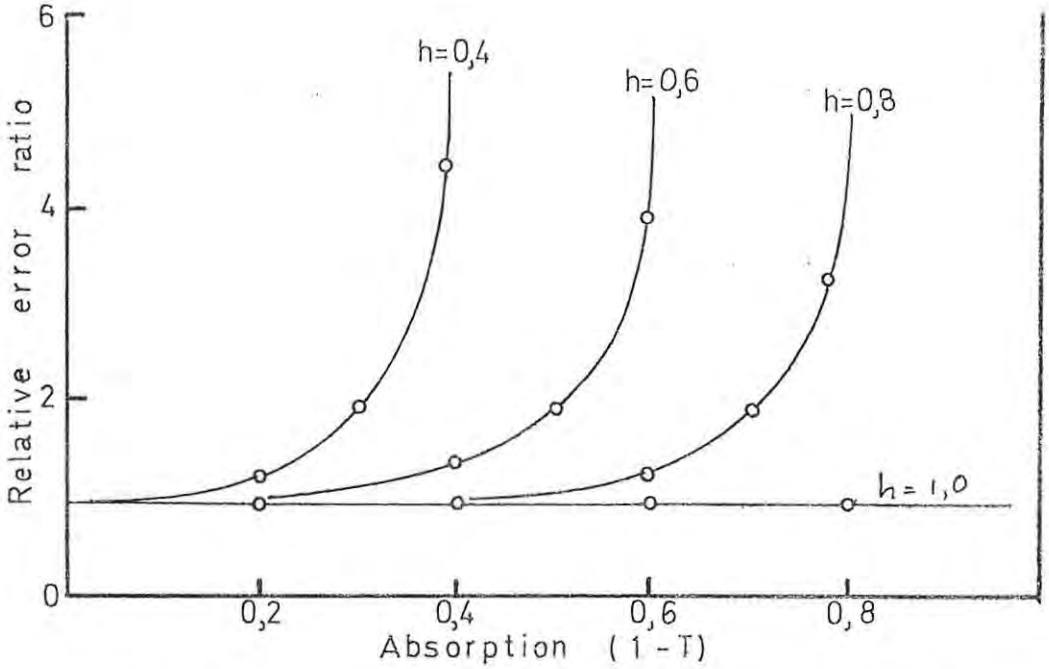

Figure 3.2. Relative error ratio as a function of absorption, for different values of h.

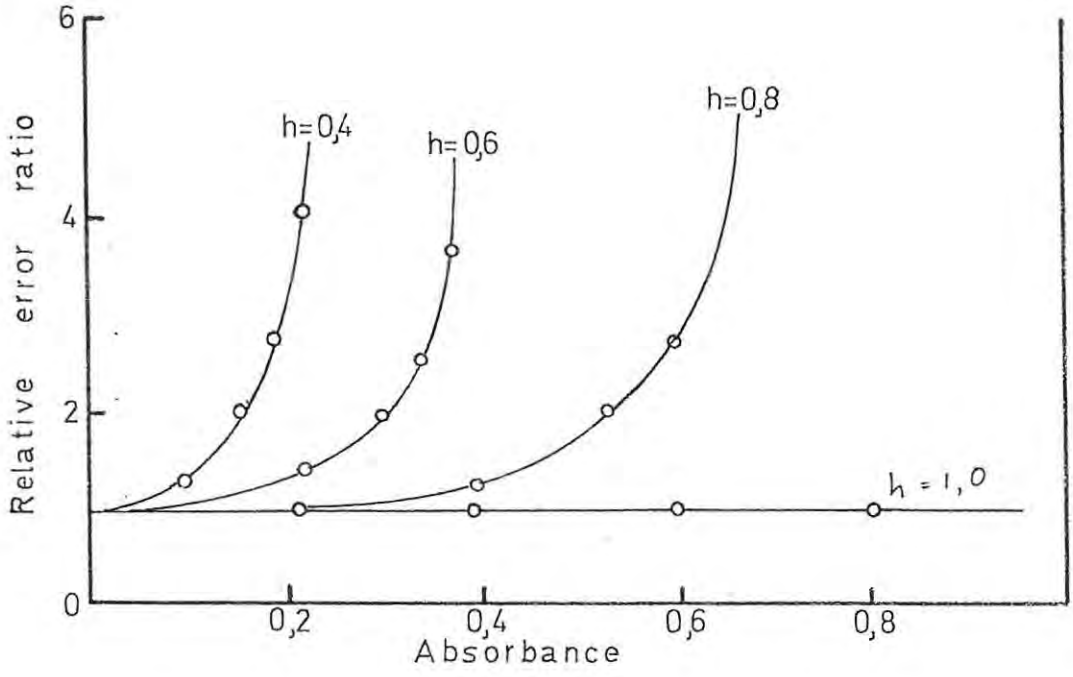

Figure 3.3. Relative error ratio as a function of absorbance, for different values of h.

curve. These authors have derived expressions for ideal growth curves, and have calculated the growth curve for magnesium. Figure 3.4 shows their calculated growth curve, together with growth curves calculated with the aid of equation (3.12) for different values of h.

Rubesca and Svoboda [27] and L'Vov [51], in particular, have studied the influence of various factors, including line width ratios, hyperfine structure, and resonance broadening, on the shape of the growth curve. The analytical curves, derived from the theoretical growth curves which the former calculated for different ratios of the hyperfine structure component separation to half-widths, and for different half-width ratios, are shown in figures 3.5 and 3.6, respectively, which also show analytical curves calculated on the basis of equation (3.12). Table 3.2 gives the values of h for the best fit in each case, and compares the various sets of calculated absorbances.

3.3 Particle volatilization and calibration curvature

Relatively little attention has been paid to possible effects on calibration curvature of incomplete volatilization of sample material in the flame, although it is well known that this can give rise to non-linearity of analytical curves [25, 52]. The flame emission studies of Leyton [53] showed that, whereas calcium chloride gave a response linear with respect to concentration, calcium phosphate gave a response which varied approximately as the 4/5th power of concentration. Zeegers et al. [25] used data, obtained by Schuhknecht and Schinkel [54] with a variety of flames, to illustrate the effect of incomplete solute vaporization on the shapes of

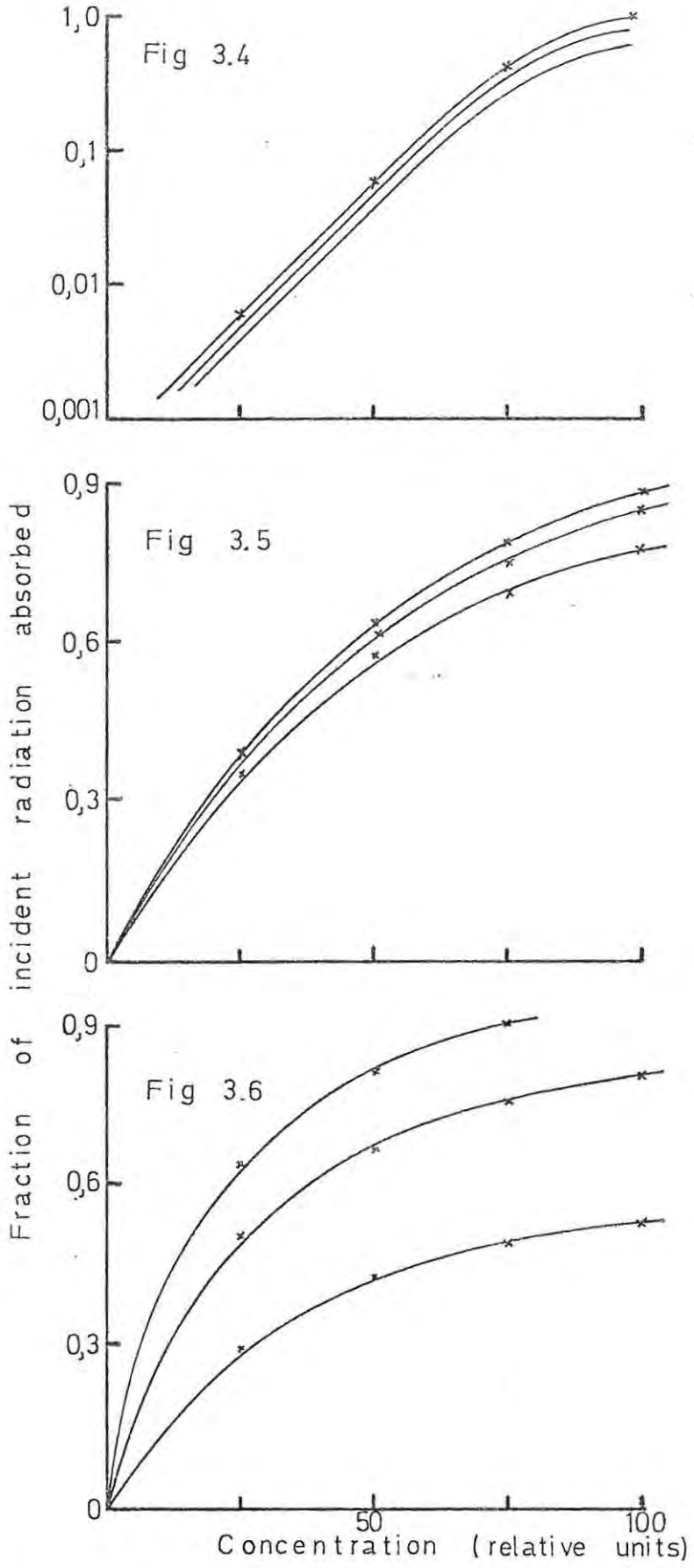

Figures 3.4 - 3.6. Comparison of theoretical growth curves (points indicated by x) and curves calculated by means of equation 3.12 (See text).

TABLE 3.2

Comparison of growth curves* calculated by Rubesca and Svoboda [27] with those calculated by equation 3.12

Per cent ABSORPTION

Relative atomic concn.	$\Delta\nu_h = 0$		$\Delta\nu_h = 0{,}5\delta$		$\Delta\nu_h = \delta$	
	Ref.27	Eq.3.12	Ref.27	Eq.3.12	Ref.27	Eq.3.12
25	39,3	39,2	39,2	38,6	36,3	35,7
50	63,2	63,1	62,2	62,1	57,5	57,2
75	77,7	77,7	75,1	75,7	69,8	70,2
100	86,4	86,4	84,2	84,0	78,1	78,0
h	1,00		0,97		0,90	

Per cent ABSORPTION

Relative atomic concn.	$\delta' = 1{,}5;\ \delta = 5$		$\delta' = \delta = 5$		$\delta' = 15;\ \delta = 5$	
	Ref.27	Eq.3.12	Ref.27	Eq.3.12	Ref.27	Eq.3.12
25	67,0	65,6	52,5	50,8	29,4	28,9
50	83,2	83,9	69,0	69,7	44,0	43,3
75	89,2	89,2	76,2	76,8	50,1	50,5
100	-	-	80,0	79,6	53,7	54,0
h	0,93		0,81		0,58	

* $\Delta\nu_h$ is the hyperfine structure component separation,
δ' is the emitted line half-width, and
δ is the absorption line half-width.

analytical curves. Roos [55] observed greater calibration curvature with chromium in the presence of iron than with chromium alone, and attributed this to incomplete volatilization in the former case.

To the knowledge of the present author, the only complete mathematical treatment of particle volatilization is that by L'Vov [56], based extensively on the work of Lykov [57]. L'Vov's concern, however, has largely been with the time required to vaporize particles of solute in flames commonly employed in atomic absorption analysis, and with interferences, and he has not discussed the possible shapes of analytical curves resulting from incomplete sample volatilization in the observation region of the flame. These authors have suggested that the rate of volatilization is controlled by heat transfer from the surrounding medium. Heat is absorbed in raising the droplet temperature and vaporizing the sample material; as the temperature of the droplet rises so the rate of vaporization increases until an equilibrium temperature is reached, when the heat absorbed by the droplets is used entirely in the vaporization process. Volatilization is therefore completed at droplet temperatures which are normally considerably lower than the temperature of the flame, especially for more volatile samples. It has also been shown [56] that vaporization of the sample would normally take place well below the boiling point of the substance concerned.

Using the equations for heat transfer and mass transfer during the vaporization process, Lykov [57] has shown that the temperature at the vaporization surface, T_d, can be expressed by equation (3.23)

$$T_d = T_f - \frac{sMD}{LRT_f}(P_d - P_f) \qquad (3.23)$$

where T_f is the absolute temperature of the flame, s is the specific heat of vaporization of the liquid in kcal/kg, M is the molecular mass of the sample material in kg/mol, D is the coefficient of diffusion of the gaseous substance at the temperature T_f in m^2/h, L is the thermal conductivity of the gas in kcal/m.h.^{o}C, P_d is the saturated vapour pressure of the substance above the droplet surface and P_f is that of the substance in the flame, both in torr, and R is the gas constant (= 0,062 torr. m^3/mol.^{o}C).

Since the vapour pressure of the substance in the flame will be much lower than the saturated vapour pressure above the droplet surface, equation (3.23) can be rewritten as follows:

$$T_f - T_d = \triangle T = \frac{sMD}{LRT_f} P_d \qquad (3.24)$$

The rate of vaporization has been expressed by Lykov [57] in terms of the amount of heat acquired by the droplet

$$dm/dt = \frac{\pi d^2 \alpha}{s} \triangle T \qquad (3.25)$$

where d is the diameter of the droplet (in m), and α is the coefficient of heat transfer in kcal/m^2.h.^{o}C.

For the vaporization of small droplets,

$$\alpha = \frac{2L}{d} ; \qquad (3.26)$$

hence, combining equations (3.24), (3.25) and (3.26), the rate of vaporization may be expressed by

$$dm/dt = \frac{2\pi MD}{RT_f} P_d \cdot d \qquad (3.27)$$

The mass of the substance in a droplet is given by

$$m = \frac{\pi d^3 \rho}{6} \tag{3.28}$$

$$\therefore \quad d = \left(\frac{6}{\pi \rho}\right)^{1/3} m^{1/3} \tag{3.29}$$

where ρ is the density of the liquid in kg/m^3. In order to calculate the shape of the resulting analytical curve, it is convenient to work in terms of the mass of sample which is <u>not</u> vaporized, so that the rate expression becomes

$$-dm/dt = \frac{2\pi MD}{RT_f} P_d \cdot d \qquad \text{(from 3.27)}$$

$$= \left(\frac{48\pi^2}{\rho}\right)^{1/3} \frac{MDP_d}{RT_f} m^{1/3} \tag{3.30}$$

Assuming that the vapour pressure P_d of the sample material remains constant, independent of the amount of material comprising the droplet at any given time, equation (3.30) may be rearranged and integrated as follows:

$$-dm/dt = \left(\frac{48\pi^2}{\rho}\right)^{1/3} \frac{MDP_d}{RT_f} m^{1/3} \tag{3.31}$$

$$\therefore \quad \int dt = -1/k_1 \int m^{1/3}\, dm \tag{3.32}$$

where $$k_1 = \left(\frac{48\pi^2}{\rho}\right)^{1/3} \frac{MDP_d}{RT_f} \tag{3.33}$$

$$\therefore \quad t = -\frac{1,5}{k_1} m^{2/3} + \text{constant} \tag{3.34}$$

When $t = o$, $m = m_o$ (m_o is the mass of the particle before any vaporization has taken place)

$$\therefore \quad t = -\frac{1,5}{k_1} m^{2/3} + \frac{1,5}{k_1} m_o^{2/3} \tag{3.35}$$

and $$m^{2/3} = m_o^{2/3} - \frac{k_1 t}{1,5} \tag{3.36}$$

For a fixed observation height in the flame, t will be a constant, and hence we may write

$$m^{2/3} = m_o^{2/3} - k_2 \qquad (3.37)$$

where $$k_2 = \frac{k_1 t}{1,5} \qquad (3.38)$$

In practice, m_o will be proportional to the concentration $\underline{c}$ of the sample solution (in kg/m^3), and the response, A, obtained will be approximately* proportional to $m_o - m$ ($m_o - m$ is the amount of sample material which volatilizes prior to reaching the observation zone in the flame).

Let $$m_o = k_3 c \qquad (3.39)$$

and $$m_o - m = k_4 A \qquad (3.40)$$

$$\therefore \quad m = m_o - k_4 A \qquad (3.41)$$

$$= k_3 c - k_4 A \qquad (3.42)$$

$$\therefore \quad (k_3 c - k_4 A)^{2/3} = (k_3 c)^{2/3} - k_2 \qquad (3.43)$$

$$\therefore \quad k_3 c - k_4 A = \left[(k_3 c)^{2/3} - k_2\right]^{3/2} \qquad (3.44)$$

and $$A = \frac{k_3 c - \left[(k_3 c)^{2/3} - k_2\right]^{3/2}}{k_4} \qquad (3.45)$$

$$= \frac{c - \left(c^{2/3} - k_2/k_3^{2/3}\right)^{3/2}}{k_4/k_3} \qquad (3.46)$$

In equation (3.46), $\left(c^{2/3} - k_2/k_3^{2/3}\right)^{3/2}$ is proportional to m, the mass which does not volatilize below the

---

* Approximately, since no allowance has been made, inter alia, for the effect of the concentration of sample material in the flame on the degree of dissociation of the sample vapour, ionization effects, etc.

observation height specified by the value of t in k_2 (equation 3.38). Therefore

$$c - (c^{2/3} - k_2/k_3^{2/3})^{3/2}$$

may be looked upon as the "effective concentration", i.e., it is proportional to the amount of sample material which volatilizes prior to passing through the observation zone and which, consequently, gives rise to the measured response.

For the sake of clarity, it has thus far been assumed that the particles entering the flame in a conventional atomic absorption spectrometer are of uniform size, and can therefore be fully described in terms of the radius r or diameter d (equations 3.24 - 3.29). This is manifestly not true in practice, and several attempts have been made to measure the size distribution of the droplets produced by pneumatic nebulizers as normally employed in atomic absorption analysis [58-60].

In order to produce an accurate model of particle volatilization and its effect on the shape of atomic absorption working curves, it is necessary to take the drop size distribution into account in the mathematical treatment outlined above. The data have been taken from reference [58]; it has been assumed that droplets greater than 15μ in diameter would be deposited on the walls of the mixing chamber and burner feed tube, and need not therefore be considered further. The drop-size distribution pattern is shown in Table 3.3.

For a given concentration of analyte it may be assumed that the diameter of a dried particle before volatilization commences will be proportional to the diameter of the droplet

T A B L E 3.3

Drop-size distribution pattern assumed in this work

Drop-size interval (μ)	Frequency (%)
0,0 - 1,0	1,6
1,0 - 2,0	6,9
2,0 - 3,0	16,1
3,0 - 4,0	16,1
4,0 - 5,0	14,6
5,0 - 6,0	14,6
6,0 - 7,0	6,3
7,0 - 8,0	6,3
8,0 - 9,0	2,8
9,0 - 10,0	2,8
10,0 - 11,0	2,5
11,0 - 12,0	2,5
12,0 - 13,0	2,5
13,0 - 14,0	2,2
14,0 - 15,0	2,2

from which that particle is derived, so that the particle-size distribution in the flame is directly related to the drop-size distribution produced by the nebulizer/cloud-chamber system. It is also assumed that, within the concentration limits normally encountered in atomic spectroscopy, the analyte concentration does not significantly influence the drop-size distribution pattern.

In any assumed distribution of drop sizes, the degree of volatilization of each individual drop may be calculated for given values of the various parameters (T_f, D, P_d, t, etc.) and the size of the drop, relative to the volatilization which would occur if the drops were all of uniform size. Multiplication by the factor $F_i / \leq F_i$ (where F_i is the relative frequency of occurrence of any drop-size interval $d_i \pm \Delta d$), followed by summation over the complete drop-size range, will give the "effective concentration" mentioned above. Figure 3.7 compares the shapes of analytical curves calculated at 2350°K [56] for the element strontium with and without taking drop-size distribution into account. The values of the parameters used in these calculations are shown in Table 3.4. The observation height was taken as 0,3 cm, and volatilization was assumed to be the only factor affecting the shapes of the curves. It can be seen that curvature commences at a lower concentration when a distribution in droplet size is assumed: this is due to the effect of the (few) larger droplets which contain a relatively high proportion of the total transported sample mass. Drop-size distribution has been assumed present in the discussion which follows.

As a test of the accuracy of the mathematical model, experimental analytical curves were obtained for strontium (as strontium nitrate) at several different observation heights in

a slightly lean air-acetylene flame; all measurements were made in emission at 610 nm (SrOH band) in order to eliminate (i) the influence of possible self-absorption, and (ii) effects due to other spectral factors which could cause significant deviations from linearity in absorption measurements, such as hyperfine structure, source line profiles, etc. In order to obtain meaningful results at particular heights in the flame, an aperture stop, ca. 2 mm x 2 mm, was positioned between the burner and the monochromator.

T A B L E 3.4

Parameters for calculating strontium oxide volatilization curves

$s = 6{,}3 \times 10^2$ kcal/kg	Flame gas velocity =
$M = 0{,}1036$ kg/mol	$3{,}60 \times 10^4$ m/h
$D = 3{,}3$ m^2/h	$\rho = 4{,}5 \times 10^3$ kg/m^3
$T_f = 2350^\circ$K, etc.	$L = 0{,}188$ kcal/m.h.$^\circ$C

P_d and T_d were computed by an iterative process using the expression [61] $\text{Log}P_d = (-0{,}2185\ A/T_d) + B$ where $A = 1{,}34827 \times 10^5$ and $B = 12{,}601974$

The measured curves were compared with a set of theoretical curves calculated for the volatilization of strontium oxide* at the same values of the observation height as were used above. The results (figure 3.8) show the excellent agreement which was

---

* Vapour pressure data were available for strontium oxide but not for strontium chloride; for this reason solutions of strontium nitrate were used, as this would decompose into the oxide at a temperature well below that of the flame.

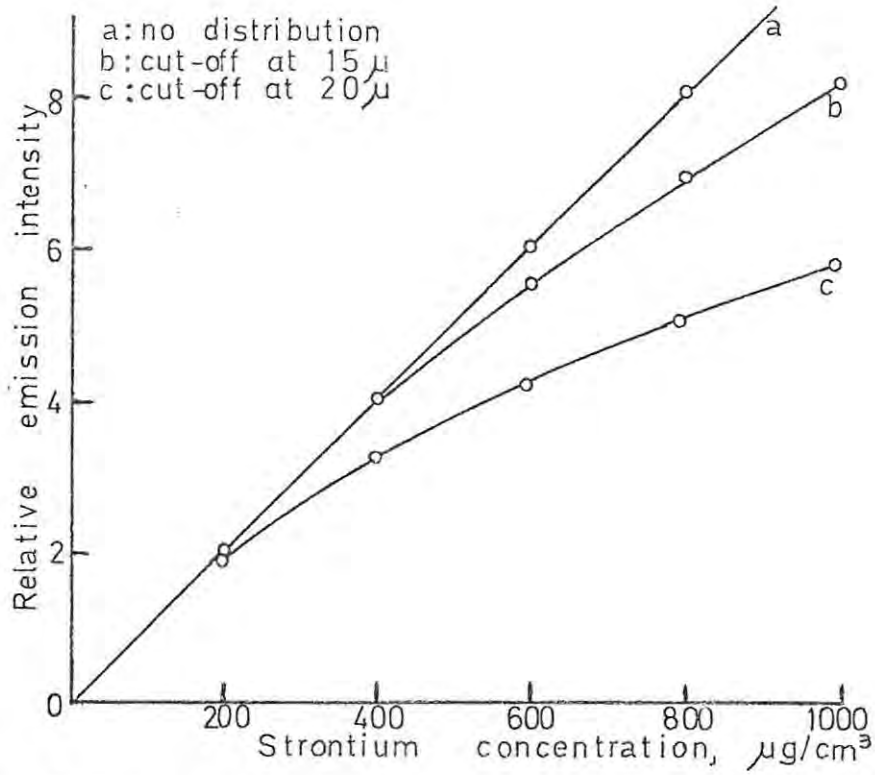

Figure 3.7. Effect of particle distribution and size (b,c) on analytical curves.

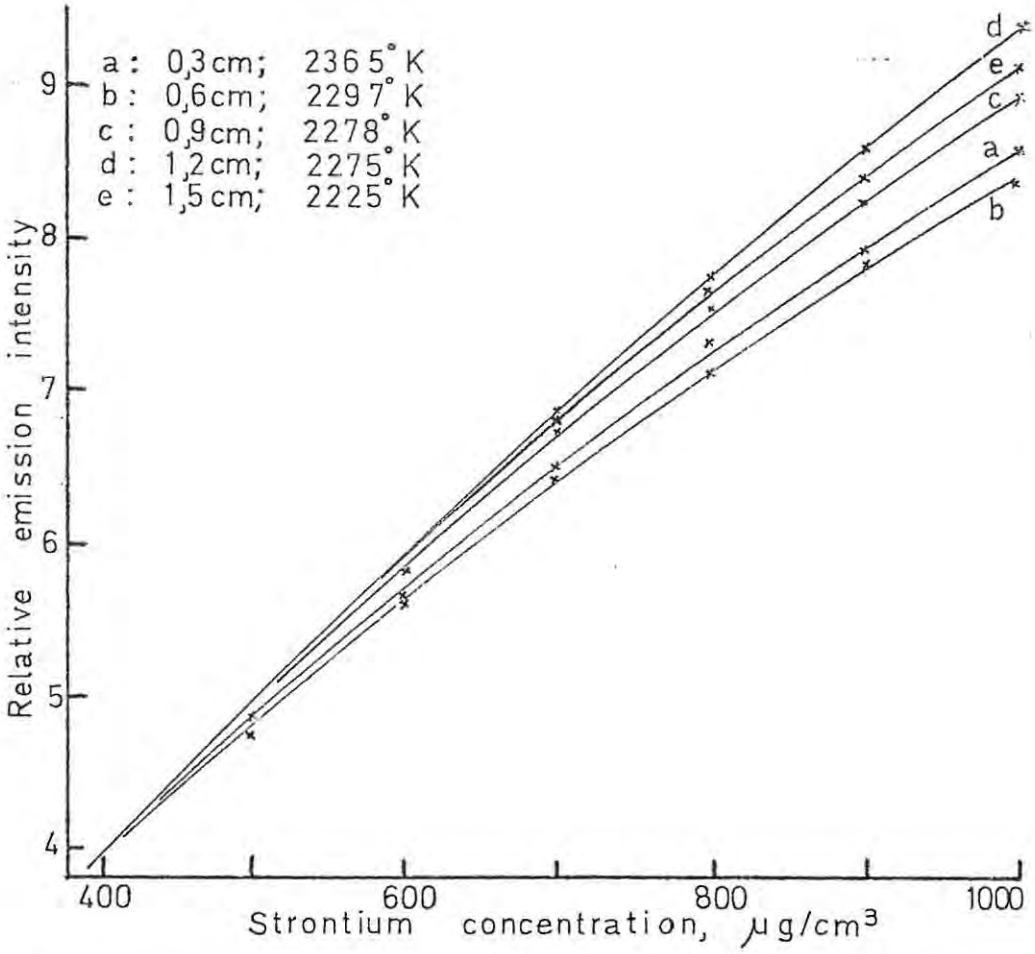

Figure 3.8. Comparison of calculated curves (unbroken lines) and measured intensities (x) for strontium. Observation height and temperature as indicated.

obtained between theory and experiment. Since the temperature of the flame would not be expected to remain constant with increasing observation height, different values of T_f were used in the calculation of the volatilization curves shown in figure 3.8; these are indicated on the figure itself.

It is obvious that some uncertainty exists in the values of many of the parameters used in these calculations, such as the latent heat of vaporization of strontium oxide (calculated from vapour pressure data by means of the Clapeyron-Clausius equation [62]), the coefficient of diffusion, D, of the gaseous substance, and the distribution pattern and limiting size of the droplets entering the flame. In addition, considerable uncertainty exists in the value which should be assigned to the temperature of the flame. Literature values quoted for the maximum temperature of the air-acetylene flame range from 2470°K to 3000°K [63]. L'Vov [56] favours a value of 2400°K for the reducing air-acetylene flame, which would decrease to ca. 2350°K upon aspiration of an aqueous solution. Fulton [64] has measured the temperature gradient in a stoichiometric air-acetylene flame and has found a drop in temperature of some 230°K between heights of 4 mm and 12 mm in the flame. In the present work, temperature values of between 2400°K and 2200°K have led to the best agreement between theory and experiment; however, this may be a reflection of inaccuracy in the assumed value of one or more of the other parameters. Thus, changing the limiting droplet dimension from 15μ to 20μ would necessitate a higher value of T_f for comparable results.* At the same time, the derivation does not allow for radiative heat losses by the droplets or the effect of particle size on vapour

---

* See figure 3.7.

pressure [52]. Due to the scarcity of vapour pressure data, in particular, it has not been possible to test the suggested model by calculating volatilization curves for elements which might be of interest in an air-acetylene flame, other than strontium.

Nevertheless, the agreement between theory and experiment found for the strontium oxide system is most encouraging - in particular, the fact that the calculated curves have exactly the correct shape for assumed values of T_f which are at least approximately correct - and enables definite conclusions to be drawn concerning the effects of (i) concentration, (ii) flame temperature and, (iii) observation height.

Concentration : Despite the fact that strontium oxide is relatively involatile (m.pt. = 2800°K, vapour pressure at 2400°K ≈ 2 torr), it is only at very high concentrations that incomplete volatilization occurs. It follows from this that most elements normally determined in an air-acetylene flame should not show line curvature due to volatilization effects unless the concentration of analyte is high, or an interfering species is present which causes a considerable decrease in vapour pressure of the particles at the temperature of the flame.

Flame temperature : Reference to calculated "absorbances" (Table 3.5 and figure 3.9) shows that the temperature of the flame may have a considerable effect on the degree of volatilization of the sample material. Thus a change in flame temperature of two degrees may produce a noticeable change in the measured response, while a change of five degrees may cause differences of 2% or more. It is not surprising, therefore, that the extent of chemical interference encountered in atomic absorption

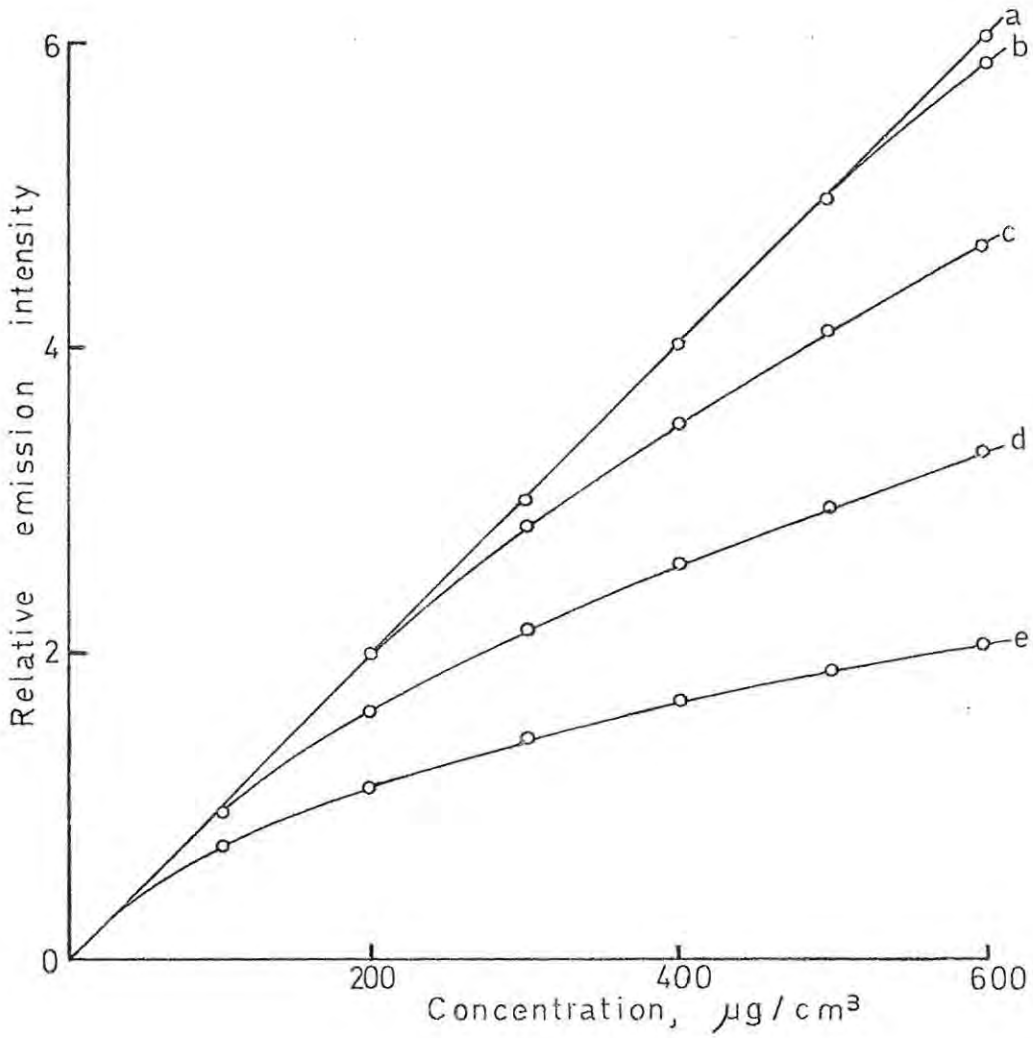

Figure 3.9. Calculated effect of flame temperature on the analytical curve for strontium.
a = 2300°K; b = 2250°K;
c = 2200°K; d = 2150°K;
e = 2100°K

spectrometry generally depends markedly on the flame conditions employed [52], since these will affect flame temperature.

Observation height : The effect of observation height per se is shown in Table 3.6; these results have been calculated on the assumption of a constant, arbitrary temperature of 2250°K. In practice, however, flame temperature varies with observation height, and these two parameters must be considered in combination. Frequently, as the observation height increases the temperature of the observation zone drops, so that these factors tend to counteract one another. The overall result, nevertheless, appears to be a general increase in the degree of volatilization of larger particles, at least until an observation height of nearly 1,5 cm (figure 3.8) is reached. This is consistent with the effect of observation height on interference reported elsewhere [65].

3.4 Summary

In order to express the degree to which analytical curves deviate from Beer's law, equation (3.12) was derived; this equation contains the quantity h which is directly related to the extent of deviation (and thus to the shape of the resultant curve), and is completely independent of the measured sensitivity. The initial justification for the use of equation (3.12) was seen in the linearization of analytical curves for cobalt, iron and nickel (figure 3.1) by means of a purely mechanical procedure involving scale expansion. However, it has also been shown that the equation is able accurately to represent the shape of calculated atomic absorption growth curves (figures 3.4 - 3.6).

Figure 3.10 compares measured analytical curves for five different elements with the curves calculated by means of equation (3.12). Some typical absorbances are given in Table 3.7. The agreement between the measured absorbances and the calculated values is seen to be quite acceptable.

It must be emphasized that equation (3.12) was derived in order to assess the effect of deviations from Beer's law on precision. At no stage was it envisaged that this equation would be used in the computation of sample concentrations from measured absorbances; it is therefore of interest to record that this work has formed the basis of the successful curve linearization process adopted by the manufacturers of the Pye Unicam SP1900 atomic absorption spectrometer.

From the work done on sample volatilization it appears that, although incomplete volatilization leads to bending of the analytical curve, the effect is unlikely to be significant unless an interfering matrix (e.g. chromium in a matrix of iron) is present, or concentrated analyte solutions are employed. In general, other factors are likely to have a far greater influence on the shape of the analytical curve.

T A B L E 3.5

Calculated* relative intensity of emmission or absorbance for different flame temperatures

Concn., $\mu g/cm^3$	Flame temperature, ^oK				
	2100	2150	2200	2250	2300
100,0	70,7	94,1	100,0	100,0	100,0
200,0	110,7	159,5	196,8	200,0	200,0
300,0	141,4	211,0	278,7	300,0	300,0
400,0	166,9	255,5	348,9	399,8	400,0
500,0	188,7	294,4	411,3	494,4	500,0
600,0	208,3	330,0	468,4	582,3	600,0

*Observation height assumed to be 1,2 cm

T A B L E 3.6

Calculated* relative intensity of emission or absorbance at different observation heights

Concn., $\mu g/cm^3$	Observation height, cm				
	0,3	0,6	0,9	1,2	1,5
100,0	92,7	100,0	100,0	100,0	100,0
200,0	155,7	195,4	200,0	200,0	200,0
300,0	205,4	274,8	298,1	300,0	300,0
400,0	248,1	342,8	387,0	399,8	400,0
500,0	285,6	403,5	466,8	494,4	500,0
600,0	319,8	458,7	539,6	582,3	598,3

*Flame temperature assumed to be 2250^oK

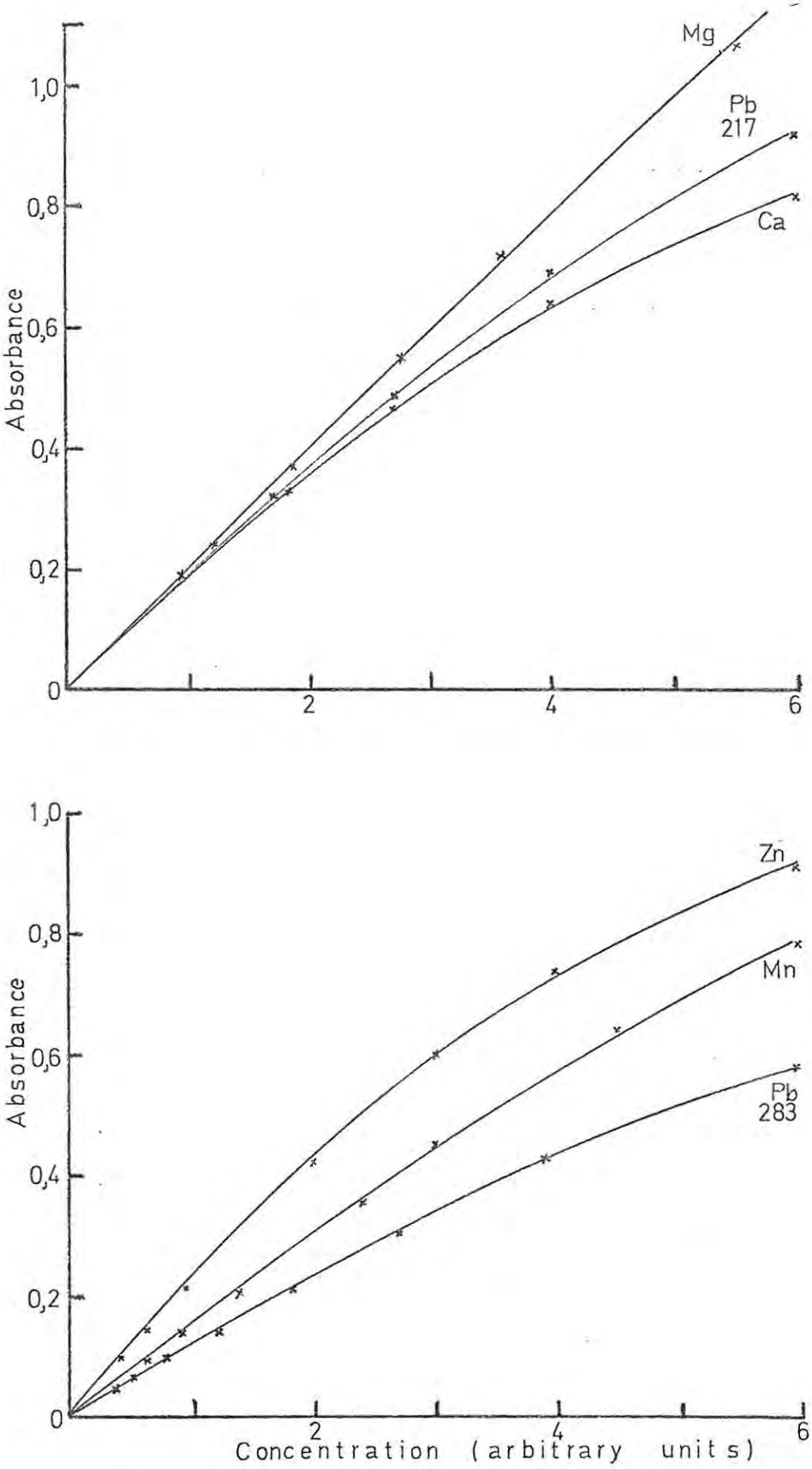

Figure 3.10. Experimental analytical curves (unbroken lines) and calculated values (x) for several elements.

T A B L E 3.7

Comparison of analytical curves obtained experimentally for several elements, with those calculated by means of equation (3.19)

Calcium

Concn. $\mu g/cm^3$	Absorbances Exptl.	Calcd.
1,8	0,069	0,067
2,7	0,103	0,101
4,0	0,149	0,148
6,0	0,222	0,219
9,0	0,323	0,321
13,3	0,452	0,455
20,0	0,627	0,633
30,0	0,818	0,815

$h = 0,90$

Lead (217,0 nm)

Concn. $\mu g/cm^3$	Absorbances Exptl.	Calcd.
3,3	0,042	0,042
7,5	0,098	0,095
11,0	0,143	0,138
17,0	0,216	0,212
25,0	0,306	0,308
40,0	0,480	0,479
60,0	0,680	0,684
90,0	0,921	0,919

$h = 0,94$

Magnesium

Concn. $\mu g/cm^3$	Absorbances Exptl.	Calcd.
0,09	0,029	0,037
0,18	0,067	0,073
0,41	0,165	0,164
0,61	0,248	0,244
0,92	0,367	0,364
1,38	0,544	0,544
1,84	0,717	0,722
2,76	1,076	1,064

$h = 0,99$

Manganese

Concn. $\mu g/cm^3$	Absorbances Exptl.	Calcd.
0,9	0,050	0,048
1,8	0,100	0,095
2,7	0,149	0,142
4,1	0,221	0,216
6,1	0,317	0,314
9,0	0,445	0,448
13,5	0,625	0,635
18,0	0,790	0,785

$h = 0,92$

Chapter 4

ERROR FUNCTIONS IN ATOMIC ABSORPTION SPECTROMETRY

4.1 Error functions in spectrophotometry

In an effort to show ranges of concentration which might be determined spectrophotometrically with low relative analytical error, Ringbom [66] and Ayres [67] plotted per cent transmittance (or absorption) against the logarithm of the analyte concentration. They found that, if a sufficient concentration range was investigated, an S-shaped curve always resulted whether or not the system under investigation followed Beer's law. If the system obeyed Beer's law, the point of inflexion occurred at ca. 63% absorption; if not, the inflexion was at some lower value, but the general shape of the curve remained the same. Such a curve generally had a considerable portion which was nearly a straight line and corresponded to the region of maximum slope, and it was suggested that this portion of the curve indicated directly the optimum range of concentration for the particular spectrophotometric analysis. Ramirez-Munoz has discussed the relationship between sensitivity and precision [68] and sensitivity and accuracy [14] in atomic absorption spectrometry, and has suggested the Ringbom-Ayres plot as a suitable criterion for selecting that concentration range corresponding to greatest precision of measurement in atomic absorption analysis. Chakrabarti [69] obtained Ringbom-Ayres plots for the atomic absorption response of aluminium.

In his excellent discussion of photometric precision, Crawford [70] has demonstrated that the Ringbom-Ayres plot is insufficient in itself to specify the range for good precision.

This author pointed out that the information furnished by a Ringbom-Ayres plot must be interpreted in the light of the "Error Function" - i.e. the way in which uncertainty in the value of transmittance (dT) varies with transmittance (T) - for the particular system under investigation. Only when dT is constant, independent of T, does the Ringbom-Ayres curve indicate the range for optimum precision. According to Crawford, "conditions exist in which constancy would not be expected and cannot be assumed". Although a number of workers [16-20] have discussed precision in atomic absorption spectrometry, only one investigation of error functions associated with this technique has been reported*, and that very recently [5]. It was felt desirable that such a study should be undertaken and should include both a theoretical treatment and practical investigations of error functions.

Since the basic spectrometric measurement is that of transmittance rather than absorbance, error functions and their effect on precision have been treated largely from the point of view of an instrument with a read-out linear in transmittance. The equivalent statements for a response linear in absorbance are given wherever applicable.

4.2 Sources of error and theoretical error functions in atomic absorption spectrometry

Following Cahn [71], Crawford has outlined three basic kinds of dT vs T behaviour. A consideration of possible error sources in atomic absorption spectrometry has led the present

---

* Except for the publication, in a slightly modified form, of the present author's own work reported in this thesis. See Spectrochim. Acta 24B, 255 (1969); 25B, 539 (1970); and 28B, 407 (1973).

author to define a fourth and a fifth error function, both of which could be particularly relevant to atomic absorption analysis:

(a) dT proportional to T;
(b) dT proportional to $\sqrt{T}$;
(c) dT constant;
(d) dT proportional to TlogT; and
(e) dT proportional to $\sqrt{1-T}$.

dT proportional to T

Several sources of error, such as flame absorption noise, changes in lamp intensity, contamination introduced during sample preparation, and light scattering and/or molecular absorption by extraneous material in the flame, would cause a change in the absorbance (dA) of an aspirated solution which would be independent of the actual absorbance of the sample, so that dA = a constant. (4.1)

But $A = -\log T$ (4.2)

$dA = -k.dT/T$ (4.3)

and $dT \propto T$ (since dA constant).

In this case, the relative precision is greatest (dA/A is a minimum) when $A = \infty$ or $T = 0$.

dT independent of T

Scale reading errors on linear T scale (including meter or recorder "deadspace"), and zero transmittance drift (dark current drift) are possible error sources which may introduce inaccuracies in atomic absorption procedures. In either of these cases the error in transmittance (dT) is independent of the transmittance. The same is true of electronic (baseline) noise

and flame (emission) noise, both of which produce an uncertainty in estimating the value of the signal, an uncertainty which is independent of the actual magnitude of the signal.

In this case the optimum value for T can be shown to be 36,8%:

Since $$dA = -k\frac{dT}{T} \qquad (4.3)$$

and since dT is constant,

$$\frac{dA}{A} = \frac{k'}{T.\log T} = \frac{k''}{T.\ln T} \qquad (4.4)$$

Differentiating with respect to T,

$$\frac{d}{dT}\left(\frac{dA}{A}\right) = \frac{-k''(\ln T+1)}{(T.\ln T)^2} \qquad (4.5)$$

For dA/A to be a minimum, we must have

$$\ln T+1 = 0$$

$$\therefore \quad \ln T = -1$$

$$\therefore \quad -\log T = 0,434$$

and $$T = 36,8\% \text{ or } A = 0,434.$$

dT proportional to $\sqrt{T}$

If the number of photons arriving at the photocell is N, then the standard deviation due to statistical variations [70] will be given by

$$dN = \sqrt{N} \qquad (4.6.)$$

Since $$T = I/I_o \qquad \text{(from 3.1)}$$

$$T + dT = \frac{I+dI}{I_o+dI_o} = \frac{N+dN}{N_o+dN_o} \qquad (4.7)$$

where N_o is the number of photons corresponding to the incident intensity I_o.

$$\therefore \quad T + dT = \frac{N + \sqrt{N}}{N_o + \sqrt{N_o}} \tag{4.8}$$

$$= \frac{N}{N_o + \sqrt{N_o}} + \frac{\sqrt{N}}{N_o + \sqrt{N_o}} \tag{4.9}$$

But $N_o + \sqrt{N_o} \approx N_o$ since N_o large.

$$\therefore \quad T + dT = \frac{N}{N_o} + \frac{\sqrt{N}}{N_o} = T + \frac{\sqrt{N}}{N_o} \tag{4.10}$$

and $$dT = \frac{\sqrt{N}}{N_o} \tag{4.11}$$

or $$dT \propto \sqrt{N} \tag{4.12}$$

If N_o is constant, then $T \propto N$.

Hence $dT \propto \sqrt{T}$

It can be shown that, under these conditions, the precision will be greatest when the transmittance is 13,5%, as follows:

From (4.3) above, $dA = \frac{-k.dT}{T}$

If $dT \propto \sqrt{T}$,

then $$dA = \frac{-k'.\sqrt{T}}{T} \tag{4.13}$$

and $$\frac{dA}{A} = \frac{k'}{\sqrt{T}.\log T} = \frac{k''}{\sqrt{T}.\ln T} \tag{4.14}$$

where k, k', and k'' are constants, and ln is $\log_e$.

Differentiating (4.14), we have

$$\frac{d}{dT}\left(\frac{dA}{A}\right) = \frac{-k''(\tfrac{1}{2}\ln T + 1)}{T.\sqrt{T}.(\ln T)^2} \tag{4.15}$$

The condition for dA/A to be a minimum is that the right hand side of equation (4.15) be equal to zero.

$$\therefore \quad \tfrac{1}{2}\ln T = -1$$

or $$\log T = -0,868$$

$$A = 0,868 \text{ or } T = 13,5\%$$

These are the values of A and T for the greatest precision.

dT proportional to TlogT

Any factor causing variations in the absorptivity a (or, sensitivity) or the concentration c of atoms in the flame, when the magnitude of the variation is itself proportional to a or c, would be expected to give rise to a TlogT error function. Thus changes in the apparent sensitivity are caused by fluctuations in flame temperature and/or gas mixture, or by monochromator drift. Similarly, factors affecting c, such as the sample uptake rate, efficiency of nebulization, and volumetric errors during sample preparation would cause this type of behaviour, as would fluctuations in flame dimensions. This latter is of particular relevance in atomic absorption analysis. In each of these instances the absolute magnitude of the possible error produced (dc) will be proportional to c.

Since $A = abc$ (from 3.1)

$\therefore$ $dA = ab.dc.$ (for constant a,b) (4.16)

But $dc \propto c$

$\therefore$ $dA \propto A$ or $dA = k'A$ (4.17)

$A = -\log T$ (4.2)

$\therefore$ $dA = -0,434.dT/T$ (4.18)

Combining (4.17) and (4.18) to eliminate dA.

$$-k'A = 0,434.dT/T \quad (4.19)$$

Replacing A by -logT, we have

$$k'\log T = 0,434.dT/T \quad (4.20)$$

$\therefore$ $dT = 2,303k'T\log T$ (4.21)

or $dT \propto T\log T$

A similar result follows for corresponding variations in a. It follows from (4.17) above that dA/A is constant, so that the relative precision is independent of A (or T).

dT proportional to $\sqrt{1-T}$

Such an error function can arise from statistical variations in the absorption process in the flame. Such errors are likely to be small; they are nevertheless included in this discussion for the sake of completeness.

This error function may be derived as follows:

The standard deviation for the absorption process will be given by

$$dN_a = \sqrt{N_a} \qquad (4.22)$$

where N_a is the mean number of photons absorbed. If the total number of photons is N_o, then

$$T = \frac{N_o - N_a}{N_o} \qquad (4.23)$$

and

$$T + dT = \frac{N_o-(N_a + dN_a)}{N_o} \qquad (4.24)$$

$$= \frac{N_o - N_a}{N_o} - \frac{dN_a}{N_o} \qquad (4.25)$$

$$= T - \sqrt{N_a}/N_o \qquad (4.26)$$

$$\therefore \quad dT = -\sqrt{N_a}/N_o \qquad (4.27)$$

If N_o is constant, then

$$dT \propto \sqrt{N_a} \qquad (4.28)$$

But $N_a \propto 1-T$ (for constant N_o)

$$\therefore \quad dT \propto \sqrt{1-T} \ . \qquad (4.29)$$

Since

$$dA = -k.dT/T \qquad (4.3)$$

$$\therefore \quad dA = -k\sqrt{1-T}/T \qquad (4.30)$$

and

$$\frac{dA}{A} = \frac{k\sqrt{1-T}}{T.\log T} = \frac{k'\sqrt{1-T}}{T.\ln T} \qquad (4.31)$$

Using equation (4.31) it is possible to find the optimum transmittance for a system giving rise to such an error function. Differentiating, we have

$$\frac{d}{dT}\left(\frac{dA}{A}\right) = \frac{-T.\ln T - 2(1-T)(\ln T+1)}{2\sqrt{1-T}(T.\ln T)^2} \qquad (4.32)$$

For the right hand side to be equal to zero, we must have

$$T.\ln T = -2(1-T)(\ln T+1) \qquad (4.33)$$

and $T = 0{,}515$ or $A = 0{,}288$.

In chapter 3 an expression was derived for the relative error, dc/c (equation 3.19); this expression should be valid whether the system under investigation obeys Beer's law or not.

$$dc/c = \frac{-dT}{2{,}303(T+h-1).\log[h/(T+h-1)]} \qquad (3.19)$$

By substituting for dT in equation (3.19) it is possible to obtain a general expression for the relative error. Such an expression, which will apply whether or not the system in question obeys the absorption law, evaluates the effect on the relative error both of the extent of deviation from Beer's law and of the particular error function.

$$\frac{dc}{c} \propto \frac{-dT}{(T+h-1).\log[h/(T+h-1)]} \qquad (4.34)$$

(i) If $dT \propto T$, then

$$\frac{dc}{c} \propto \frac{-T}{(T+h-1).\log[h/(T+h-1)]} \qquad (4.35)$$

(ii) If dT constant, then

$$\frac{dc}{c} \propto \frac{-1}{(T+h-1).\log[h/(T+h-1)]} \qquad (4.36)$$

(iii) If $dT \propto \sqrt{T}$, then

$$\frac{dc}{c} \propto \frac{-\sqrt{T}}{(T+h-1).\log[h/(T+h-1)]} \qquad (4.37)$$

(iv) If $dT \propto T\log T$, then

$$\frac{dc}{c} \propto \frac{-T\log T}{(T+h-1).\log[h/(T+h-1)]} \qquad (4.38)$$

(v) If $dT \propto \sqrt{1-T}$, then

$$\frac{dc}{c} \propto \frac{-\sqrt{1-T}}{(T-h-1).\log[h/(T+h-1)]} \qquad (4.39)$$

The error function $dT \propto T\log T$ needs further modification, however. Since this behaviour arises out of the dynamic nature of the atom reservoir (flame) in conventional atomic absorption spectrometry, and depends on the absorption characteristics of the light beam from the hollow cathode lamp, it is clear that when T approaches a value of 1 - h, the error function $dT \propto T\log T$ approaches zero. Hence dT can have no real meaning for values of T less than 1 - h. In order to fulfil this condition, dT must be h-dependent, and can be re-written in the form

$$dT \propto T'\log T' \qquad (4.40)$$

where $$T' = (T + h - 1)/h \qquad (4.41)$$

Substitution of equations (4.40) and (4.41) into equation (3.19) leads to the result

$$\frac{dc}{c} \propto \frac{(T+h-1).\log[h/(T+h-1)]}{h.(T+h-1).\log[h/(T+h-1)]} \qquad (4.42)$$

or $$\frac{dc}{c} \propto \frac{1}{h} \qquad (4.43)$$

Irrespective, therefore, of the extent of deviation from Beer's law, the relative error for a TlogT - type error function does not vary with transmittance or absorbance; however the relative error does increase with increasing deviation from Beer's law (decreasing value of h).

The same will be true of the function $dT \propto \sqrt{1 - T}$: when T reaches a value of 1 - h, i.e. when all the absorbable radiation has been absorbed, the function must reach a maximum value. Again, T in the equation for this error function must be replaced by T' (equation (4.41), so that

$$dT \propto \sqrt{1 - T'} \qquad (4.44)$$

$$\propto \sqrt{1 - \frac{T+h-1}{h}} \qquad (4.45)$$

$$\propto \sqrt{\frac{1 - T}{h}} \qquad (4.46)$$

Substitution into equation (4.34) of equation (4.46) gives

$$\frac{dc}{c} \propto \frac{\sqrt{(1-T)/h}}{(T+h-1).\log[h/(T+h-1)]} \qquad (4.47)$$

The error functions $dT \propto T$, dT constant, and $dT \propto \sqrt{T}$ are not directly related to the specific light-absorption characteristics of the system, and therefore are not dependent on the value of h.

Figure 4.1 shows the variation of dc/c with transmittance, for several values of h, for each of the error functions discussed above.

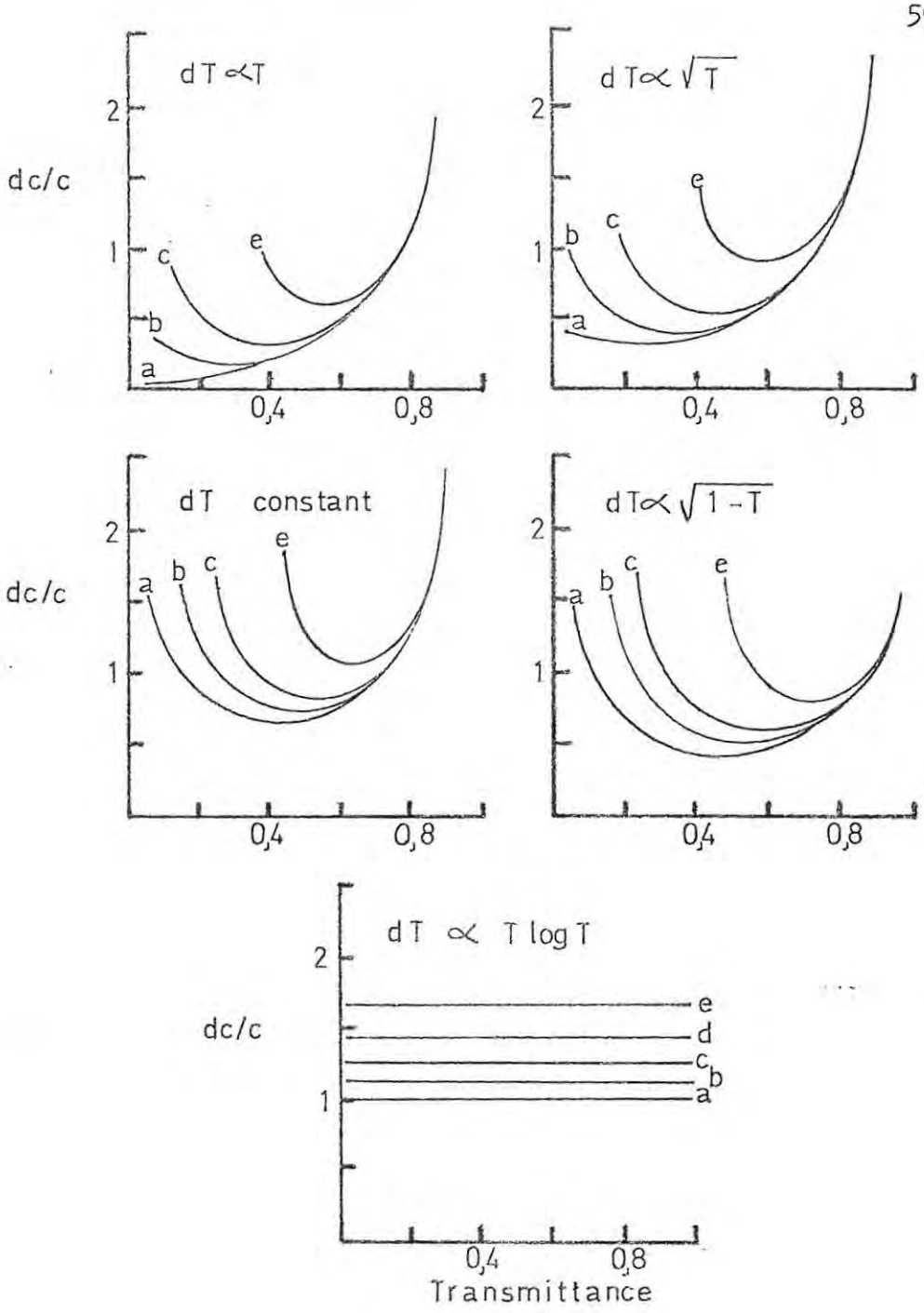

Figure 4.1. Variation of dc/c (arbitrary units) with transmittance for several values of h, for individual error functions.

4.3 Quantitative evaluation of atomic absorption error functions

In order to compare the various error functions directly with one another, each function may be expressed in such a way that the area under the curve of dT vs T between the limits T = 1 and T = 1 - h is constant; hence

$$dT_1 = \frac{0,5T}{h(1-h/2)} \qquad (4.48)$$

$$dT_2 = 0,5/h \qquad (4.49)$$

$$dT_3 = \frac{0,75\sqrt{T}}{1-(1-h)^3/2} \qquad (4.50)$$

$$dT_4 = -4,61\ \frac{(T+h-1)}{h} \log \frac{T+h-1}{h} \qquad (4.51)$$

$$dT_5 = \frac{0,75\sqrt{1-T}}{h^3/2} \qquad (4.52)$$

These error functions may then be combined as the sum of their squares to give an expression for the overall, observed error function F, thus

$$F = \sqrt{(k_1 dT_1)^2 + (k_2 dT_2)^2 + (k_3 dT_3)^2 + (k_4 dT_4)^2 + (k_5 dT_5)^2} \qquad (4.53)$$

The overall relative error will then be given by

$$\frac{dc}{c} = \frac{F}{(T+h-1).\log\ [h/\ (T+h-1)]} \qquad (4.54)$$

It is possible to programme a computer to find the values of k_1, etc., which give the best fit of the function F (equation 4.53) to a set of experimentally-determined values for dT (measured at different values of T). The magnitude of each constant is then a direct measure of the extent to which a particular error function contributes to the general noise level. The computer flow-diagrams are shown in figure 4.2.

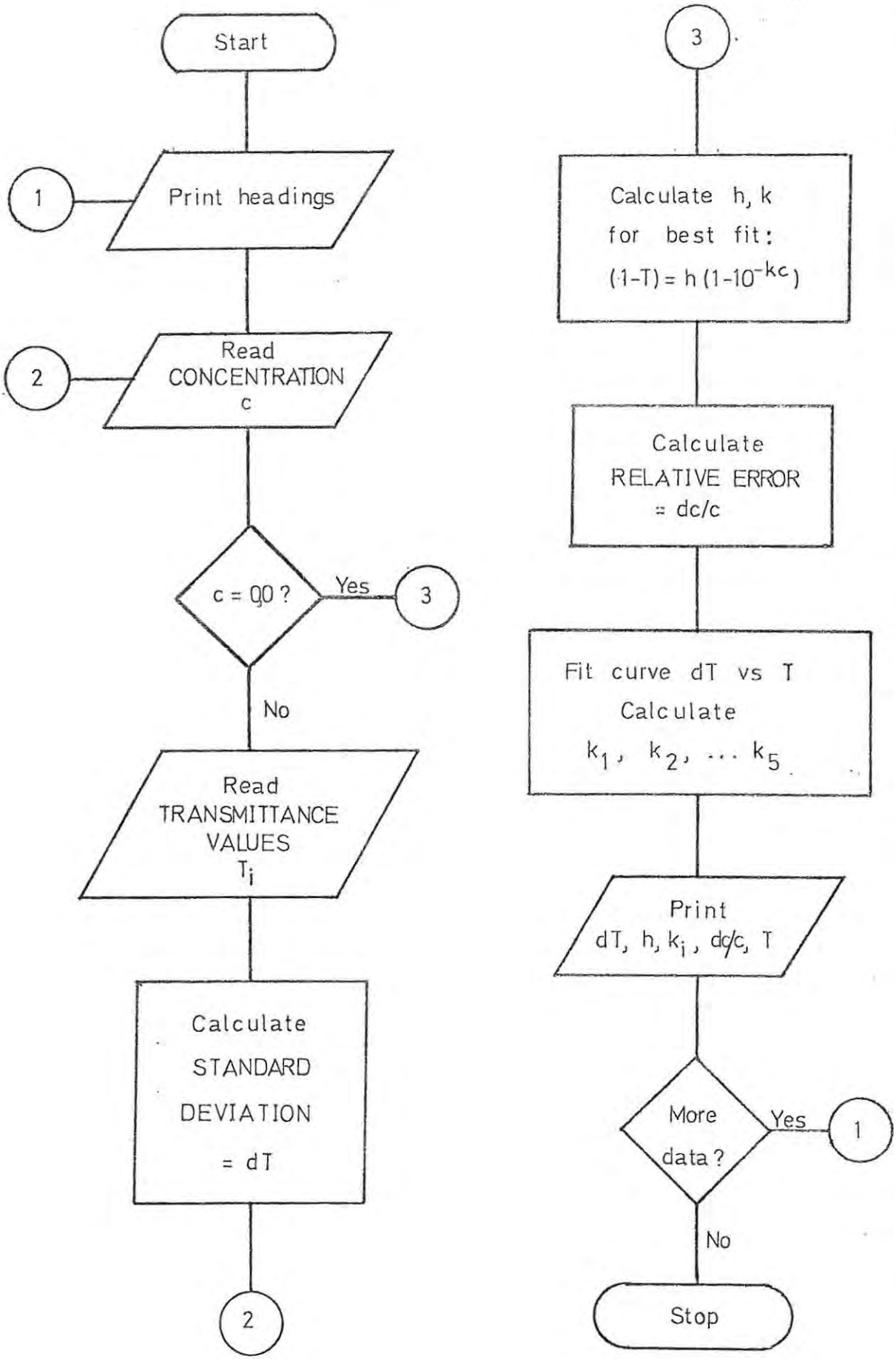

Figure 4.2. Computer flow diagram for the quantitative evaluation of error functions.

In order to verify the form of individual error functions, instrumental parameters were adjusted in such a way as to enhance one source of noise relative to all others, where possible. In this way, error functions could be obtained which approximated to one or other of the individual functions outlined previously (e.g. equations 4.48 - 4.52). The following typical sets of conditions were used:

(a) The monochromator slit width was reduced to the minimum value possible (about 0,005 mm) and the electronic gain increased to compensate for the low intensity of lamp emission reaching the monochromator. The flame was not lit, and no solution was aspirated. A variable attenuator placed in front of the monochromator slit was used to vary transmittance from 1,0 to 0,0. Under these conditions the overall electronic noise factor was emphasised over other sources of noise, and the graph obtained (figure 4.3) approximates to a $dT \propto T$ error function.

(b) As for (a) above, but with a large slit width (ca. 0,5 mm) and minimum gain setting in order to emphasize photomultiplier shot noise. The results (figure 4.4) indicate increased line curvature due to an increased $dT \propto \sqrt{T}$ contribution.

(c) A zinc lamp was operated at 5 mA with a monochromator wavelength setting of 213,9 nm and a highly absorbing air-acetylene flame, thus enhancing absorption noise from the flame. Variation in transmittance

was obtained by increasingly off-setting the lamp from the true optical path; distilled water only was aspirated into the flame. The results are shown in figure 4.5, and indicate, predictably, a $dT \propto T$ type error function.

(d) A chromium lamp was operated at a current of 5 mA, with the monochromator set on a non-absorbing line at 423 nm. A strongly-emitting nitrous oxide-acetylene flame was used, and a solution containing calcium (100 $\mu g/cm^3$) was aspirated. In this way, flame emission noise was considerably increased relative to other noise factors. Again, the range 1,0 - 0,0 transmittance was covered by off-setting the hollow cathode lamp from the true optical path, thus blocking off increasing proportions of the light from the lamp prior to its passage through the flame. A nearly constant noise level was obtained (figure 4.6).

(e) A series of calcium solutions, covering the range 0 - 100 $\mu g/cm^3$, was aspirated for calcium under normal flame conditions. The wavelength was set at 422,7 nm. In order to enhance dynamic flame noise, the instrument was operated inside a fume cupboard with the fan on: sufficient draught was produced to cause slight fluctuations within the flame. Electronic and flame emission noise were kept to a minimum by using a calcium lamp which emitted a high intensity of resonance radiation: both a low amplifier gain and a small slit width could therefore

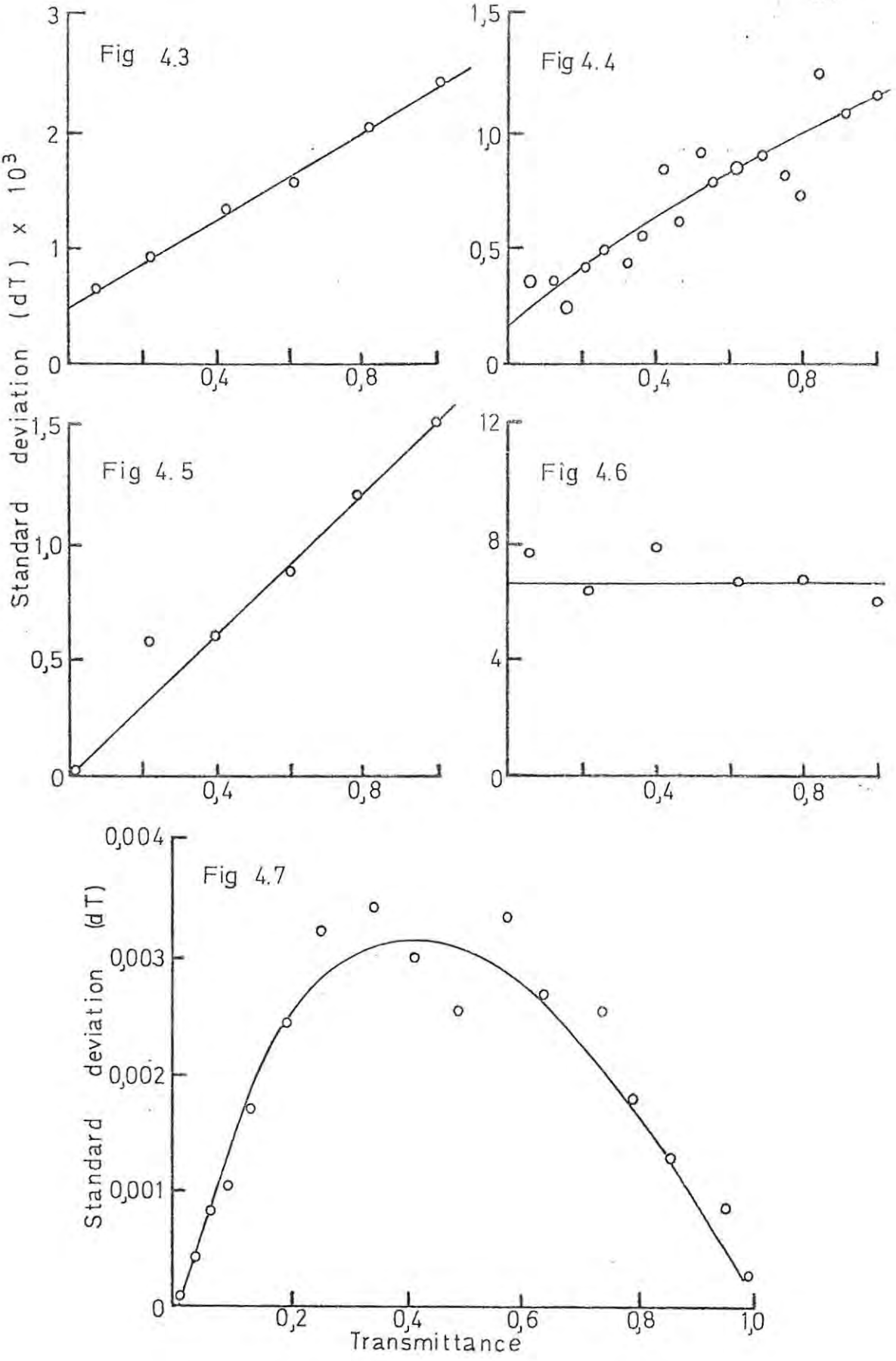

Figures 4.3 - 4.7. Variation of standard deviation with transmittance for individual noise sources.

be employed. The results are shown in figure 4.7, and, allowing for a small $dT \propto T$ and/or $dT \propto \sqrt{T}$ contribution, approximate very closely to a TlogT error function (unbroken line).

The error functions obtained under real analytical conditions, designated composite error functions, were evaluated for nine elements commonly determined by atomic absorption analysis. For each element, a set of standard solutions was prepared covering the range from approximately 2x to 600x the expected analytical sensitivity ($\mu g/cm^3$ per 1% absorption) of the element concerned. Instrumental conditions were adjusted in accordance with the manufacturer's recommendations, and 20 readings were obtained for each solution. Standard deviations (dT) were computed for each set of 20 readings. From the value of the mean transmittance (T) and the known concentration (c) of each solution, the best value of the constant $\underline{h}$ was calculated for each element. Finally, the best value for each of the coefficients k_{1-5} was computed from the known values of c_i, T_i, dT_i and $\underline{h}$ for every element studied. The results are given in Table 4.1. Figure 4.8 shows some typical results obtained for dT as a function of T, together with the calculated curves.

For calcium, the above procedure was repeated for different settings of the monochromator slit width, thus giving rise to sets of results related to different values of $\underline{h}$ ($\underline{h}$ decreases with increasing slit width). The results are shown in Table 4.2. Since in none of the cases examined did the constant k_5 have a significant value ($k_5 \leq 0{,}0002$), it has not been included in Tables 4.1 and 4.2.

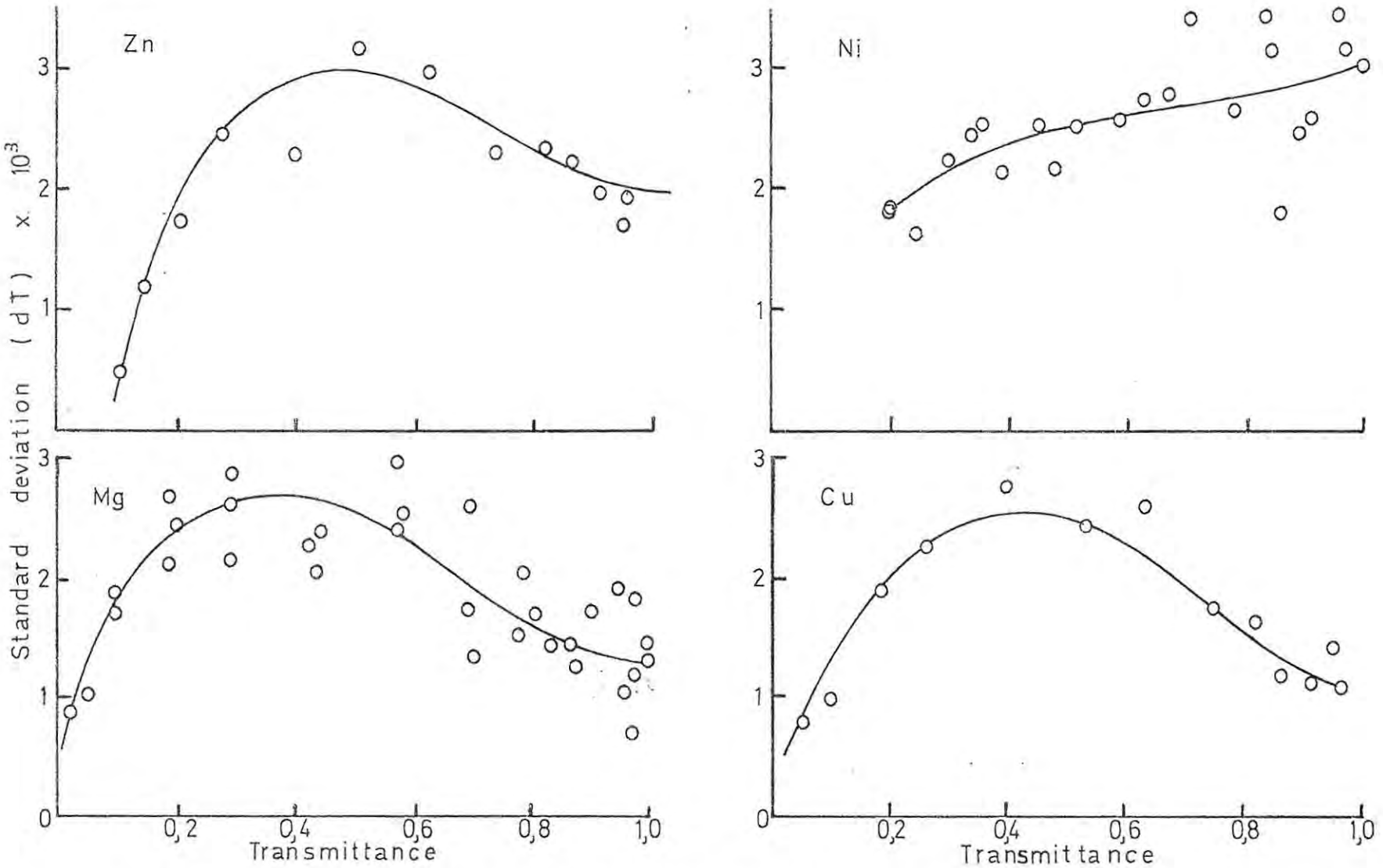

Figure 4.8. Standard deviation dT (o) as a function of transmittance. Unbroken lines indicate the calculated variation of dT with T.

T A B L E 4.1

Composite error functions* for different elements

	h	k_1	k_2	k_3	k_4
Calcium	0,96	0,0009	0,0007	0,0015	0,0026
	0,90	0,0008	0,0008	0	0,0034
Chromium	0,83	0,0003	0	0,0018	0,0017
	0,81	0,0009	0	0,0016	0,0018
Copper	0,96	0,0002	0,0013	0,0011	0,0033
	0,95	0	0,0014	0,0016	0,0034
Iron	0,85	0	0	0,0020	0,0027
	0,81	0,0011	0,0009	0,0016	0,0030
Lead	0,96	0,0020	0,0017	0,0016	0,0044
(217.0 nm)	0,96	0,0014	0,0016	0,0016	0,0033
Lead	0,92	0	0,0026	0	0,0034
(283.3 nm)	0,88	0	0,0021	0	0,0029
Magnesium	1,00	0	0,0012	0,0013	0,0035
Manganese	0,95	0,0016	0,0015	0,0013	0,0030
	0,92	0,0001	0,0014	0,0011	0,0036
Nickel	0,84	0,0026	0,0027	0,0007	0,0022
Zince	0,93	0,0015	0,0009	0,0020	0,0037
	0,91	0,0004	0,0012	0,0018	0,0024

* The various sets of results for a given element are not duplicates, but were obtained under different instrumental conditions.

T A B L E 4.2

Composite error functions for calcium with varying slit width

Slit width	h	k_1	k_2	k_3	k_4
0,02 mm	0,99	0,0019	0,0020	0,0009	0,0033
0,05 mm	0,98	0,0005	0,0008	0,0013	0,0027
0,10 mm	0,97	0	0,0009	0,0015	0,0029
0,20 mm	0,89	0,0005	0,0011	0,0016	0,0024
0,50 mm	0,76	0	0,0008	0,0016	0,0028
1,00 mm	0,64	0,0003	0,0014	0,0010	0,0023

4.4 Optimum working range

Because of differences in the extent to which different elements, or the same element under different conditions, follow Beer's law, it is difficult to quote a general working range for atomic absorption analysis in terms of absorbance, and the present author has suggested [22] that such an optimum range is better expressed in terms of multiples of sensitivity of the absorbing species rather than in terms of a measured response such as transmittance or absorbance.

We have

$$1 - T = h(1 - 10^{-abc}) \qquad (3.12)$$

By definition, the sensitivity equals that concentration which will give a transmittance of 0,99, i.e. 1% of absorption;

$$\therefore \quad 0{,}01 = h(1 - 10^{-abc}) \qquad (4.55)$$

$$\text{and} \quad -abc = \log\left(1 - \frac{0{,}01}{h}\right) \qquad (4.56)$$

By the binomial expansion,

$$\log\left(1 - \frac{0{,}01}{h}\right) = -\frac{0{,}0044}{h} \qquad (4.57)$$

Hence, when the concentration equals the analytical sensitivity,

$$1 - T = h(1 - 10^{-0{,}0044/h}) \qquad (4.58)$$

and in general,

$$1 - T = h(1 - 10^{-0{,}0044N/h}) \qquad (4.59)$$

$$\text{or} \quad T = 1 - h(1 - 10^{-0{,}0044N/h}) \qquad (4.60)$$

$$\text{and} \quad T + h - 1 = h.10^{-0{,}0044N/h} \qquad (4.61)$$

where N is the concentration expressed as multiples of the sensitivity.

The value of T may be substituted into the equation for the relative error (equation 3.19) to give

$$\frac{dc}{c} \propto \frac{-dT}{(10^{-0,0044N/h})0,0044N} \qquad (4.62)$$

dT can be equated with any of the individual error functions or with F, the expression for the composite error function(equation 4.53). The variation of dc/c with N may then be calculated under any given conditions. Figure 4.9 shows the variation in dc/c with N for some of the composite error functions given in Table 4.1.

It has been pointed out by Ayres [67], amongst others, that definition of the limits of an optimum working range is largely arbitrary, since the relative error changes continuously with change in concentration. He has suggested that the concept of optimum range could be made more meaningful "by giving the upper and lower limits of concentration between which the relative analysis error, for a given photometric error (i.e. dT) will not exceed some specified value". However, Ayres was considering but one type of error function, viz. dT constant. In the present work dT (or F) has varied with T, and a different definition of "optimum" is therefore necessary.

It is proposed, for the purpose of this work, to define the optimum working range as that range of concentration for which the relative error is never greater than a fixed percentage of the minimum value given by the particular composite error function under consideration. This "limiting value" may be set at 110%, 125% or even 150%, depending on the needs of the individual analyst. On the basis of this definition the optimum ranges found in

practice for many different metals, calculated for each of the three limiting values quoted above, are shown in Table 4.3. The ranges are quoted in terms of concentration, expressed as multiples of the analytical sensitivity (designated N).

Figure 4.9 shows the variation of dc/c with N for several elements. The minima for these and similar curves drawn for each error function listed in Table 4.1 occur in the range 90x to 150x the sensitivity (or, 0,35 - 0,61 absorbance units). This is in good agreement with the results reported by Weir and Kofluk [19], and is somewhat lower than the values suggested by Price [26]. It is clear from figure 4.9 that there is a common region of best precision in the range 80x - 140x the sensitivity for the different elements. However, for many elements there is a flat portion of the curve which extends far beyond the limits quoted above (e.g. magnesium, up to nearly 200x the sensitivity). Reference to Table 4.3 indicates the optimum range for the various elements in terms of the amount by which the relative error is increased over the minimum value: keeping the relative error within 125% of the minimum value gives a range of less than 40x to greater than 260x the sensitivity for many elements. If 110% is selected as the criterion for "optimum", the range is shortened to about 50x - 200x the sensitivity.

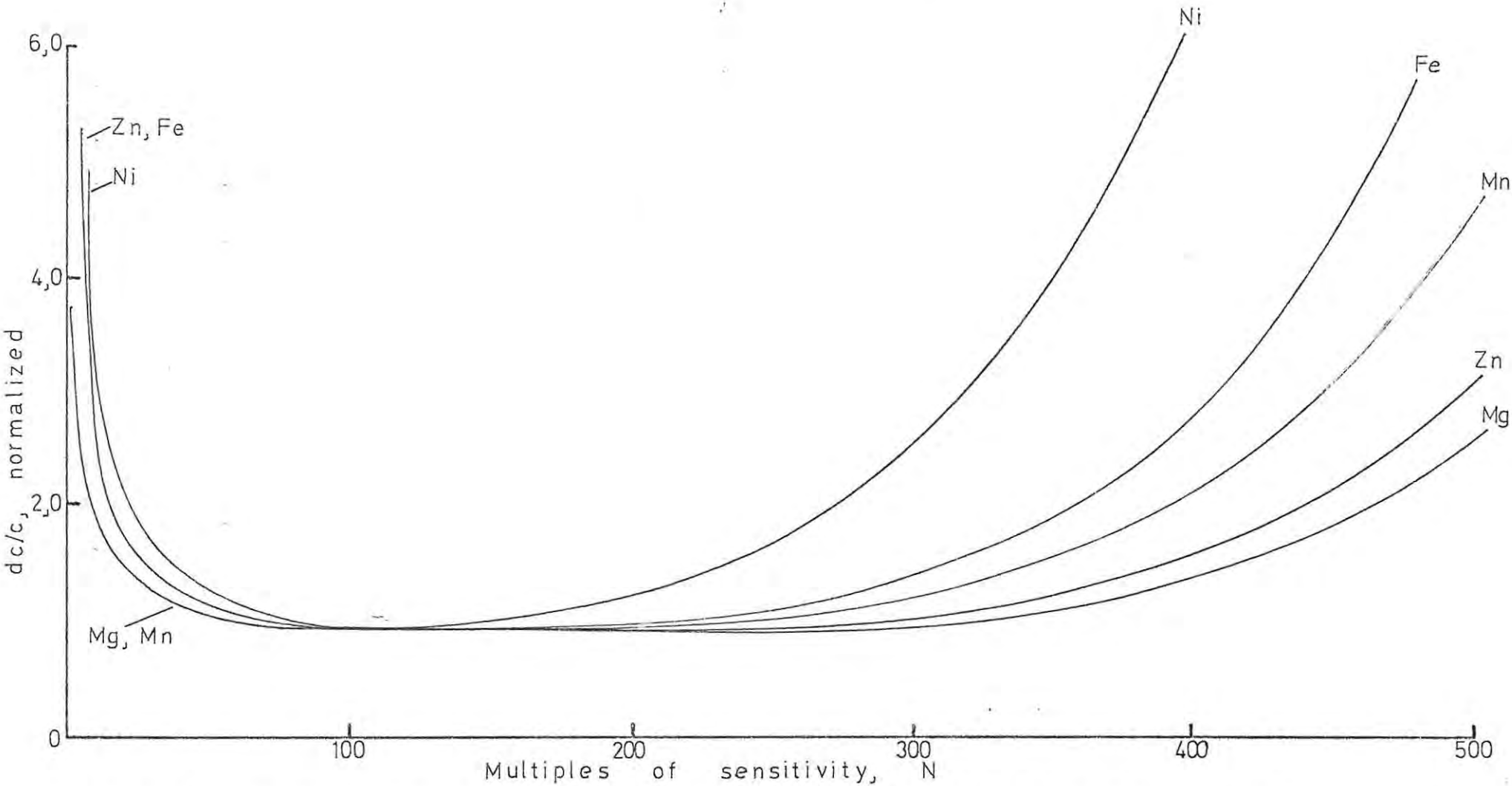

Figure 4.9. Relative error (normalized to an arbitrary minimum value of 1,0) as a function of concentration, for several elements.

TABLE 4.3

Optimum working ranges for different elements

Element	h	Optimum working ranges					
		110%		125%		150%	
		Multiples of sensitivity	Absorbance	Multiples of sensitivity	Absorbance	Multiples of sensitivity	Absorbance
Calcium	0,96	54 - 286	0,23 - 1,0	35 - 342	0,15 - 1,0	24 - 390	0,10 - 1,0
	0,90	26 - 283	0,11 - 0,86	16 - 337	0,07 - 0,92	11 - 382	0,05 - 0,95
Chromium	0,83	57 - 191	0,23 - 0,60	40 - 232	0,17 - 0,66	28 - 271	0,12 - 0,70
	0,81	57 - 191	0,23 - 0,58	39 - 230	0,16 - 0,63	28 - 268	0,12 - 0,66
Copper	0,96	33 - 256	0,14 - 0,98	21 - 313	0,09 - 1,0	14 - 361	0,06 - 1,0
	0,95	41 - 248	0,18 - 0,93	26 - 302	0,11 - 1,0	18 - 349	0,08 - 1,0
Iron	0,85	50 - 219	0,21 - 0,67	33 - 266	0,14 - 0,73	22 - 308	0,09 - 0,76
	0,81	45 - 198	0,19 - 0,59	30 - 241	0,13 - 0,64	21 - 280	0,09 - 0,67
Lead (217,0 nm)	0,96	53 - 264	0,23 - 1,01	35 - 318	0,15 - 1,0	24 - 365	0,10 - 1,0
	0,96	54 - 242	0,23 - 0,94	36 - 294	0,16 - 1,0	25 - 341	0,11 - 1,0
Lead (283,3 nm)	0,92	37 - 183	0,16 - 0,69	24 - 230	0,10 - 0,81	16 - 274	0,07 - 0,90
	0,88	34 - 177	0,15 - 0,63	23 - 223	0,10 - 0,73	15 - 265	0,07 - 0,79
Magnesium	1,00	37 - 286	0,16 - 1,0+	23 - 346	0,10 - 1,0+	15 - 396	0,07 - 2,0
Manganese	0,94	56 - 230	0,24 - 0,86	38 - 279	0,16 - 0,97	26 - 324	0,11 - 1,0
	0,92	31 - 238	0,13 - 0,83	19 - 292	0,08 - 0,93	13 - 338	0,06 - 0,99
Nickel	0,84	61 - 157	0,25 - 0,54	45 - 190	0,19 - 0,61	33 - 224	0,14 - 0,67
Zinc	0,93	53 - 282	0,23 - 0,95	34 - 336	0,15 - 1,0	23 - 383	0,10 - 1,0
	0,91	52 - 211	0,22 - 0,75	35 - 258	0,15 - 0,85	24 - 302	0,10 - 0,91

4.5 Discussion

There is no evidence in the chemical literature of any previous attempt to specify the component error functions associated with atomic absorption measurements, nor has there been any quantitative evaluation of the contribution of individual error functions to the composite function which is met with in practice. Such quantitative evaluation as is described in this chapter enables an assessment to be made of the importance of different sources of noise during atomic absorption measurement.

During the course of this work, techniques were developed by means of which the overall error functions could be analysed and quantitative weightings assigned to each contributing function. The only real problem encountered was the poor precision of the basic data themselves - the computed standard deviations - giving rise to the scatter of the points as observed, for instance, in figure 4.8. This is inherent in the very nature of the data as measured, and could be rectified only with integrating read-out equipment which was not generally available to the author.

The results obtained show very clearly the consistently large contribution from the TlogT component as indicated by the values of k_4. This confirms the generally accepted conclusion, based on other observations, that the flame is normally the most serious single source of noise in atomic absorption spectrometry. However, flame noise may be divided into three different components as indicated below; the investigations described in this chapter have shown which constituent part is the main contributor to atomic absorption noise.

(a) Flame emission noise, produced in the a.c. amplifier circuit due to the d.c. photocurrent

caused by emission from the flame. In this case, dT is constant (figure 4.6);

(b) flame absorption noise, caused by changes in the absorptivity of the flame gases, due in turn to fluctuating fuel flow rates and variations in the refractive index of the flame. Here, dT is proportional to T (see figure 4.5); and

(c) dynamic flame noise, due to changes in the flame path length or atomic population caused by fluctuations in flame temperature, efficiency of nebulization, or reducing properties of the flame. These factors produce the TlogT error function (figure 4.7).

The experimental results presented in this chapter have shown the last-mentioned noise source (c) to be the most significant component of the overall noise level.

As discussed in chapter 3, the effect of deviation from Beer's law on the precision of analysis is to superimpose, upon the existing error function, a second function whose magnitude increases (i) as the absorbance increases, and (ii) as the system deviates increasingly from Beer's law. This second function, the relative error ratio (equation 3.22) is shown graphically in figure 3.2. The net result of deviations from Beer's law is, therefore, an overall decrease in precision and a shortening of the dynamic working range, in terms of absorbance, for optimum precision. However, the working range in terms of multiples of sensitivity is less affected by such

deviation. As has been indicated above, the question of a generalized optimum working range is somewhat problematic. The range 50x - 200x the measured analytical sensitivity is likely to approximate, under most conditions, to that giving best precision in atomic absorption analysis. However, the limits of this range are, by their very nature, somewhat arbitrary and therefore somewhat flexible.

Chapter 5

INSTRUMENTAL FACTORS AND THEIR EFFECT ON PRECISION

Apart from the studies by Erdey and co-workers [16-18] and by Hermann and Lang [24] mentioned in the Introduction, no investigations into the effect of variations in instrumental conditions on atomic absorption precision appear to have been published. Instrumental settings normally employed are those corresponding to the most favourable sensitivity for a particular element; these conditions may not necessarily be those for optimum precision. It was therefore felt desirable that such an investigation be undertaken.

Other than the operating wavelength, five instrumental parameters may normally be varied by the operator. These are observation height, fuel:oxidant ratio, lamp current, amplifier gain and monochromator slit width. Of these, the observation height and fuel:oxidant ratio may be varied independently of each other and of all other parameters; however, lamp current, gain and slit width form a triad of which only two may be varied independently. The third member of this group must be adjusted in such a way as to give 100% transmittance at zero analyte concentration, and can therefore not be considered an independent variable.

5.1 Interrelationship between slit width, amplifier gain and lamp current

In order to minimize the number of factors contributing to the overall noise level, the combined effect of gain and slit width was evaluated under conditions which did not involve aspiration of sample solutions; that is, at 100%

transmittance (distilled water aspirated) and zero transmittance (lamp offset from optical path). The slit width was varied from 0,5 mm to 0,03 mm, and the gain adjusted to give 100% transmittance at the operating wavelength of the element concerned. The lamp current was maintained at a constant value of between 5 mA and 10 mA, and a lean flame was used with an observation height of 1,0 cm. After obtaining forty-eight readings of the transmittance, the lamp was rotated out of the optical path, and a further forty-eight readings obtained without altering any of the other instrumental settings. Standard deviations were then calculated for each set of forty-eight readings. Results for the elements calcium, chromium, cobalt, copper, iron, lead (217 nm and 283 nm), magnesium, manganese, nickel and zinc were obtained in this way, and are shown in Table 5.1 and figure 5.1. From these results it is clear that increasing the gain has no noticeable effect until a setting of 9 or 9,5 is reached - a setting which is not normally used in practice. This means, in turn, that a very wide range in amplifier gain is available to the analyst without any risk of adversely affecting the precision of measurement.

Similar readings were obtained at 100% T for the effect of lamp current on precision: using a fixed slit width of 0,1 mm, lamp current was varied over the range 4 mA to 20 mA, but within the general restriction that the gain setting should not exceed 8,5; in this way, any significant variation in standard deviation could be attributed to the effect of lamp current alone. The results are given in Table 5.2 and indicate that an increase in lamp current above ca. 10 mA generally has

T A B L E 5.1(a)

Effect of gain on precision (dT) at 100% transmittance

Gain Setting	Normalized* standard deviations at 100% transmittance										
	Ca	Cr	Co	Cu	Fe	Pb 217	Pb 283	Mg	Mn	Ni	Zn
1,0 - 1,9	1,60	1,14		1,33	1,19		1,07	1,00		1,06	
2,0 - 2,9	1,27	1,29	1,00	1,00	1,19		1,00	1,06	1,25	1,06	1,23
3,0 - 3,9	1,00	1,14	1,00	1,10	1,14		1,22	1,12	1,00	1,06	1,33
4,0 - 4,9	1,53	1,00		1,24	1,00		1,00	1,24	1,17	1,00	1,07
5,0 - 6,9	1,47		1,42		1,24	1,13	1,14	1,00	1,42		1,23
7,0 - 8,9		1,21	1,42	1,67		1,00		1,18	1,50	1,06	1,00
9,0 - 9,9		1,36			1,68	1,07	1,93			1,47	1,10
9,9 +			3,17			2,54			2,25		

* All values normalized to an arbitrary minimum value for each element of 1,00

T A B L E 5.1(b)

Effect of gain on precision (dT) at 0% transmittance

Gain Setting	Standard deviations at 0% transmittance, x 10^3										
	Ca	Cr	Co	Cu	Fe	Pb 217	Pb 283	Mg	Mn	Ni	Zn
1,0 - 1,9	0,4	0,5	0,5	0,5	0,5		0,3	0,5		0,5	
2,0 - 2,9	0,6	0,5	0,4	0,5	0,3		0,4	0,5	0,5	0,1	0,7
3,0 - 3,9	0,5	0,5	0,3	0,3	0,5		0,5	0,5	0,4	0,4	0,4
4,0 - 4,9	0,5	0,3		0,4	0,4		0,5	0,5	0,4	0,5	0,4
5,0 - 6,9	0,4		0,4		0,3	0,4	0,4	0,6	0,4		0,5
7,0 - 8,9		0,5	0,4	0,8		0,5		0,4	0,6	0,3	0,4
9,0 - 9,9	0,7	0,7		1,0	0,5	0,6	0,6			0,4	0,5
9,9 +			0,5			1,1			0,9		

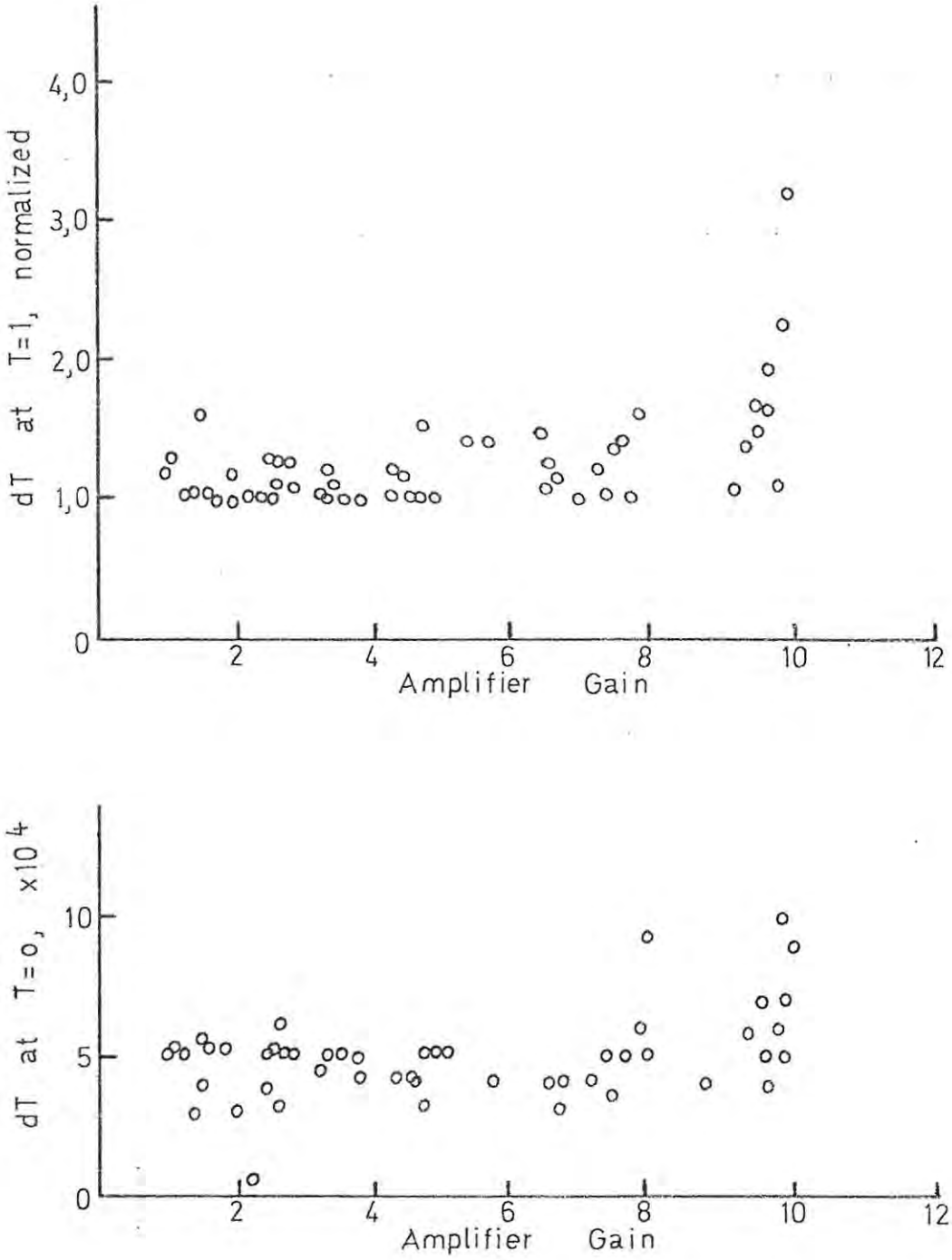

Figure 5.1. Effect of amplifier gain on precision, expressed as the standard deviation dT.

a negligible effect on precision, but lower lamp currents tend to give rise to poor precision.

T A B L E 5.2

Effect of lamp current (in mille-amperes, mA) on precision (dT) at 100% transmittance

Cobalt		Chromium		Iron		Manganese		Nickel	
mA	dT	mA	dT	mA	dT	mA	dT	mA	dT
5	0,0025	5	0,0023	4	0,0023	4	0,0014	5	0,0020
10	0,0020	10	0,0016	8	0,0015	8	0,0011	10	0,0015
15	0,0014	15	0,0019	12	0,0012	12	0,0012	15	0,0015
18	0,0014	18	0,0020	16	0,0009			18	0,0018

Apart from any possible effect of lamp current directly on the extent of variation in lamp output, a further important factor must be borne in mind - the influence of lamp current on calibration curvature. In chapter 3 it was shown that the adverse effect of increasing curvature could be quantitatively expressed by the relative error ratio (equation 3.22). A brief investigation was therefore conducted into the effect of lamp current on calibration curvature. Using a fixed slit width of 0,1 mm, lamp current was varied as described previously and standard solutions of the analyte were aspirated under constant conditions. The extent of deviation from Beer's law was evaluated by computer, and is shown in Table 5.3, where the values of $\underline{h}$ indicate the extent to which Beer's law is obeyed under given conditions.

T A B L E 5.3

Effect of lamp current (mA) on calibration curvature (h)

Cobalt		Chromium		Iron		Manganese		Nickel	
mA	h	mA	h	mA	h	mA	h	mA	h
5	0,77	5	0,78	5	0,82	3	0,93	5	0,79
10	0,76	10	0,80	10	0,76	6	0,93	10	0,60
15	0,69	15	0,80	15	0,75	9	0,91	15	0,62
18	0,66	18	0,79	18	0,71	12	0,90	18	0,58

5.2 Effect of fuel flow rate and observation height

In order to investigate the effects of observation height and fuel flow rate on precision, a different approach to that described above was employed. Observation height was varied from 0,3 cm to 1,5 cm in steps of 0,3 cm; different fuel flow rate settings corresponded to a lean flame (1200 cm^3/min), stoichiometric conditions (1600 cm^3/min), a slightly rich flame (2000 cm^3/min), and a luminous flame (2400 cm^3/min). The air flow rate was maintained at 5 dm^3/min throughout. For each element, therefore, twenty sets of conditions were employed.

For each of the elements investigated, a series of aqueous standard solutions was prepared covering the range from approximately 10x to 2000x the optimum analytical sensitivity. Concentrations of successive solutions were in the ratio of $1 : \sqrt{2}$. The transmittance of each of five of these standard solutions was measured under given instrumental conditions,

the solutions being so chosen as to cover the range from 1,0 to 0,2 transmittance in approximately equal steps, wherever possible. Twenty readings of transmittance were then made on a further solution of the element concerned; the solution chosen had a concentration of between 50x and 100x the observed sensitivity, since this was the region found previously to give a constant, minimum relative error (see chapter 4, and especially figure 4.9). The results were fed to an IBM 1901 computer which was programmed to calculate the values of h and ab (chapter 3), the standard deviation in terms of both transmittance (dT) and concentration (dc), and the per cent relative error (dc/c). The results for a given element (twenty different instrumental settings) were normalized by the computer, and finally average normalized values for all the elements, taken together, were obtained for each different set of instrumental conditions. The results obtained for chromium and zinc are shown in Tables 5.4 and 5.5; the overall averaged results are given in Table 5.6.

5.3 Error function in double-beam instrumental systems

During a brief visit to the laboratories of Pye Unicam Limited in Cambridge, England, it was possible to study the form of the error function(s) to be expected from a double-beam atomic absorption spectrometer. As before, aqueous calibration standards covering the absorbance range 0,0 - 1,0 (approximately) were prepared for several elements. The solutions were aspirated using the recommended instrumental settings for the element concerned (Table 5.7), and integrated absorbances (4 second integration time) were digitally displayed. Standard deviations were calculated from 20 replicate readings for each solution, and the

T A B L E 5.4

Effect of instrumental conditions* on precision and line curvature - chromium

Calculated values of dT

0,0019	0,0031	0,0024	0,0020
0,0038	0,0032	0,0027	0,0034
0,0050	0,0047	0,0033	0,0028
0,0065	0,0052	0,0044	0,0042
0,0068	0,0080	0,0055	0,0042

Calculated values of dc/c

1,30	7,34	5,28	2,77
2 04	1,90	1,75	1,93
2,21	1,80	1,60	1,06
3,03	2,38	1,76	1,69
3,86	3,16	2,16	1,56

Calculated values of h

0,54	0,45	0,35	0,26
0,70	0,73	0,68	0,69
0,70	0,78	0,76	0,80
0,61	0,79	0,78	0,81
0,50	0,78	0,79	0,82

* From left to right, fuel flow rate = 1200; 1600; 2000; 2400 cm^3/min, respectively.

* From top to bottom, observation height = 0,3; 0,6; 0,9; 1,2; 1,5 cm, respectively.

T A B L E 5.5

Effect of instrumental conditions* on precision and line curvature - zinc

Calculated values of dT

0,0041	0,0030	0,0023	0,0023
0,0039	0,0032	0,0021	0,0027
0,0026	0,0028	0,0023	0,0025
0,0022	0,0024	0,0024	0,0027
0,0024	0,0020	0,0025	0,0021

Calculated values of dc/c

1,64	1,41	1,23	1,10
1,63	1,23	0,89	1,09
0,89	0,93	0,88	0,87
0,76	0,82	0,83	0,89
0,82	0,69	0,89	0,71

Calculated values of h

0,76	0,77	0,76	0,75
0,82	0,80	0,81	0,79
0,84	0,85	0,85	0,84
0,86	0,86	0,85	0,85
0,86	0,86	0,84	0,85

* From left to right, fuel flow rate = 1200; 1600; 2000; 2400 cm^3/min, respectively.

* From top to bottom, observation height = 0,3; 0,6; 0,9; 1,2; 1,5 cm, respectively

T A B L E 5.6

Mean overall normalized values for dT, dc/c, and h

Normalized values for dT

1,06	1,11	0,88	1,07
1,10	1,04	1,00	1,21
0,91	0,92	0,89	1,04
0,93	1,04	0,92	0,94
1,16	0,97	0,86	0,99

Calculated values of dc/c

1,20	1,88	1,37	1,63
0,98	0,96	1,10	1,16
0,77	0,76	0,75	0,88
0,79	0,85	0,76	0,78
1,06	0,81	0,71	0,79

Calculated values of h

0,86	0,82	0,78	0,73
0,94	0,93	0,91	0,90
0,95	0,97	0,97	0,96
0,95	0,98	0,98	0,98
0,93	0,98	0,98	0,98

Variations in fuel flow rate and observation height as in Tables 5.4. and 5.5.

contributions of individual error functions computed as outlined previously (section 4.3).

The results are displayed in two different ways in figures 5.2 and 5.3. In the former, the standard deviation in absorbance, dA, is plotted as a function of absorbance, while the latter shows the dT vs T behaviour for the calculated composite error function, for several of the elements examined. These results show quite clearly the considerable contribution made by the TlogT - type error function to the overall noise pattern. [If $dT \propto T\log T$, then $dA \propto A$; hence a linear plot of dA vs A is indicative of a large TlogT contribution.] It is clear from figures 5.2 and 5.3 that other forms of the individual error function also are present, but that their contribution is far less important over the normal working range of concentration or absorbance than is that from the TlogT function. At or near the detection limit, this state of affairs is reversed. The computed values of the individual contributions are given in Table 5.8, in the form of the values of the constants k_1 - k_4 as previously defined.

T A B L E 5.7

Operating conditions for several elements

	Obs. ht. cm	Fuel flow cm^3/min	Slit width mm
Calcium	1,0	1200	1,0*
Chromium	0,8	1400	0,1
Copper	0,8	1000	0,1
Magnesium	0,7	1000	0,1
Nickel	0,5	1200	0,1
Zinc	0,7	1000	0,2

* Large value used in order to test for flame emission noise.

T A B L E 5.8

Contributions to double-beam composite error function

	k_1 $dT \propto T$	k_2 dT const.	k_3 $dT \propto \sqrt{T}$	k_4 $dT \propto T\log T$
Calcium	0,00	0,0009	0,00	0,0022
Chromium	0,00	0,0018	0,0007	0,0043
Copper	0,00	0,0019	0,00	0,0063
Magnesium	0,0005	0,00	0,0008	0,0020
Nickel	0,0013	0,0019	0,0008	0,0028
Zinc	0,0020	0,00	0,00	0,0049

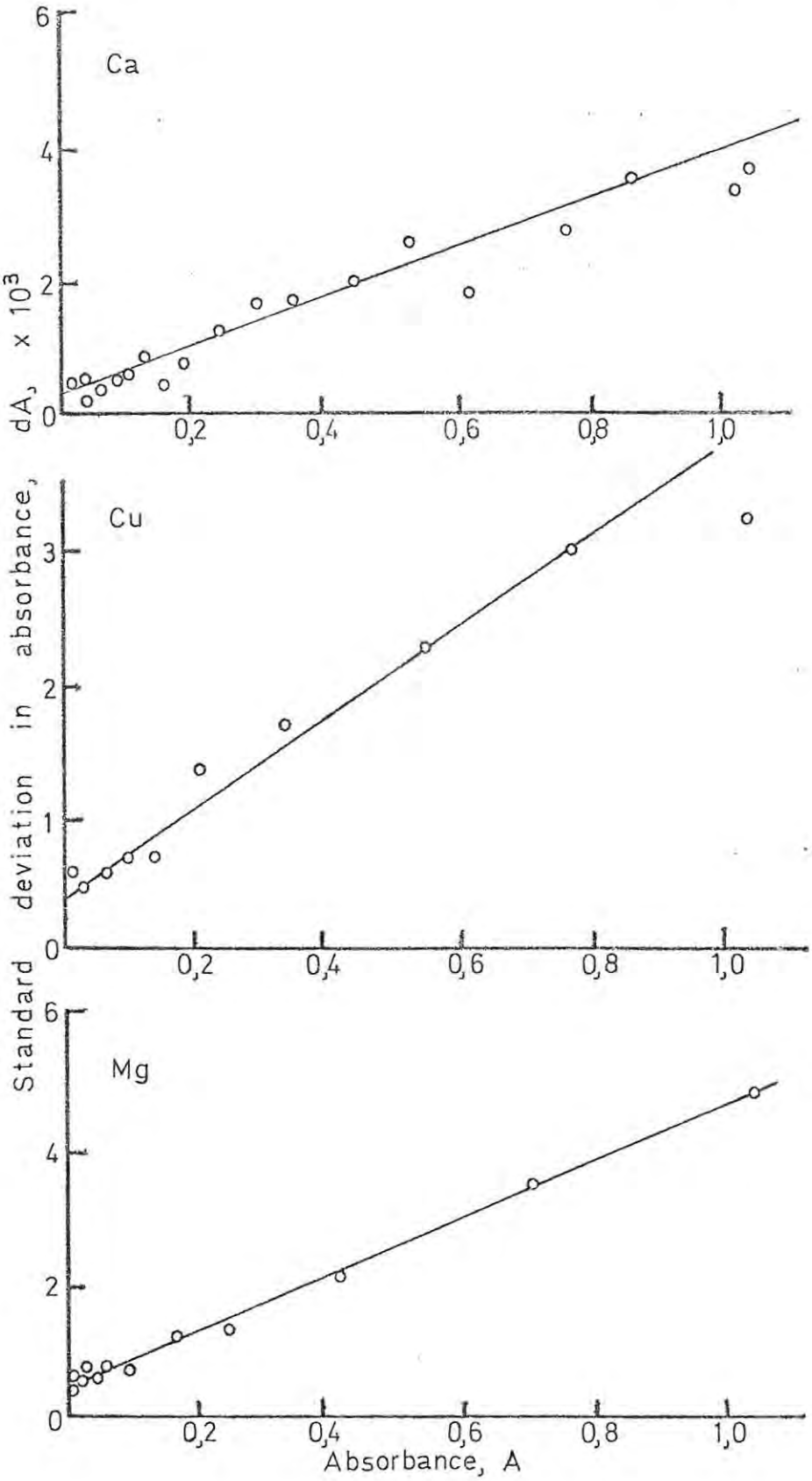

Figure 5.2. Plots of dA vs A for several elements; double-beam operation.

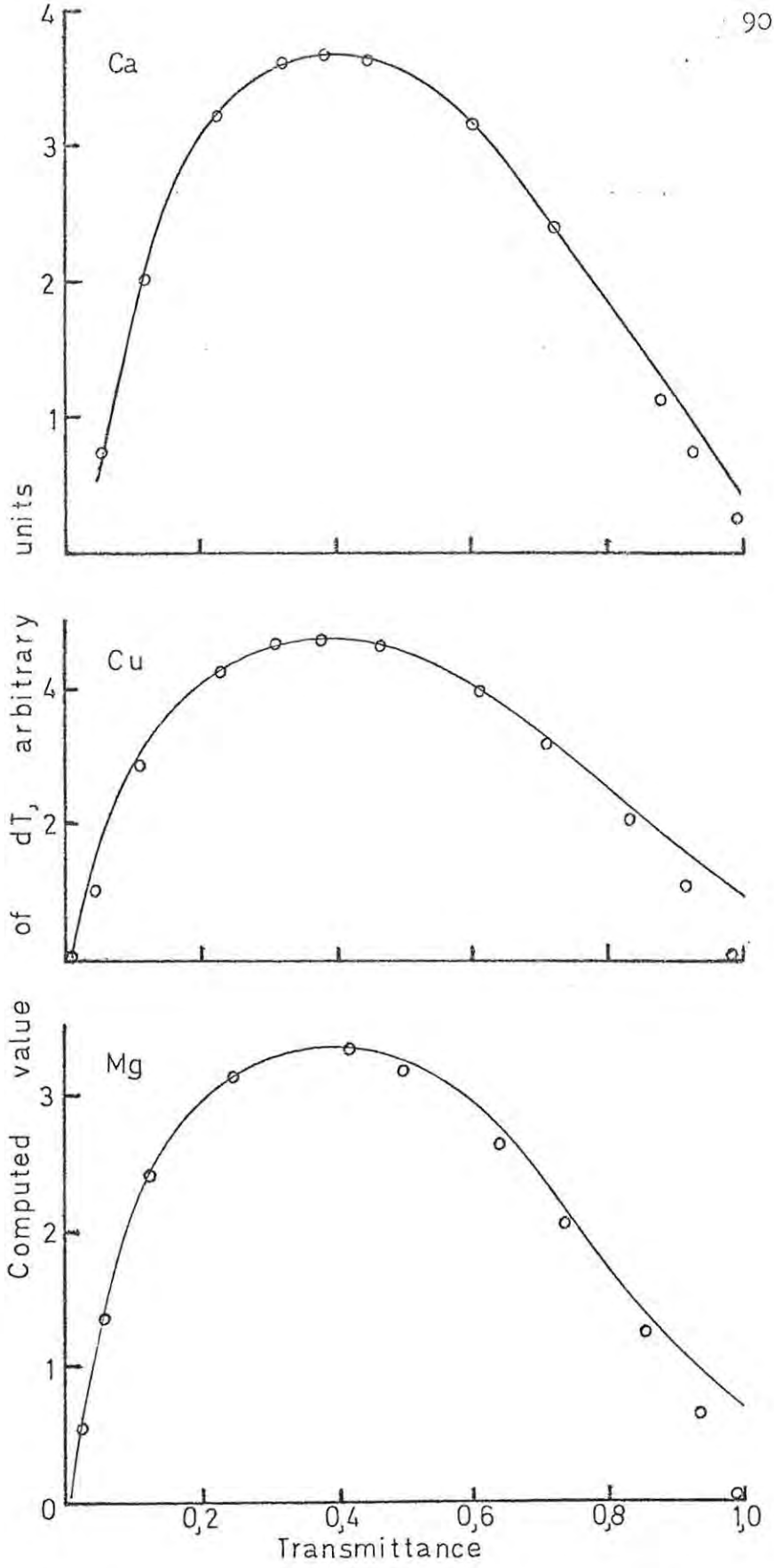

Figure 5.3. Calculated error function curves (dT vs T) for double-beam operation, compared with pure TlogT plots (o).

5.4 Precision and the sample matrix

The investigations reported thus far in this chapter were performed with simple aqueous solutions of the elements concerned - either in pure water or very dilute acid. In order to assess the effect, on precision, of the presence of the sample matrix, standard deviations were measured for synthetic solutions corresponding to samples of cement (largely a matrix of calcium and silica) with and without added lanthanum, steel (a matrix of iron) with and without addition of a releasing agent for chromium, and fruit juice (a matrix of soluble organic species including citric acid and sugar). A solution containing a matrix of lanthanum ion only (as the chloride) with added trace metals was also used in the investigation.

The composition of the different solutions is summarized in Table 5.9; the results, each calculated from forty-eight separate readings of transmittance, are shown in Table 5.10.

5.5 Discussion

The combined effect of changes in gain and slit width settings was measured at 100% transmittance and zero transmittance for each element studied, as described in section 5.1. At 100% transmittance electronic noise, which gives rise to error functions of the form $dT \propto T$ and $dT \propto T$, is at its maximum value.

Any significant change in the electronic contribution to noise would therefore noticeably change the level of fluctuation at 100% transmittance. That such a change did not occur until very high values of the amplifier gain setting were reached ($\sim 9,5$) indicates that the overall electronic contribution to

T A B L E 5.9

Sample matrices

Sample	Approximate composition
Cement	2000 $\mu g/cm^3$ Ca + 1000 $\mu g/cm^3$ SiO_2
Cement + lanthanum	As above + 0,5 g% La^{3+} as chloride
Fruit juice	1 g% citric acid
Steel	0,5 g% iron in H_2SO_4/H_3PO_4
Steel + magnesium sulphate	As above + 2,5 g% $MgSO_4$
Lanthanum	0,5 g% La^{3+} as chloride

T A B L E 5.10

Effect of sample matrix on precision for several elements

Type of matrix	dT for individual elements			
	Cr	Fe	Ni	Zn
-	0,0031	0,0023	0,0020	0,0022
Cement		0,0021		0,0019
Cement + La^{3+}		0,0023		0,0023
La^{3+} only		0,0020		0,0019
Fruit juice		0,0022		0,0021
Steel	0,0029		0,0024	
Steel + $MgSO_4$	0,0032		0,0020	

noise must be fairly small. The bulk of the fluctuation at 100% transmittance must therefore be caused either by lamp fluctuations or by flame (absorption) noise, both of which would give rise to

a $dT \propto T$ error function. Evaluation of standard deviations with and without the flame lit showed clearly (Table 5.11) that lamp noise is the major contributor to the fluctuations normally observed at 100% transmittance except in the case of zinc and, possibly, lead. It is to be expected, therefore, that the use of a double-beam atomic absorption spectrometer would lead to a considerable improvement in the precision here. That this is indeed the case is clear from the results (Table 5.8) for a double-beam system. Although these data are not directly comparable with, for instance, those given in Tables 4.1 and 4.2. because of differences in instrumentation (such as integration time), nevertheless the "$dT \propto T$" contribution appears to be substantially reduced in double-beam operation. The only significant exception is zinc which, because of the low wavelength of the zinc resonance line (213,9 nm), is subject to flame absorption noise whether single-beam or double-beam optics are employed. As a result of this general decrease in the $dT \propto T$ contribution, the composite error functions obtained during double-beam operation have approximated fairly closely to a TlogT function.

T A B L E 5.11

Standard deviations at 100% transmittance with and without flame

Element	Operating Wavelength nm	Standard deviation	
		Flame	No Flame
Calcium	422,7	0,0011	0,0011
Copper	324,8	0,0011	0,0014
Iron	248,3	0,0024	0,0018
Lead	217,0	0,0018	0,0010
Lead	283,2	0,0023	0,0013
Magnesium	285,2	0,0013	0,0014
Manganese	279,5	0,0016	0,0014
Zinc	213,9	0,0042	0,0011

The only error function contributing significantly to the noise level at zero transmittance is dT = a constant; this can be caused by flame (emission) noise, fluctuations in dark current, or other residual electronic fluctuations such as amplifier noise. Since the standard deviation at zero transmittance remained effectively constant despite changes in gain and slit width (which would be directly related to the flame emission noise), the observed fluctuations could be due to dark current variations. However, the effect is small enough as to be unimportant, the observed standard deviations being of the order of one 20th of one per cent transmittance, and may equally well be due to insufficient resolution on the part of the digital voltmeter which displayed transmittance values to only the third significant figure.

Table 5.6 shows the "average" effect which changes of fuel flow rate and observation height exert upon the precision of measurement and upon calibration curvature. Reference to this table indicates that there is very little overall difference in standard deviation (in terms of transmittance), no matter which set of conditions is used; with only one exception (a lean flame, observation height set at 1,5 cm) does the normalized value of dT differ from the average value by more than 14%. The values of the relative error, however, reveal a much larger divergence, varying from 0,69 to 1,98 (relative to a mean value of 1,00). The condition giving rise to a higher relative error is primarily a low observation height (0,3 - 0,6 cm). Inspection of Table 5.6 reveals that this is the same condition giving rise to larger deviations from Beer's law (smaller value of $\underline{h}$), so that changes in relative error are dictated largely by variations in the degree

of conformity to Beer's law. It is therefore calibration graph curvature which, to a large extent, determines the magnitude of the relative error.

In work previously published by the present author [55, 65] it was shown that interference effects, generally speaking, are more severe (i) in fuel-rich flames, and (ii) when the observation height is small; these observations were attributed to less complete volatilization of the sample material under such conditions. This suggestion finds apparent confirmation in the observed variations in the values of h reported in Tables 5.4 - 5.6 : when the observation height is small or, to a lesser extent, when the flame is fuel-rich, a greater degree of bending of the analytical curve is observed and shows itself in a lower value for h. This is also seen very clearly in the results presented for manganese (Table 5.12). Under normal conditions, as discussed in

T A B L E 5.12

Dependence of line curvature on instrumental conditions for manganese

Calculated values of h			
0,68	0,57	0,58	0,52
0,88	0,78	0,68	0,62
1,00	0,98	0,96	0,77
1,00	1,00	1,00	0,94
1,00	1,00	1,00	1,00

Variations in fuel flow rate and observation height as in Tables 5.4 and 5.5.

chapter 3, incomplete volatilization should not be noticeable unless interfering ions also are present. However, in the course

of a survey such as is reported in this chapter, a wide range of different instrumental settings has been employed. Several combinations of observation height and fuel:oxidant ratio give rise to extremely poor sensitivity for some elements such that solution concentrations of six or seven hundred $\mu g/cm^3$ (or more) are necessary before the absorbance reaches a value of 0,6 - 0,8. It is under such conditions that these elements exhibit significant line curvature due to incomplete volatilization. This is not inconsistent with the results presented in chapter 3.

A further trend in the variation of $\underline{h}$ is apparent when considering those elements - particularly calcium and chromium - which readily form oxides in the flame, namely a decrease in the value of $\underline{h}$ in a lean flame at larger observation heights. The values for chromium are shown in Table 5.4. For such elements, partial oxidation of the atoms in the flame before passing through the observation zone causes a serious deterioration in sensitivity higher in the (lean) flame. This necessitates the use of larger analyte concentrations in the aqueous solution; together with the expected decrease in flame temperature, this will completely offset the advantage of working at a larger observation height.

Generally speaking, therefore, best analytical precision is attained under the following instrumental conditions:

(i) a lamp current of about 10 mA, provided this does not exceed the permissible maximum for the cathode material employed, or less;

(ii) an observation height of 0,9 - 1,2 cm and a a fuel flow rate of 2000 cm^3/min, corresponding to an acetylene:air ratio slightly richer than that for a stoichiometric flame;

(iii) a slit width of less than 0,1 mm - preferably about 0,05 mm, provided that this does not necessitate a gain setting of greater than 9.

It must be emphasized that these are generalized settings, and some individual elements (e.g. chromium; see Table 5.4) require analytical conditions which differ significantly from the "average". Of considerable interest is the fact that small lamp currents give rise to poor precision but less significant calibration curvature than lamp currents of 10 - 15 mA.

Chapter 6

SOLVENT EXTRACTION - A COMPARATIVE STUDY OF PRECISION

Solvent extraction is well-known as a useful adjunct in atomic absorption analysis, and has been used, inter alia, in the analysis of brine [72], blood and urine [73], fine chemicals [74], biological materials [75], and foodstuffs [76]. Groenewald [77] has recently summarised the effect, upon results obtained by analytical techniques involving solvent extraction, of such factors as the mutual solubility of the solvents, the solvent volume ratio, and the ionic strength of the aqueous phase, and has indicated the magnitude of the errors which may arise in different cases.

The main advantages of solvent extraction procedures are:

(i) the separation of traces of the analyte from the bulk of the sample matrix;

(ii) separation of the analyte from interfering ions which may be present in the sample; and

(iii) increased atomic absorption response due both to an increased concentration of analyte in the organic layer and to the so-called "organic solvent effect".

Although solvent extraction has been much used in conjunction with atomic absorption analysis, very little attention has been given to the effect which a solvent extraction step has on the precision of analysis vis-à-vis direct analysis of the aqueous solution itself. The work described in this chapter was undertaken in order to obtain information which could assist the analyst in deciding whether or not to use solvent extraction

in a particular situation from the point of view of analytical precision. Naturally, there may be other, possibly overriding, factors which would also have to be considered.

6.1 Apparatus and reagents

Stock solutions of copper and lead (1000 $\mu g/cm^3$ each in very dilute perchloric acid) were prepared from the pure metals. These solutions were further diluted as required.

Reagent solution: 10 g of diethylammonium diethyldithiocarbamate (DDDC) were dissolved in 1,0 dm^3 of analytical reagent grade amyl acetate. This solution was stored in an amber bottle and dispensed by means of an all-glass repetitive pipette (supplied by Labindustries, California, U.S.A.).

Buffer solution, pH4 : analytical reagent grade sodium acetate (25 g) and sodium chloride (50 g) were dissolved in about 200 cm^3 of water, the pH adjusted to between 4 and 4,5 with analytical reagent grade hydrochloric acid, and the solution transferred to a separating funnel (500 cm^3 capacity). The mixture was then extracted with two separate 20 cm^3 portions of a solution of DDDC in chloroform (1% w/v) and finally with 20 cm^3 of pure amyl acetate. The lower aqueous layer was run into a 250 cm^3 volumetric flask, and the solution diluted to volume with water.

During the extractions described in this chapter, separation of the organic and aqueous phases was hastened by centrifugation. For ease of operation, special centrifuge tubes were constructed from "pyrex" glass. These had a total capacity of 55-60 cm^3, and were provided with a narrow neck (1,5 cm internal diameter) so that even a small volume of extractant (e.g., 2 cm^3) formed a layer about 1 cm deep in the neck, greatly

facilitating aspiration of the organic layer. The centrifuge tubes were fitted with interchangeable ground glass stoppers.

6.2 Choice of solvent

Currently, the organic solvent most widely used in atomic absorption analysis is iso-butyl methyl ketone. However, this solvent is relatively soluble in water (1,9 g per 100 cm^3), and is therefore not particularly useful when the ratio of aqueous phase to organic phase is large. Amyl acetate, on the other hand, has a solubility in water of 0,16 - 0,18 g per 100 cm^3, and is readily available in analytical reagent grade quality as a mixture of iso-amyl and n-amyl isomers. At the same time, the burning properties of amyl acetate in an atomic absorption flame are as favourable as those of iso-butyl methyl ketone. Table 6.1 shows the effect of differing volumes of aqueous phase on the concentration of copper extracted into the organic phase, for both iso-butyl methyl ketone and amyl acetate. As can be seen, because of the greater aqueous solubility of iso-butyl methyl ketone, there is a considerable volume ratio effect using this solvent.

TABLE 6.1

Volume-ratio effects for iso-butyl methyl ketone and amyl acetate

Aqueous volume cm^3	Organic solution added, cm^3	Ratio Aq./Org.	iso-Butyl methyl ketone		Amyl acetate	
			Absorbance	Cu recovery*,%	Absorbance	Cu recovery*,%
25	5	5,0	0,370	100	0,268	100
50	5	10,0	0,400	108	0,281	105
100	5	20,0	0,545	147	0,290	108
200	5	40,0	2,0	550	0,293	109

* Relative to absorbance for sample extracted from 25 cm^3 aqueous solution.

Before adopting amyl acetate as the preferred solvent for extraction studies, it was necessary to confirm that the organic extracts were sufficiently stable, and that there would not be a change in the analyte absorbance (in the flame) with time. Different 40 cm^3 portions of the same copper solution (1,0 $\mu g/cm^3$) were extracted with 5 cm^3 portions of DDDC reagent solution over the course of a normal working day. One set of such extracts was placed in a dark cupboard immediately after extraction; a second, equivalent set was placed near a window in the laboratory (but not in direct sunlight). The copper in each organic layer was measured immediately after the final extraction had been performed. In this way, readings were obtained for solutions stored either in the dark or in relatively bright daylight for periods of up to six hours.

In neither case was there any detectable difference in the copper concentrations of any of the extracted samples. Identical results were obtained for the extraction of lead.

These results indicate that extraction of both copper and lead into amyl acetate using DDDC reagent produces organic phases which are stable for at least six hours in bright daylight. Hence no precautions to shield extracted samples from normal laboratory light are required.

Amyl acetate was therefore selected as solvent for this investigation, and was used as the analytical reagent grade material without further purification.

6.3. Results

6.3.1. Precision of aqueous measurement

Copper solutions containing 0,05; 0,1; 0,2; 0,5 and 1,0 $\mu g/cm^3$ of the metal, and solutions of lead containing 0,25;

0,50; 1,0; 2,5 and 5,0 $\mu g/cm^3$ of lead, respectively, were aspirated eleven times under normal working conditions (see Table 6. 2); ten values of the absorbance were read off the digital voltmeter each time and averaged to obtain the mean absorbance for each separate aspiration. These mean absorbance values were then used to calculate the standard deviation of measurement for each solution aspirated. These are given in Table 6.3, which also shows the coefficients of variation for the respective solutions.

T A B L E 6.2

Conditions for determining copper and lead

Parameter	Copper	Lead
Wavelength, nm	324,8	283,3
Slit width, mm	0,1	0,1
Observation height, cm	0,8	0,8
Acetylene flow (aqueous solvent)	1200 cm^3/min	1200 cm^3/min
Acetylene flow (organic solvent)	700 "	900 "

T A B L E 6.3

Precision of measurement of aqueous solutions

Copper			Lead		
Concn. $\mu g/cm^3$	Standard deviation $\mu g/cm^3$	Coefficient variation, %	Concn. $\mu g/cm^3$	Standard deviation $\mu g/cm^3$	Coefficient variation, %
0,05	0,0085	17	0,25	0,055	22
0,1	0,0089	8,9	0,5	0,038	7,6
0,2	0,0088	4,4	1,0	0,067	6,7
0,5	0,011	2,2	2,0	0,042	2,1
1,0	0,011	1,1	5,0	0,045	0,9

6.3.2 Repeatability measurements on extracted samples

Ten x 40 cm^3 samples of each of the solutions used in section 6.3.1 were extracted with 2,5; 5,0 and 10,0 cm^3 portions of the reagent solution after adjustment of the pH to 4. The mean absorbance for copper and lead was determined for each extract; standard deviations were then calculated for each set of ten extracted samples for every original solution. The results are tabulated in Table 6.4.

In order to be able to calculate detection limits for copper determined after extraction, the standard deviation for the blank (0,00 $\mu g/cm^3$ level) was calculated from the results for ten replicate blank extractions, using both 2,5 and 5,0 cm^3 portions of the reagent. Buffer solution (pH = 4) was added as before. For copper, the standard deviations obtained were 0,00088 absorbance units (for 5,0 cm^3 of organic reagent) and 0,0011 units (for 2,5 cm^3 of organic reagent); for copper in the aqueous solutions, the standard deviation at the blank level was found by extrapolation to be 0,00021 absorbance units. The corresponding figures for lead were 0,0012 (for 5,0 cm^3 extractant), 0,0007 (for 2,5 cm^3 extractant), and 0,0009 (aqueous solution).

6.4 Discussion

The effect of introducing a solvent extraction step on the overall efficiency of atomic absorption analysis can conveniently be discussed under four different headings, viz. sensitivity, detection limit, precision, and convenience.

6.4.1 Sensitivity

The sensitivity of the determination is improved in proportion to the ratio aqueous phase : organic phase in the system.

T A B L E 6.4

Precision for extracted samples

Copper concn.* $\mu g/cm^3$	Coefficient of variation, %, for copper extracted into:		
	10,0 cm^3 of reagent solution	5,0 cm^3 of reagent solution	2,5 cm^3 of reagent solution
0,05	-	7,7	10,0
0,10	2,6	4,4	5,0
0,20	1,8	2,6	2,5
0,50	1,3	2,3	2,1
1,00	1,0	1,3	-
Concn. factor	x 4	x 8	x 16

Lead concn.* $\mu g/cm^3$	Coefficient of variation, %, for lead extracted into:		
	10,0 cm^3 of reagent solution	5,0 cm^3 of reagent solution	2,5 cm^3 of reagent solution
0,25	-	7,3	1,3
0,50	2,6	3,3	6,1
1,00	2,6	2,4	3,2
2,00	1,3	2,4	3,5
5,00	1,3	1,2	-
Concn. factor	x 4	x 8	x 16

*Concentration in the aqueous solution (40 cm^3) prior to extraction.

An additional improvement by a factor of 2 - 2,5 is obtained through the so-called "organic solvent effect". This effect has been carefully studied by Elwell and Gidley [78], who have shown it to be due largely to more efficient nebulization of the sample solution and not, as has at times been suggested, to an increased up-take rate of the organic solution. The overall result has been an improvement in sensitivity of approximately 10x, 20x and 40x for 10 cm^3, 5 cm^3 and 2,5 cm^3 of organic extractant, respectively.

6.4.2 Detection limit

The values for detection limit arrived at on the basis of the definition given in the Introduction indicate that solvent extraction techniques lower the detection limit significantly, although perhaps not to the extent expected. The limit of detection found for aqueous copper solutions aspirated directly is of the order of 0,016 $\mu g/cm^3$; extraction methods lead to values of about 0,002 $\mu g/cm^3$ (for 5 cm^3 reagent) and 0,001 $\mu g/cm^3$ (for 2,5 cm^3 reagent), an improvement of up to 16-fold. The corresponding detection limits for lead are 0,02 $\mu g/cm^3$ (5 cm^3 reagent), 0,006 $\mu g/cm^3$ (2,5 cm^3 reagent), and 0,08 $\mu g/cm^3$ (aqueous solution). Extraction thus leads to an improvement in the detectibility of lead by a factor of 14. It should be noted that, for the purpose of establishing detection limits in the solvent extraction method, the standard deviation of the background was calculated from the results for ten separate blank extractions, and not from the background fluctuations for one sample read ten times as was done in the case of the aqueous solutions. Similarly, in measuring the analytical precision, standard deviations for extraction were calculated from the results for replicate extractions, whereas

the aqueous standard deviations were computed from replicate readings on the same sample. In this way, allowance could be made for the additional operation necessitated by introducing a solvent extraction step.

6.4.3 Precision

Reference to Tables 6.3 and 6.4 shows the effect which extraction has on the precision of analysis. In either case - organic extract or aqueous solution - the coefficient of variation shows a general decrease as the concentration of analyte increases. Of particular importance, however, is the fact that the coefficient of variation for the organic extracts is significantly lower, at lower concentrations, than for direct aqueous analysis. For copper, this gives rise to a cross-over point in the region 0,5 - 1,0 $\mu g/cm^3$: at concentrations greater than 1,0 $\mu g/cm^3$, aqueous solutions show slightly more favourable coefficients of variation than those subjected to prior extraction. The corresponding cross-over point for lead occurs at about 2,0 $\mu g/cm^3$.

Expressed differently, the cross-over point in either instance occurs when the metal-ion concentration (in the aqueous solution) has a value of approximately 5 - 10 x the measured analytical sensitivity in units of $\mu g/cm^3$ per 1% absorption.

6.4.4 Convenience

Introduction of an extraction process naturally prolongs the time taken for the analysis. However, the fact that this type of work may be performed, from start to finish, in a single centrifuge tube means that the whole operation may be performed relatively rapidly. Centrifugation can be used to advantage to accomplish the rapid separation of the two phases, so that the

time required for the extraction is reduced to a minimum. At the same time, the whole operation becomes extremely simple and straightforward, and the dangers of contamination and loss of sample material are virtually excluded. The use of organic solvents which are lighter than water, such as iso-butyl methyl ketone or amyl acetate, means that the organic layer may be aspirated directly from the centrifuge tube without any need to separate the phases physically from one another.

Solvent extraction methods may thus be used to advantage in the determination of traces of metals by atomic absorption spectrometry. Not only are the detection limit and sensitivity considerably improved by extraction, but the precision of measurement is increased significantly when the analyte concentration before extraction is less than about 5x - 10x the sensitivity of the analyte as measured in aqueous medium.

Chapter 7

ANALYTICAL PRECISION IN ATOMIC ABSORPTION SPECTROMETRY

In order to assess the potential of atomic absorption spectrometry for the analysis of real samples - as opposed to synthetically-prepared aqueous solutions - procedures were devised for the analysis of several materials with widely differing properties and drawn from various areas of industrial analysis. The accuracy of the methods was established by analysing a number of internationally-recognised standard samples, or by comparison with other acceptable methods where standard samples were not available; recovery investigations were also performed. The precision of each method was ascertained by replicate analysis. The materials selected for analysis were cement, steel and cast iron, and fruit juice. Each of these contains a number of elements susceptible to determination by atomic absorption spectrometry, and each requires a different approach in respect of sample pre-treatment. The constituent elements occur over widely-divergent concentration ranges. Since the individual methods have been published elsewhere, a brief outline only will be given here covering sample preparation and dissolution procedures, interferences, and the selection of optimum instrumental conditions.

7.1 Integration and true instrumental precision

Irrespective of the type of read-out device employed, atomic absorption measurements always involve an integration or signal-averaging process of one type or another. Thus the operator may estimate the mean position of a fluctuating meter, or draw the best straight line through the instrumental noise trace superimposed upon an absorption peak from a potentiometric recorder.

Neither of these methods can be used to obtain a quantitative measure of true instrumental precision, however. Since the repeatability of instrumental readings would be a limiting factor in the overall precision of any method of analysis involving atomic absorption spectrometry, it was considered desirable that such information should be obtained. This was accomplished by means of an atomic absorption spectrometer incorporating true integration facilities (see chapter 2, section 2.1.2; chapter 5, section 5.3), in contrast with the equipment used during the major portion of the work reported in this thesis.

For several elements, series of standard solutions were prepared which covered the absorbance range from ca. 0,2 - 0,8; twenty readings were obtained for each solution using a four second integration period. The results are shown in Table 7.1, and include coefficients of variation in terms of both absorbance (dA/A) and concentration (dc/c); from these it can be seen that the limiting (minimum) coefficient of variation, when instrumental fluctuations only are taken into account, is of the order of 0,4% - 0,5%.

7.2 Sample preparation

Sample material for atomic absorption analysis is normally required - at the present stage in the development of atomic absorption technology - to be presented to the instrument in solution form. Thus it is necessary to dissolve completely each analysis element in the sample, unless the material is already in liquid form. There are, however, additional considerations which need to be borne in mind when preparing a sample solution suitable for atomic absorption analysis: (i) the viscosity of the solution

T A B L E 7.1

Instrumental precision obtained with integrating read-out display

CALCIUM h = 0,94			COPPER h = 0,98		
A	dA/A*	dc/c*	A	dA/A*	dc/c*
0,10	0,59	0,60	0,09	0,74	0,74
0,23	0,57	0,58	0,13	0,52	0,52
0,44	0,46	0,49	0,33	0,51	0,52
0,61	0,30	0,34	0,54	0,43	0,44
0,85	0,41	0,57	0,76	0,40	0,43
1,01	0,33	0,62	1,02	0,31	0,36

MAGNESIUM h = 1,00			NICKEL h = 0,91		
A	dA/A*	dc/c*	A	dA/A*	dc/c*
0,10	0,74	0,74	0,12	0,99	1,01
0,17	0,71	0,71	0,26	0,72	0,75
0,25	0,53	0,53	0,44	0,53	0,59
0,42	0,49	0,49	0,61	0,57	0,72
0,71	0,49	0,49	0,78	0,35	0,55
1,04	0,46	0,46	1,02	0,35	2,79

ZINC h = 0,96		
A	dA/A*	dc/c*
0,12	1,70	1,71
0,24	1,41	1,43
0,37	0,95	0,98
0,66	0,87	0,96
0,88	0,77	0,95
1,09	0,44	0,69

*Both dA/A and dc/c are expressed as percentages

must not differ significantly from that of the calibration standards, so that inaccuracies due to viscosity effects do not occur; (ii) the overall dissolved solids concentration must not be so large as to cause rapid clogging of the burner slot; (iii) a high acid concentration, apart from introducing possible interferences, will cause gradual pitting and corrosion of burner heads, nebulizers, etc., and is therefore to be avoided.

Cement: Two procedures are available to the analyst wishing to dissolve siliceous materials in such a way that silica is not precipitated. These are (i) fusion of the sample with salts such as sodium carbonate, sodium or potassium hydroxides, or lithium metaborate, and (ii) attack by hydrofluoric acid with or without addition of a second mineral acid. Fusion methods, although routine in geological and geochemical analysis, result in analysis solutions with very high salt concentrations which may clog the burners used in atomic absorption work; in addition, there is the danger of contamination. It was therefore decided to investigate the possibility of using hydrofluoric acid attack for the complete dissolution of cement samples. Three possible sources of error must be guarded against.

(a) Loss of silicon through volatilization as SiF_4, resulting in a low value for silicon. However, according to Langmyhr and Graff [79], virtually no silicon is lost by volatilization when silica (or other siliceous material) is dissolved in an excess of hydrofluoric acid, provided that the solution is not heated. This has been found to hold true also for cement dissolved in a cold mixture of hydrochloric and hydrofluoric acids.

(b) Uptake of silicon and other elements by hydrofluoric acid attack of glass volumetric apparatus used in the analysis.

This was, in fact, observed with the concentrations of hydrofluoric acid required to dissolve cement samples, and is shown graphically in figure 7.1. Such attack could be completely eliminated by adding boric acid to the hydrofluoric acid before transferring the solution to glass apparatus.

(c) Loss of calcium, magnesium, iron and aluminium by precipitation of such salts as CaF_2, MgF_2, $FeAlF_5$. Addition of boric acid was found to bring such precipitated material back into solution.

Fruit juice: The determination of metals in material of biological origin is normally performed after the sample has been ashed. Both dry ashing (normally at about 500-550°) and wet oxidation with nitric-perchloric acid mixtures have been used successfully in the analysis of foodstuffs, plant material and biological tissue. The applicability of both these techniques to the analysis of fruit juice was investigated. Dry ashing was found to be unsatisfactory because of the very nature of the sample itself: attempted evaporation to dryness of fruit juice - a necessary preliminary to ashing of the sample at an elevated temperature - was found to produce a molasses-type residue which proved to be extremely resistant to ashing. At the same time there was considerable danger of sample loss through sputtering, and it was concluded that dry ashing was not a suitable technique for use with fruit juices.

Wet oxidation with a mixture of nitric and perchloric acids, on the other hand, proved to be completely satisfactory for samples of this type. The oxidation proceeded smoothly, needed little attention from the operator, and a solution suitable for

analysis was readily obtained. However, such a procedure suffers from two main disadvantages: (i) the process is time-consuming, taking 4 - 6 hours to reach completion, and (ii) any tin in the original sample is precipitated as stannic oxide by the acid mixture employed. For these reasons, the possibility was investigated of using straight aqueous dilution of the fruit juice for atomic absorption analysis.

In order to ascertain the effect of viscosity on such a direct method, known quantities of iron were added to successive dilutions of natural orange juice. These were aspirated, and the apparent concentration of iron determined for each solution. In order to eliminate possible interferences [80] these determinations were performed using a nitrous oxide-acetylene flame. The results are shown in Table 7.2 and figure 7.2. From these results it can be seen that, with increasing dilution, the effect of viscosity becomes less and less important, and a 1 : 5 dilution of the juice is sufficient to minimize any error incurred. A 1 : 5 dilution is also adequate to prevent blocking of burner slots by the sample solutions.

T A B L E 7.2

Effect of dilution on the recovery of iron

Volume of juice in 100 cm^3	Dilution factor	Iron present,* $\mu g/cm^3$	Iron found, $\mu g/cm^3$	Recovery, %
80,0 cm^3	1,25	104	98	94
40,0 "	2,5	102	99	97
25,0 "	4	101	100	99
20,0 "	5	101	100	99
10,0 "	10	100	100	100
5,0 "	20	100	100	100

* Undiluted juice sample contained 5,0 $\mu g/cm^3$
A further 100 $\mu g/cm^3$ was added after dilution

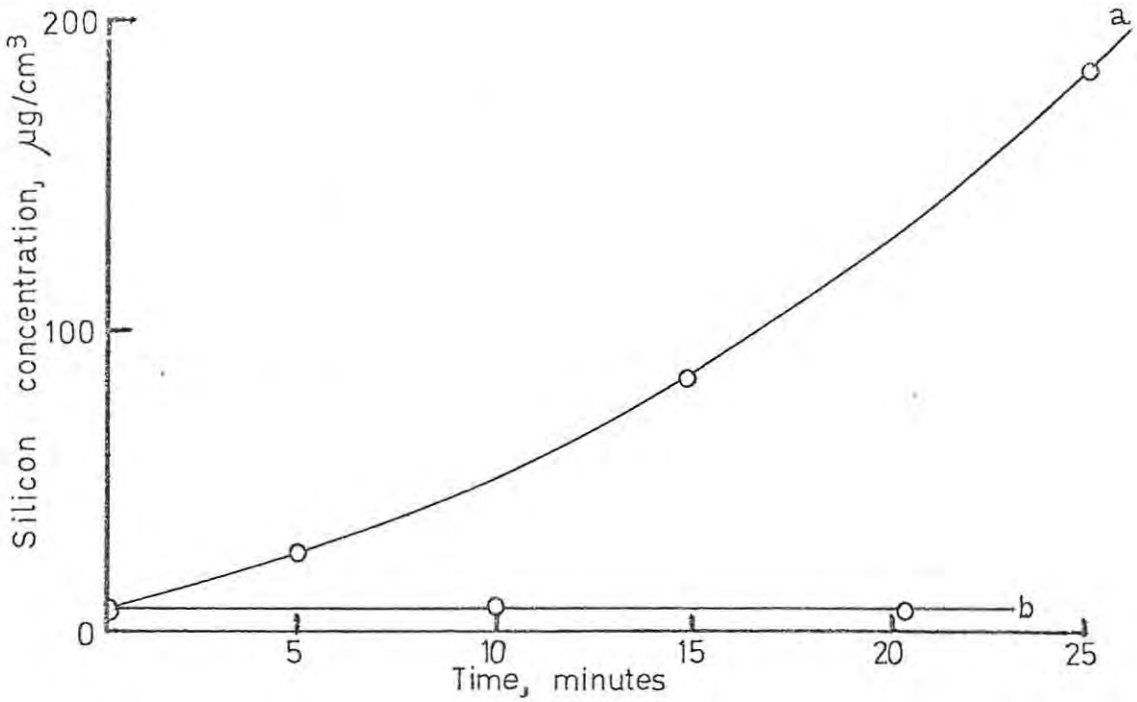

Figure 7.1. Dissolution of silica from glassware in the presence of hydrofluoric acid.
a - hydrofluoric acid only,
b - boric acid added.

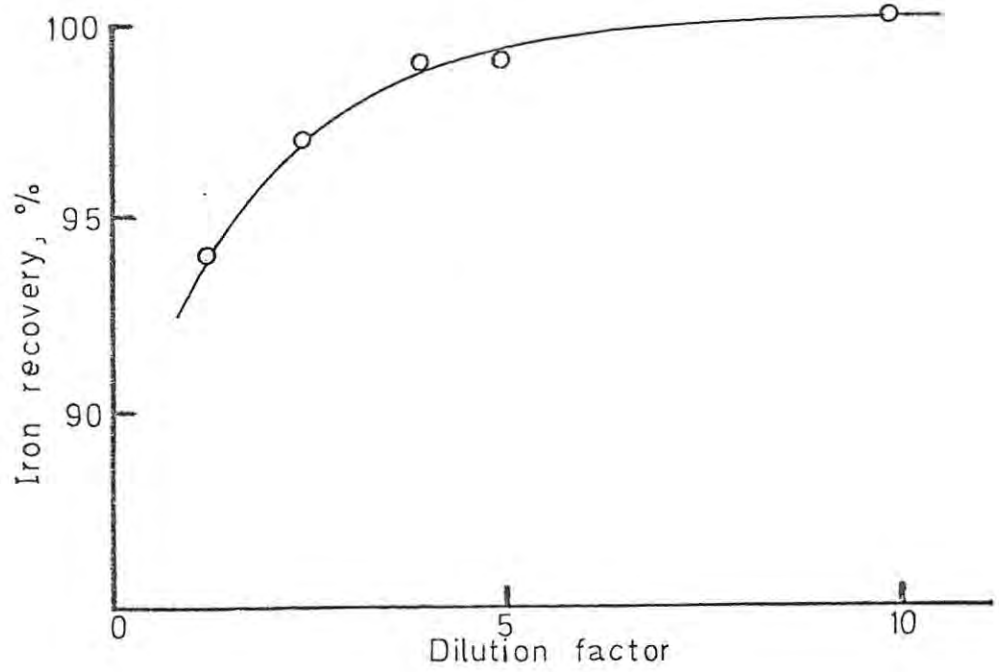

Figure 7.2. Effect of dilution on recovery of 50 µg/cm³ iron added to fruit juice.

As an additional check on the validity of using a simple dilution of the juice sample for atomic absorption analysis, extensive measurements were made of the recovery of added amounts of each of the elements determined. The results are shown in Table 7.3. With few exceptions, recoveries for individual elements lie between 96% and 104% of the expected values, indicating that the accuracy of the proposed procedure is equal to that normally expected from atomic absorption analysis.

T A B L E 7.3

Recoveries of added elements

Element	Added $\mu g/cm^3$	Pineapple Juice: Mean natural concn. $\mu g/cm^3$	Pineapple Juice: Recovered $\mu g/cm^3$	Orange Juice: Mean natural concn. $\mu g/cm^3$	Orange Juice: Recovered $\mu g/cm^3$
Iron	3,0 6,0	3,6	2,8 ; 2,8 5,9 ; 5,9	5,1	2,9 ; 3,0 6,0 ; 6,2
Manganese	2,5 5,0	12,0	2,5 ; 2,4 4,8 ; 4,8	0,3	2,5 ; 2,5 4,85 ; 4,95
Tin	10,0 20,0	47,0	9,0 ; 11,5 19,0 ; 19,0	36,0	10,3 ; 10,0 22,5 ; 22,5
Zinc	1,25 2,50	3,1	1,13 ; 1,13 2,38 ; 2,23	5,4	1,20 ; 1,20 2,45 ; 2,45
Calcium	100 200	82	98 ; 99 195 ; 190	85	101 ; 101 201 ; 201
Sodium	20,0 40,0	19,8	20,0 ; 20,0 40,2 ; 40,2	26,2	20,1 ; 19,1 39,4 ; 40,0
Magnesium	100 200	119	104 ; 102 206 ; 203	73,2	104 ; 105 206 ; 208
Potassium	500 1000	1652	462 ; 496 1000 ; 982	1238	514 ; 510 980 ; 960

Steel: There is very little difficulty in obtaining solutions of steel samples suitable for atomic absorption analysis. A mixture of sulphuric and phosphoric acids ("Spekker-acid") was found convenient since moderate quantities of tungsten could be kept in solution; precipitation of the tungsten frequently resulted in co-precipitation of significant quantities of chromium and molybdenum. Also, in sulphuric-phosphoric acid solution, interferences in the determination of chromium and molybdenum, if not fully eliminated, were found to be less severe than in hydrochloric or sulphuric acid medium. Except when silicon was to be determined, a sulphuric-phosphoric acid mixture was used for the dissolution of steel samples. For the determination of silicon in steel, a dissolution procedure is required which will retain the silicon in solution. Clarke [81] has described a rapid method for the dissolution of steels and cast irons which does not result in precipitation of the silica; hydrochloric acid attack, followed by treatment with hydrogen peroxide, results in the complete dissolution (except for carbon) of samples containing less than about 1% of silicon.

7.3. Interferences

The major interferences occurring during the analysis of the sample materials have been discussed elsewhere, [55, 65, 82-34]. These are briefly as follows:

(a) Suppression of calcium, iron and manganese response by the presence of silicate ions in sample solutions of cement. Addition of lanthanum fully overcomes the depressive effect of silicate both on calcium, iron and manganese, and also on magnesium and zinc, the latter two being affected far less than the

former group. This releasing action is summarized in Table 7.4.

(b) Enhancement of silicon absorption by elements such as calcium which are present in cement. This is shown in Table 7.5. Again, addition of lanthanum eliminates the interference.

(c) Depression of iron response by citric acid present in fruit juice. Such interference was fully eliminated by the addition of phosphoric acid.

(d) Depression of chromium absorbance by iron is encountered during the analysis of steel. Ammonium chloride and sodium sulphate (or chloride) are frequently recommended as releasing agents for chromium. Preliminary investigations revealed that neither ammonium nor sodium salts were suitable as releasing agents for chromium in the presence of phosphoric acid, and an alternative interference suppressor was therefore sought. Potassium sulphate was found to act more successfully than either the sodium or ammonium salts mentioned above, but even more effective releasing action was provided by magnesium sulphate. Apart from the differences, noted above, with respect to their effectiveness in phosphoric acid medium, these four releasing agents (ammonium chloride, and sodium, potassium and magnesium sulphates) appear to operate in very much the same way. In each case, greatest enhancement is obtained under fuel-rich conditions when, in fact, the enhancement more than compensates for the suppressive effect of iron. Very little enhancement occurs in a lean flame, and addition of such reagents to pure chromium solutions produces very little change in chromium response under any flame conditions. It thus appears that the presence of iron assists, in some way not yet fully understood, with the overall enhancement produced by,

for example, magnesium sulphate. From the practical point of view, this phenomenon leads to one very important consideration which is that, in order to obtain results of even moderate accuracy, iron must be present in similar amounts in both standard solutions and samples. It is not sufficient to prepare standard solutions containing only chromium and the relevant releasing agent. The main function of such a releasing agent is, therefore, to counteract the depressive effect of the iron, thus improving the sensitivity of chromium in the presence of iron.

T A B L E 7.4

Releasing action of lanthanum on interference by silicon

Silicon concentration, $\mu g/cm^3$	Absorbance for			
	Fe*	Fe + La	Mn*	Mn + La
0	0,164	0,166	0,092	0,092
160	0,135	0,167	0,060	0,092
320	0,124	0,166	0,045	0,090
480	0,122	0,166	0,043	0,090

*40 $\mu g/cm^3$ iron and 10 $\mu g/cm^3$ manganese

T A B L E 7.5

Enhancement of silicon response by calcium and iron

Concentration of added ion $\mu g/cm^3$	Apparent silicon concentration $\mu g/cm^3$	
	Calcium added	Iron added
0	200	200
500	218	230
1000	229	240
1500	235	243
2000	238	244

Because the presence of the releasing agent may have a residual effect of its own on the response of the analysis element, it is strongly recommended that releasing agents, in equal concentration, be added to both standard solutions and samples alike.

7.4 Operating conditions

The choice of instrumental conditions under which an analysis is performed is important, since it may affect three important factors, viz. precision, analytical sensitivity, and the extent to which possible interferences may occur.

As discussed in chapters 3 and 5, the precision of analysis is determined largely by the curvature of the calibration graph: increasing curvature generally leads to worsening precision (larger coefficients of variation). It is therefore desirable that the value of h be maintained as large as possible. From the data presented in chapter 5, it can be seen that larger values of h generally occurred when the observation height was relatively large and the flame not too rich; such conditions were frequently found also to approximate to those required for good analytical sensitivity. In addition, it has been shown that interferences are generally more severe (i) when the observation height is small and (ii) when the flame is very rich [55]. Such conditions were therefore avoided wherever possible.

Table 7.6 summarises the suggested operating conditions for a number of different elements. These recommendations are based on the work reported in chapter 5 of this thesis. Due to instrumental difficulties, no investigation of precision in a nitrous oxide-acetylene flame could be made; the conditions

recommended for silicon and aluminium, therefore, are those corresponding to best sensitivity. (In practice, sensitivity in a nitrous oxide-acetylene flame is critically dependent upon the instrumental conditions employed, and even a slight deviation from optimum leads to extremely poor sensitivity.)

7.5 Analytical methods

Methods are here presented for the atomic absorption analysis of cement, steel (both for silicon and for a number of alloying or residual constituents) and fruit juice. Most of these methods have been published by the present author, and references to the original papers are given where appropriate.

7.5.1 Analysis of cement [84]

Weigh 0,500 g of the powdered sample into a 100 cm^3 polythene or PTFE beaker. Wash down the sides of the beaker with about 20 cm^3 of water. Add, with stirring, 10 cm^3 of hydrochloric acid (sp. gr. 1,16), breaking up any gritty particles with the end of the stirring rod. When the sample has dissolved (except for any precipitated silica) rinse down the glass rod, remove it from the beaker, and add 1,0 cm^3 of hydrofluoric acid (40% w/v). Carefully swirl the mixture until all precipitated silica has dissolved, then add 50 cm^3 of boric acid solution (4% w/v) and mix thoroughly. Transfer the solution quantitatively to a 200 cm^3 volumetric flask, add 20 cm^3 of stock lanthanum chloride solution (5% La^{3+}) and dilute to the mark with water (Solution A). Solution A is used for the determination of aluminium, iron, manganese, silicon, sodium, strontium and zinc.

Transfer 10,0 cm^3 of solution A to a 100 cm^3 volumetric flask. Add 5 cm^3 of hydrochloric acid and 9,0 cm^3 of stock lanthanum chloride solution, and dilute to the mark with water (Solution B).

T A B L E 7.6

Recommended instrumental settings for the elements

Element	Wavelength nm	Slit width mm	Acetylene flow cm^3/min	Oxidant	Observation height, cm
Aluminium	309,3	0,05	4000	N_2O	1,2
Calcium	422,7	0,05	2000	air	1,2
Chromium	357,9	0,05	2400	air	1,2
Cobalt	241,0	0,05	2000	air	1,5
Copper	324,8	0,05	1600	air	1,2
Iron	248,3	0,05	2000	air	0,9
Lead	283,1	0,05	2000	air	1,2
Lead	217,0	0,10*	2000	air	1,2
Magnesium	285,2	0,05	1200	air	1,2
Manganese	279,5	0,05	1200	air	1,2
Silicon	251,3	0,05	4200	N_2O	1,0
Zinc	213,9	0,10*	1600	air	1,5

* The slit width for lead (217 nm) and zinc can be reduced if the lamp intensity permits of this.

With a 10 cm air-acetylene burner head, the most suitable calcium and magnesium concentration ranges within which to work are approximately 3-30 $\mu g/cm^3$ and 0,25 - 2,5 $\mu g/cm^3$ respectively. These concentration ranges require a 50 or 100-fold dilution of the original sample solution (Solution A, above). Using a 1-cm (emission) burner head for absorption, however, the method becomes less sensitive for both calcium and magnesium by a factor of 5 - 10, making it possible to work with much higher concentrations of these elements. This is demonstrated in figures 7.3. and 7.4. which show Ringbom-Ayers plots for calcium and magnesium using both types of burner head. A ten-fold dilution only of the original sample solution is then required, leading to both an increase in precision and a saving in time. This same solution may also be used for the determination of potassium, this time with a 10 cm slot burner.

7.5.2. Determination of a silicon in steel [82]

Weigh out 1 g of the material into a glass beaker and add 5 - 10 cm^3 of water followed by 10 cm^3 of hydrochloric acid. Heat the solution and add, carefully and in small portions, 10 cm^3 of hydrogen peroxide (50 vols). Boil the solution, allow to cool, filter into a 100 cm^3 volumetric flask, and dilute to the mark with water.

7.5.3 Analysis of steel (for chromium, etc.) [35, 104]

Weigh 0,5 or 1 g samples of the steel into a 300 cm^3 conical flask, add 20 cm^3 of a mixed sulphuric-phosphoric acid solution (25% w/v of each), and heat gently until the sample has dissolved. Add, with care, a total of 10 cm^3 of hydrogen peroxide (50 vols), heat to decompose the excess of peroxide,

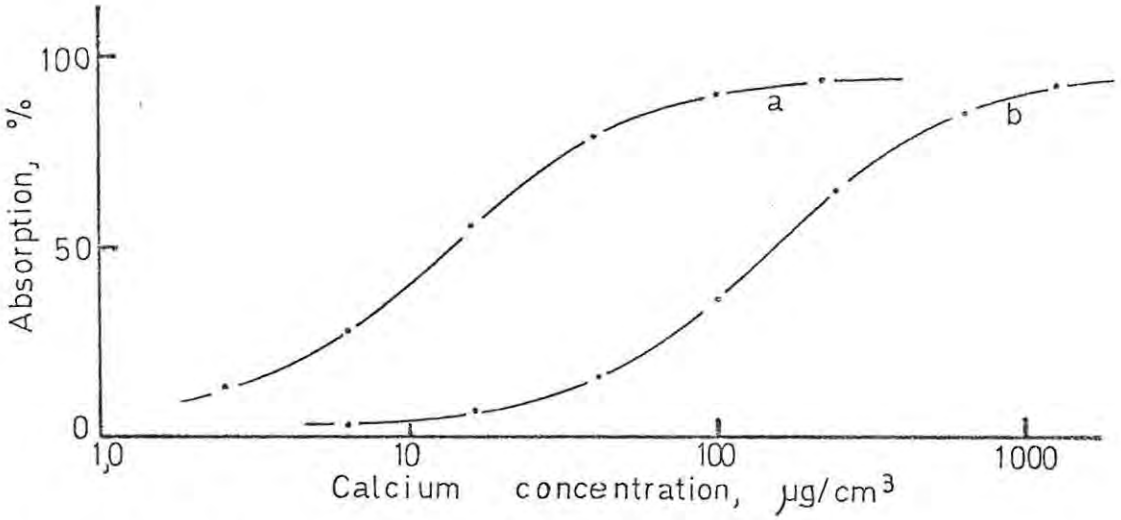

Figure 7.3. Ringbom-Ayers plots for calcium.
a - 10 cm burner head;
b - 1 cm burner head.

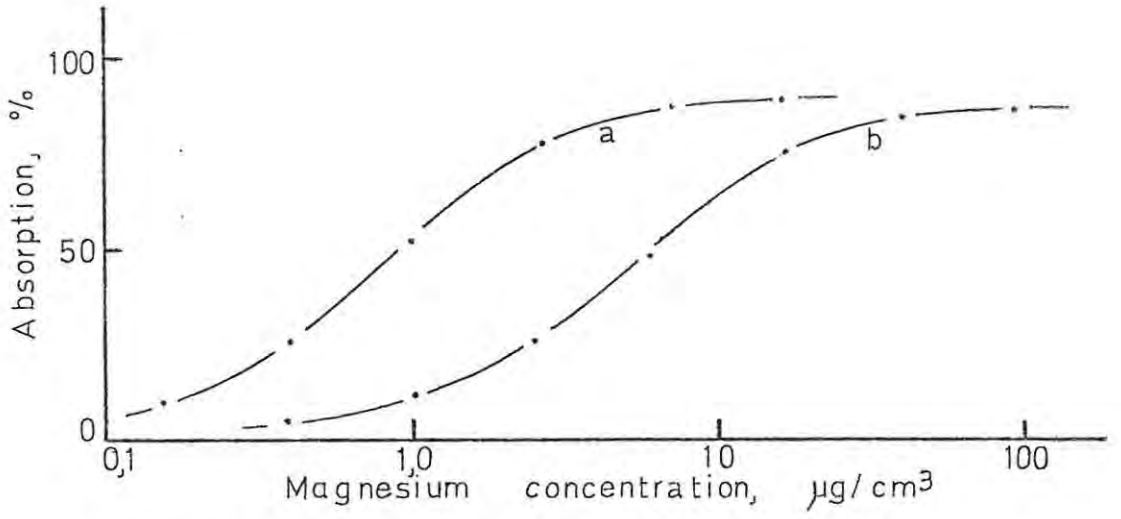

Figure 7.4. Ringbom-Ayers plots for magnesium.
a - 10 cm burner head;
b - 1 cm burner head.

cool, and transfer the solution quantitatively to a 100 cm^3 volumetric flask. Add 10.0 cm^3 of magnesium sulphate solution (25% w/v $MgSO_4.7H_2O$) and dilute to volume. If necessary, filter a small portion of this solution for analysis.

Where required, dilute this "master" solution in accordance with Table 7.7 being careful to add sufficient magnesium sulphate and iron to compensate for that lost through dilution. Both iron and magnesium sulphate should be added to the standard solutions employed.

TABLE 7.7

Suggested sample dilutions

Element to be determined	Approximate sensitivity in air-acetylene	Optimum concn. range for analysis, $\mu g/cm^3$	Concentration range of element in sample		
			0,015-0,15%	0,15-1,5%	1,5-15%
			Suggested sample dilution g/100 cm^3		
Chromium	0,4	8 - 80	1	0,5	0,05
Cobalt	0,4	8 - 80	1	0,5	0,05
Copper	0,2	4 - 40	1	0,2	0,02
Manganese	0,1	2 - 20	1	0,1	0,01
Molybdenum	2,0	40 - 400	1	1	0,2
Nickel	0,8	16 - 160	1	1	0,1

7.5.4 Analysis of fruit juice [56, 57]

Before performing the analysis it is necessary both to dilute the samples and to remove suspended matter. Removal of suspended matter is best performed by centrifugation of the original sample material; alternatively, a small portion may be filtered after dilution. In either case, dilute the sample in

accordance with Table 7.8, adding hydrochloric acid in sufficient amount to give an overall concentration of 5% v/v of concentrated acid before making up to the mark with pure water. The diluted solutions are then used for analysis.

TABLE 7.8

Suggested sample dilutions for fruit juices

Element	Optimum range, $\mu g/cm^3$	Approximate levels in fruit juice $\mu g/cm^3$	Dilution factor
Iron	10 - 100	5	5
Manganese	1,6 - 16	5	5
Tin	50 - 500	100*	5
Zinc	1,2 - 12	5	5
Calcium	3 - 30	100	10
Sodium	1 - 10	20	10
Magnesium	0,25 - 2,5	200	200
Potassium	2 - 20	1000	200

* In canned juices

7.6 Accuracy and precision of the proposed methods

The accuracy of the proposed methods was assessed either by analysing standard samples (B.C.S. or N.B.S.) of the materials concerned, or by comparing analytical results obtained by the proposed methods with those obtained by means of another, generally accepted, procedure. Standard samples of cement and steel were readily available for analysis; in the case of fruit juice, the results obtained by the proposed method utilizing simple dilution of the samples were compared with those obtained by atomic

absorption analysis after ashing the samples with a nitric-perchloric acid mixture. This combination - wet ashing followed by atomic absorption analysis - is a well-established method and is known to give excellent results for the analysis of materials of biological origin.

For each sample material analysed, standard deviations and co-efficients of variation were calculated from a series of replicate analyses - usually eleven - of the samples according to the proposed method of analysis.

The results are shown in Tables 7.9 - 7.15.

7.7 Conclusions

Atomic absorption analysis has proved to be an extremely rapid and versatile technique for the analysis of cement. Not only is it possible to determine ten elements after but one sample weighing and without any chemical separations, but the reproducibility is comparable with that expected for the accepted methods of cement analysis. The only possible exceptions are the determinations of the major constituents silicon and calcium, and the atomic absorption technique is probably inferior to classical methods for the determination of these elements in samples of this type. In the case of calcium, for instance, the reproducibility normally required by the cement chemist is of the order of $\pm$ 0,1% (coefficient of variation). This is not attainable by the atomic absorption method without very special precautions and highly sophisticated instrumentation.

When silicon occurs as a minor constituent, as for instance in steel where it is usually present to an extent less than 1%, a coefficient of variation of 2,4% of content was found; at higher

silicon levels (e.g. in cement) the precision improved significantly to give a coefficient of variation of about 1%. The lowest concentration level at which silicon can be determined with acceptable accuracy depends mainly upon sample dilution and instrumental conditions. As interfering effects may be largely overcome, the limits both of detection and determination are not influenced by the matrix elements. With a silicon sensitivity of 5 $\mu g/cm^3$ and a detection limit in aqueous solution of 2 $\mu g/cm^3$, concentrations around 20 $\mu g/cm^3$ can be measured with a coefficient of variation of about 10% or better. This represents 0,2% of silicon if a 1 g sample is made up to 100 cm^3 in solution, and is probably the practical limit of determination for silicon in steel by the method described, though clearly it may be improved by replication; lower concentrations may be determined, but with a greater proportional error.

The work performed on the analysis of steel for a number of different alloying elements, such as chromium, cobalt, manganese and nickel, confirms the ease with which the atomic absorption technique is able to be incorporated into a comprehensive scheme of analysis. This stems from the nature of the technique itself: the simplified sample pre-treatment involved, the specificity of the method combined with the wide variety of elements which may be determined, and the ease with which interferences may normally be eliminated. Reference to Table 7.13 indicates that the proposed method for the analysis of steel is capable of extremely good precision. Except for the determination of a trace of chromium (0,03%) in one sample, all the coefficients of variation obtained were better than 0,75%. The overall accuracy is

also good, although some individual estimations deviate significantly from the expected values.

Turning to the analysis of fruit juice (Tables 7.14 and 7.15), it is seen that the overall precision is entirely satisfactory, the coefficients of variation for many elements being better than 1%. The analytical results (Table 7.14) for the proposed method also agree extremely well with those obtained after ashing the samples, thus establishing the accuracy of the far shorter method involving simple aqueous dilution. It is thus unnecessary to ash fruit juice samples prior to analysis, straight dilution with water followed by centrifugation being the only sample pre-treatment that is normally required. These solutions are then aspirated directly, enabling determinations to be performed extremely rapidly. Centrifugation has been used in preference to the more tedious process of filtration in order not to detract from the overall speed of analysis.

Table 7.16 compares the precision of atomic absorption methods of analysis for the samples discussed above with that reported for other analytical techniques. The figures quoted for atomic absorption analysis have all been obtained during the course of the work reported in this thesis.

T A B L E 7.9

Results for standard cement samples

Analysis	N.B.S. 1013		N.B.S. 1015	
	Certificate %	Found A.A. %	Certificate %	Found A.A. %
Al_2O_3	3,30	3,18 3,21	5,04	4,99 5,06
Fe_2O_3	3,07*	3,21 3,17	3,27*	3,36 3,38
Mn_2O_3	0,05	0,052 0,052	0,06	0,059 0,059
Na_2O	0,20	0,19 0,19	0,16	0,017 0,016
SiO_2	24,2	24,7 23,7	20,6	21,0 20,3
SrO	0,08	0,080 0,085	0,11	0,095 0,098
CaO	64,26	64,6 63,9	61,37	60,4 59,5
MgO	1,39	1,37 1,37	4,25	4,35 4,24

*Capacho-Delgado and Manning [85] found 3,17 and 3,37 per cent Fe_2O_3 for N.B.S. 1013 and N.B.S. 1015, respectively.

T A B L E 7.10

Calculated standard deviations for cement analysis

Analysis	Standard deviation %	Coefficient of variation %
Al_2O_3	0,050	1,0
Fe_2O_3	0,023	0,7
Mn_2O_3	0,0008	1,3
SiO_2	0,25	1,2
SrO	0,0009	0,9
CaO	0,43	0,7
MgO	0,029	0,7

T A B L E 7.11

Determination of silicon in steel

Sample No.	Type	Nominal Composition	% Silicon	
			Std. Analysis	A.A.
Private sample	Cast Iron	-	2,14	2,13) 2,13)
BCS 241/1	High-speed Steel	W 19,6%; Co 5,7% Cr 5%	0,33	0,30
BCS 251/1	Low Alloy Steel	Mn 1,5%; Mo 1,6%	0,41	0,39
BCS 253/1	Low Alloy Steel	Ni 1%; Cr 1%	0,65	0,65) 0,66)
BCS 336	Stainless Steel	Cr 17,6%; Ni 9,5%	0,51	0,51) 0,53)
BCS 339	Cr - V Steel	Cr 12,4%	0,36	0,36
BCS 235	Stainless Steel	Cr 18,6%; Ni 9,4%	0,82	0,83

Coefficient of Variation

The standard deviation at the 0,5% silicon level was found to be 0,012%, giving a coefficient of variation of 2,4%.

T A B L E 7.12(a)

Analysis of synthetic steel samples for several elements

Sample No.	Chromium		Cobalt		Copper		Manganese		Nickel	
	Present %	Found %	Present %	Found %	Present %	Found %	Present %	Found %	Present %	Found %
1	3,13	3,05	3,75	3,65	-		-		3,13	3,05
2	0,50	0,48	0,50	0,50	1,00	1,00	0,50	0,52	1,00	0,98
3	15,0	15,0	-	-	-	-	-	-	7,50	7,50
4	5,0	4,88	2,00	2,00	-	-	3,00	3,12	1,52	1,52
5	0,25	0,25	0,50	0,51	0,75	0,75	1,00	1,00	1,00	1,00
6	0,50	0,50	1,00	0,96	0,50	0,50	0,50	0,49	1,00	1,00
7	3,75	3,60	3,00	2,88	0,75	0,72	-	-	-	-

T A B L E 7.12(b)

Analysis of standard steel samples

B.C.S. Sample No.	Chromium %		Cobalt %		Copper %		Manganese %		Nickel %	
	Cert.	A.A.	Cert.	A.A.	Cert.	A.A.	Cert.	A.A.	Cert.	A.A.
320	0,13	0,14 0,14	-	-	-	0,02 0,03	0,19	0,17 0,18	0,02	0,014 0,014
252/1	0,42	0,44 0,44	-		0,20	0,20 0,20	0,34	0,36 0,36		
253/1	0,99	1,01 1,03	-		-		-		-	
323	0,22	0,22 0,22	-		-	0,02 0,02	0,29	0,31 0,30	0,17	0,17 0,17
258/1	-		-		0,15	0,15	0,40	0,39	-	
336	17,3	17,3 16,8	0,63	0,60 0,64	0,11	0,11 0,11	-		9,5	8,8 8,8
220/1*	5,13	4,0 4,1	0,13	0,11 0,12	0,15	0,14 0,15	-		0,16	0,16 0,15

* A bulky precipate of tungstic oxide formed and co-precipitated a considerable proportion of the chromium

T A B L E 7.13

Precision of steel analysis, for four elements

Element %	Content, c %	Standard Deviation %	Coefficient of Variation %
Chromium (A)	0,028	0,0009	3,2
Chromium (B)	0,396	0,0028	0,7
Copper (A)	0,267	0,0009	0,32
Copper (B)	0,227	0,0009	0,38
Manganese	0,320	0,0023	0,73
Nickel	0,195	0,0012	0,59

T A B L E 7.14

Analysis of ashed and non-ashed fruit juice samples

Element determined	Concentration found ($\mu g/cm^3$)			
	Pineapple juice		Orange juice	
	Ashed	Non-ashed	Ashed	Non-ashed
Manganese	2,20; 2,20	2,09; 2,09	0,3	0,3
Zinc	3,2 ; 3,3	3,2 ; 3,1	5,8; 5,8	5,5; 5,5
Calcium	173; 171	173; 171	76; 76	76; 76
Magnesium	238; 235	238; 239	148; 149	151; 153
Potassium	1310; 1290	1280; 1290	1090; 1080	1090; 1080

T A B L E 7.15

Standard deviations ($\mu g/cm^3$ in the diluted sample) and coefficients of variation (%) for the analysis of fruit juice

Element	Standard deviations	
	Orange juice	Pineapple juice
Calcium	0,081 $\mu g/cm^3$ or 0,7%	0,145 $\mu g/cm^3$ or 0,8%
Iron	-	0,021 $\mu g/cm^3$ or 0,9%
Magnesium	0,002 $\mu g/cm^3$ or 0,5%	0,004 $\mu g/cm^3$ or 0,8%
Manganese	0,006 $\mu g/cm^3$ or 2,7%	0,028 $\mu g/cm^3$ or 3,8%
Potassium	0,092 $\mu g/cm^3$ or 1,0%	0,095 $\mu g/cm^3$ or 0,8%
Sodium	0,046 $\mu g/cm^3$ or 1,7%	0,054 $\mu g/cm^3$ or 2,9%
Tin	-	0,351 $\mu g/cm^3$ or 2,3%
Zinc	0,005 $\mu g/cm^3$ or 1,6%	0,013 $\mu g/cm^3$ or 3,1%

TABLE 7.16

Comparison of precision of atomic absorption procedures with that of other analytical methods

(a) Fruit juice and biological material

Element	Approx. concn. $\mu g/cm^3$	At. Abs. CV[a] %	Other methods		
			CV[a] %	Method[b]	Ref.
Ca	10	0,7 0,8	1,2	f. phot.	86
Fe	2	0,9	2,0	col.	87
K	10	0,8	1,0	f. phot.	86
Mg	1	-	1,2	col.	88
Mg	0,2	0,5 0,8	2,5	col.	89
Mn	0,4	2,7 3,8	2,3	col.	90
Zn	31	1,6[c] 3,1[c]	1,7 4,0	col. pol.	91 91
Zn	15	-	1,4	col.	92

(b) Steel and cast iron

Element	Approx. concn. %	At. Abs. CV[a] %	Other methods		
			CV[a] %	Method[b]	Ref.
Cr	0,4	0,7	0,9	col.	93
Cu	0,1	0,38	5	col.	94
Cu	0,2	0,32	1,2	col.	94
Mn	0,3	0,73	0,5	col.	93
Ni	0,2	0,59	0,9	grav.	95
Ni	0,2	-	0,5	col.	95
Si	0,5	2,4	1,6	n. act.	96

For explanatory notes, see page 135

TABLE 7.16 (Continued)

(c) Cement

	Approx. concn. %	At. Abs. CV[a] %	Other methods		
			CV[a] %	Method[b]	Ref.
Al_2O_3	5	1,0	0,7	col.	97
CaO	60	0,7	0,2	vol.	97
CaO	60	-	1,4	f. phot.	98
CaO	60	-	0,9	amper.	99
Fe_2O_3	5	0,7	0,7	col.	97
MgO	4	0,7	1,0	vol.	100
MgO	4	-	0,8	vol.	97
MgO	4	-	1,0	vol.	101
Mn_2O_3	0,1	1,3	2,0	col.	97
SiO_2	20	1,2	0,3	col.	97

NOTES:

a - coefficient of variation

b - col. = colorimetric
vol. = volumetric
amper. = amperometric titration
f. phot. = flame photometric
n. act. = neutron activation
grav. = gravimetric
pol. = polarographic

c - Zinc concentration approximately 0,5 $\mu g/cm^3$

Chapter 8

DISCUSSION

It has been shown in chapter 3 of this thesis that the effect of calibration curvature on precision of analysis may readily be expressed in quantitative form. In order to do this, an equation has been derived relating the transmittance (T) and concentration (c) which contains but two, independent, constants, viz. the combined factor ab, which is a measure of the analytical sensitivity, and h, which is directly related to the shape of the curve. The necessary computing techniques, which enable rapid evaluation of these constants, have also been developed. The accuracy of the derived equation for expressing the analytical curves is frequently sufficient to give a coefficient of variation in terms of absorbance, calculated over the whole curve, of between 1% and 4% for such a curve-fitting procedure. It appears that this close agreement between the calculated and measured curves is maintained irrespective of the main cause(s) of deviation from linearity. This means that analytical curves for different elements, or for the same element under different operating conditions, may be compared directly with respect to both sensitivity and degree of conformity with Beer's law.

The considerable effect which calibration curvature exerts upon precision is shown in figures 3.2. and 3.3; this is also indicated very clearly in Table 7.1, where the values of dc/c are compared directly with those of dA/A for the same analytical system. Since the analytical precision worsens rapidly as calibration curvature increases, it is of paramount importance that those instrumental parameters which may affect the linearity

of the analytical curve - lamp current, slit width, and observation height - be adjusted in such a way as to reduce calibration curvature to a minimum. It is clear from results presented in chapter 5 that instrumental factors are, generally, without significant effect on the precision except in so far as they affect the shape of the analytical curve. The importance of linearity applies whether or not integrating devices or electronic curvature correction facilities are employed.

The question of calibration curvature may also assume importance when attempts are made to work under less sensitive conditions (i.e. poorer sensitivity), so as to avoid the necessity of diluting the analyte solution. Absorption lines which are less sensitive than the normal resonance lines are known for a number of elements. However, in some cases the less-sensitive lines exhibit far greater calibration curvature and are therefore unsatisfactory. A far more acceptable procedure in such cases is to employ a shorter absorption path length, i.e. by rotating the burner head through 45° or 90°; alternatively, a different burner altogether may be employed, such as a Meker-type burner normally recommended for flame emission work. Analytical curves for the element calcium, obtained with different burner heads, or at different wavelengths, are shown in figure 8.1.

Using available vapour pressure and other data, it has been possible to calculate the degree of volatilization of strontium oxide at different heights in an air-acetylene flame. The results agree very well with the experimentally determined volatilization curves. Strontium oxide, even at concentrations of several hundred $\mu g/cm^3$, volatilizes completely at a temperature well below the melting point of the solid. This confirms L'Vov's

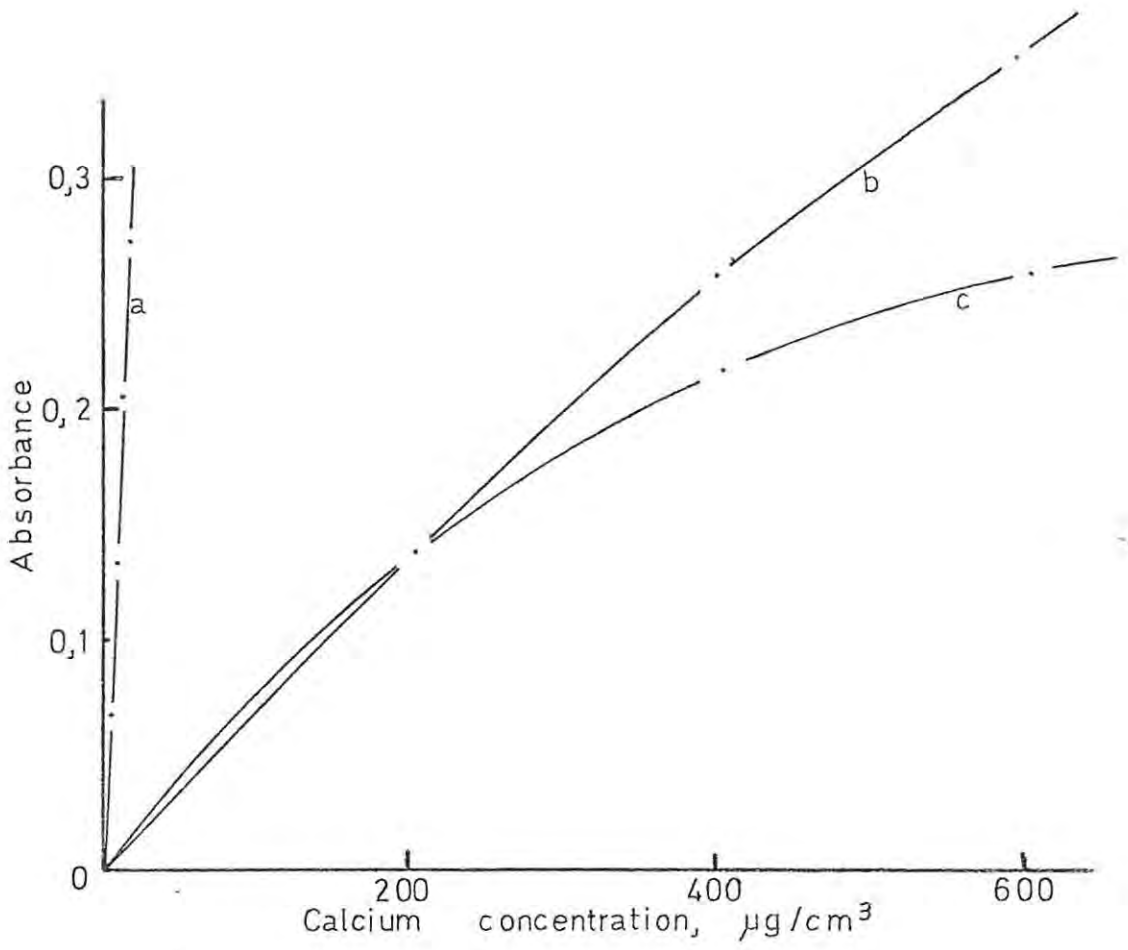

Figure 8.1. Analytical curves for calcium.

a - 422,7 nm;

b - 422,7 nm, burner rotated through an angle of 55°;

c - 393,0 nm.

observation [56] that solute vaporization would normally take place at temperatures significantly lower than the boiling point of the material concerned. With such knowledge, a new approach can be made towards understanding interference phenomena (solute vaporization interference [102] or "chemical interference"). In the past, interferences have frequently been interpreted in terms of boiling point data, where these have existed. However, since vaporization is now known to occur at temperatures far below the boiling point, boiling point data are largely irrelevant and interferences may be considered, far more realistically, in terms of the vapour pressure of the solute at or near the temperature of the flame. In most, if not all, cases of interference, that portion of the sample which volatilizes within the observation zone would do so directly from a solid matrix, so that co-precipitation effects during the evaporation of solvent from the individual droplets as they enter the burner head or the flame, and solid-solid interactions in the dried particles, are likely to be controlling factors (together with the overall vapour pressure of the resultant mixture or compound) in determining the existence or otherwise of interference in particular circumstances.

Many workers [52, 102, 103] have emphasized the fact that one of the most important factors controlling interference in atomic absorption analysis is the size of the particles of dried sample material entering the flame: the smaller the particles, the more likely is volatilization to be complete at an early stage in the transit of the material through the flame, even if the vapour pressure of the sample is relatively low. It is of the utmost importance, therefore, that particle size be reduced as far as is possible - hence, that ways and means are devised of

reducing the size of the droplets which pass from the mixing chamber to the flame. Ultrasonic nebulization, although apparently successful in producing minute drops and drastically reducing the severity of several interference effects [58], has not found general acceptance due, largely, to technical difficulties. This technique still offers a potential solution to the problem of reducing droplet size and hence to minimizing certain types of chemical interference. Whether the ultimate solution lies in conventional pneumatic, or ultrasonic, nebulization, or in some other direction, any advance in this field would be of considerable advantage, both by reducing the severity of interference, and also by improving sensitivity and the linearity of working curves.

The work described in this thesis has shown, unequivocally, that the concept of photometric error functions may be applied to atomic absorption spectrometry, and that such error functions are important for a full appreciation of the factors governing precision in this technique. Prior to the work reported here and published in three research papers [21-23], precision in atomic absorption analysis had not been interpreted in terms of error functions. The existence of individual error functions has been conclusively demonstrated, and the experimentally determined form of these individual functions has been shown to agree with that expected on theoretical grounds. It has further been shown that composite error functions, obtained under practical operating conditions, can be expressed in terms of contributions from several individual functions. Such composite error functions may then be used in estimating the concentration range corresponding to optimum precision.

Concentration ranges giving optimum precision have been expressed, in part, in terms of multiples of the analytical sensitivity ($\mu g/cm^3$ per 1% absorption) of the element concerned measured under given instrumental conditions. It was hoped that such an approach would automatically compensate for differences in the extent to which different elements conform to Beer's law, and that it would be possible to quote an optimum range which would be valid for all elements. However, this approach has not been altogether successful: although the spread in multiples of sensitivity was relatively smaller than the spread in the limiting absorbance values defining the ranges for the different elements, there was not the close agreement hoped for. This approach would work, however, for a pure TlogT error function.

Exact quantitative evaluation of the error functions has not been possible because of the spread of results for the measured standard deviations, and elaborate computerised curve-fitting procedures were necessary to obtain the best fit through the experimental points. The uncertainty in the values of individual standard deviations, caused partly by the use of a non-integrating read-out system for normal measurements, means that there is a consequent uncertainty in the exact magnitude of the contributions of individual error functions as expressed by the values of the co-efficients k_{1-4} (chapter 4). In spite of this small inherent uncertainty, it has been possible to evaluate the coefficients satisfactorily, and it has been shown that, in every case except nickel, the greatest contribution to the overall error pattern comes from the $dT \propto TlogT$ function. Quantitative evidence has therefore been produced which shows that flame fluctuations are the major single source of noise in atomic absorption

determinations. Such fluctuations arise directly out of the dynamic nature of the combustion process, leading to slight variations both in flame temperature and in flame dimensions.

If small changes in flame dimensions - whether as a result of variations in gas flow rate or the movement of air near the flame - contribute significantly to the dynamic flame noise, introduction of mechanical or physical control of the size of the flame would reduce the noise level. In order to test this possibility, metal plates (12 cm x 2 cm x 0,5 cm) were placed parallel to, and on either side of, the burner slot, a distance of ca. 4 mm apart. Holes drilled in the base of each plate allowed sufficient air through to support the secondary combustion process. Preliminary measurements on copper and calcium have shown a considerable reduction in the overall noise level: relative to normal burner operation, introduction of the parallel plates reduced the coefficient of variation (dA/A) for copper readings by 50%, and for calcium by a factor of five. These investigations are in an initial stage, and are introduced here purely as substantiating the conclusion reached during the course of this work, that dimensional flame fluctuations contribute significantly to lack of precision in atomic absorption analysis. Clearly, there is much scope for further work here.

In the case of nickel, the error functions 'dT∝T' and 'dT constant' exerted a considerable influence - to such an extent, that the form of the composite function differs markedly from that exhibited by any of the other elements investigated. This, together with a large degree of deviation from Beer's law, has resulted in an extremely restricted "optimum range" for nickel, whether expressed in terms of absorbance or multiples of

sensitivity. Further investigation has shown that a combination of factors, such as significant absorption of nickel resonance radiation by the flame gases, and hollow cathode lamp instability, are probably responsible for the observed results.

Throughout the course of the work reported in this thesis, the emphasis has been on analytically useful ranges of concentration; detection limits have been referred to only in connection with the brief solvent extraction study reported in chapter 6. It is clear from the investigations described in chapter 4 that sources of noise which are important at or near the limit of detection frequently assume far less importance at higher concentrations. Conversely, the major sources of noise at normal working concentrations - those giving rise to the TlogT-type error function - reduce to zero at very low concentrations. The limit of detection can therefore not be considered a reliable guide to instrument performance and instrumental precision at those concentrations normally of interest to the practising analytical chemist. A more realistic guide would be the signal-to-noise ratio (A/dA) at, for example, an absorbance of 0,5. This absorbance value falls within the flat minima of all the error function curves (dc/c vs N, figure 4.9) obtained during this study, and hence the signal-to-noise ratio here would be a direct measure of the maximum attainable precision for the element under investigation. An approach along these lines has been made recently by at least one instrument manufacturing company.

Instrumental factors <u>per se</u> have been found to have very little effect on the precision in terms of absorbance (dA/A). The factor of major importance in single beam instruments, after dynamic flame noise, is lamp instability. Predictably, the use

of double-beam optics causes a considerable reduction in lamp noise. Flame absorption noise becomes a significant factor in some cases, notably nickel, lead and zinc. Since this, too, is a consequence of the dynamic nature of the flame, partial shielding of the burner slot as discussed above may result in an improvement here also.

The brief investigation of precision in atomic absorption procedures involving preliminary solvent extraction was performed as a supplement to the earlier work on error functions in atomic absorption analysis: since it was known that precision worsened rapidly at low concentrations, it was considered desirable to ascertain when, if at all, introduction of a solvent extraction step would improve the analytical precision. In order to be realistic, such a comparison had to be made between the precision of measurement only (in the case of aqueous solutions) and the precision of the measurement process plus the extraction step (in the case of solvent extraction). For this reason the standard deviation of aqueous measurement was computed from successive aspirations of the same aqueous solution, whereas that for extraction was obtained by extracting ten separate portions of a given aqueous standard solution, measuring the apparent concentration of analyte in each extract, and then calculating the standard deviation from the values obtained. The results indicated quite clearly that, at least for the systems investigated, solvent extraction improved the precision of the analysis only when the concentration of the analyte in the aqueous solution was less than 5-10x the measured analytical sensitivity. It therefore assumes importance at concentrations somewhat below the lower end of the

concentration range for optimum precision. Solvent extraction may, however, be of importance at higher concentrations in cases of persistent interference, such as the determination of zinc in the presence of a matrix which exhibits significant molecular absorption at 213,9 nm.

The work described in this thesis has been concerned, almost entirely, with precision in atomic absorption analysis. However, accuracy and precision cannot be entirely separated, although they must be clearly distinguished, and the practising analyst is equally interested in both. Precision refers to the agreement among a group of experimental results, and implies nothing about their relation to the true value, whereas accuracy is a measure of the closeness of coincidence between a given result, or the mean of a series of results, and the true value. In view of the uncertain nature of "true" values, however, accuracy can often not be expressed with the same degree of exactitude as can precision. It is clear that precise values may well be inaccurate, since an error causing deviation from the true value may affect all the determinations equally, and hence not modify the closeness of the agreement between them. It is equally clear that imprecise results cannot be considered accurate because of the large inherent uncertainty which will exist within such a (non-reproducible) set of measurements.

Because of considerations such as these, it was considered desirable that both the precision and the accuracy of the analytical methods which are briefly described in Chapter 7 be evaluated, in order to avoid the situation arising where the quoted standard deviations and coefficients of variation referred to methods of doubtful accuracy. The accuracy of the

methods was established by analyzing standard samples where these were available (cement, cast iron, and steel), and by means of recovery experiments and comparison with accepted atomic absorption methods (fruit juice). The precision (standard deviations) were measured for a number of different elemental determinations for each of the analytical methods proposed. The coefficients of variation reported in Chapter 7 show that the precision of the methods is completely satisfactory; this is particularly the case where analyte concentrations in the solutions to be analyzed were within the suggested optimum range for the element concerned. This is further illustrated in figure 8.2, where coefficients of variation for all determinations in which the analyte concentration fell within the optimum range are plotted in the form of a histogram. The only estimations which gave coefficients of variation greater than one per cent were those of aluminium and silicon, both of which are determined in the nitrous oxide-acetylene flame (a system which has not been studied in the course of the present work), and sodium. Due to its ubiquity, sodium is always a likely contaminant, and hence frequently gives rise to a somewhat elevated standard deviation.

Table 7.16 compares coefficients of variation for similar samples, obtained with a variety of analytical methods, both classical and instrumental. This comparison, whilst not exhaustive, shows that atomic absorption spectrometry is able to compete favourably with other analytical methods except in so far as major constituents are concerned. In such instances atomic absorption precision falls short of that required of, and obtainable with, certain other techniques such as volumetric and gravimetric procedures.

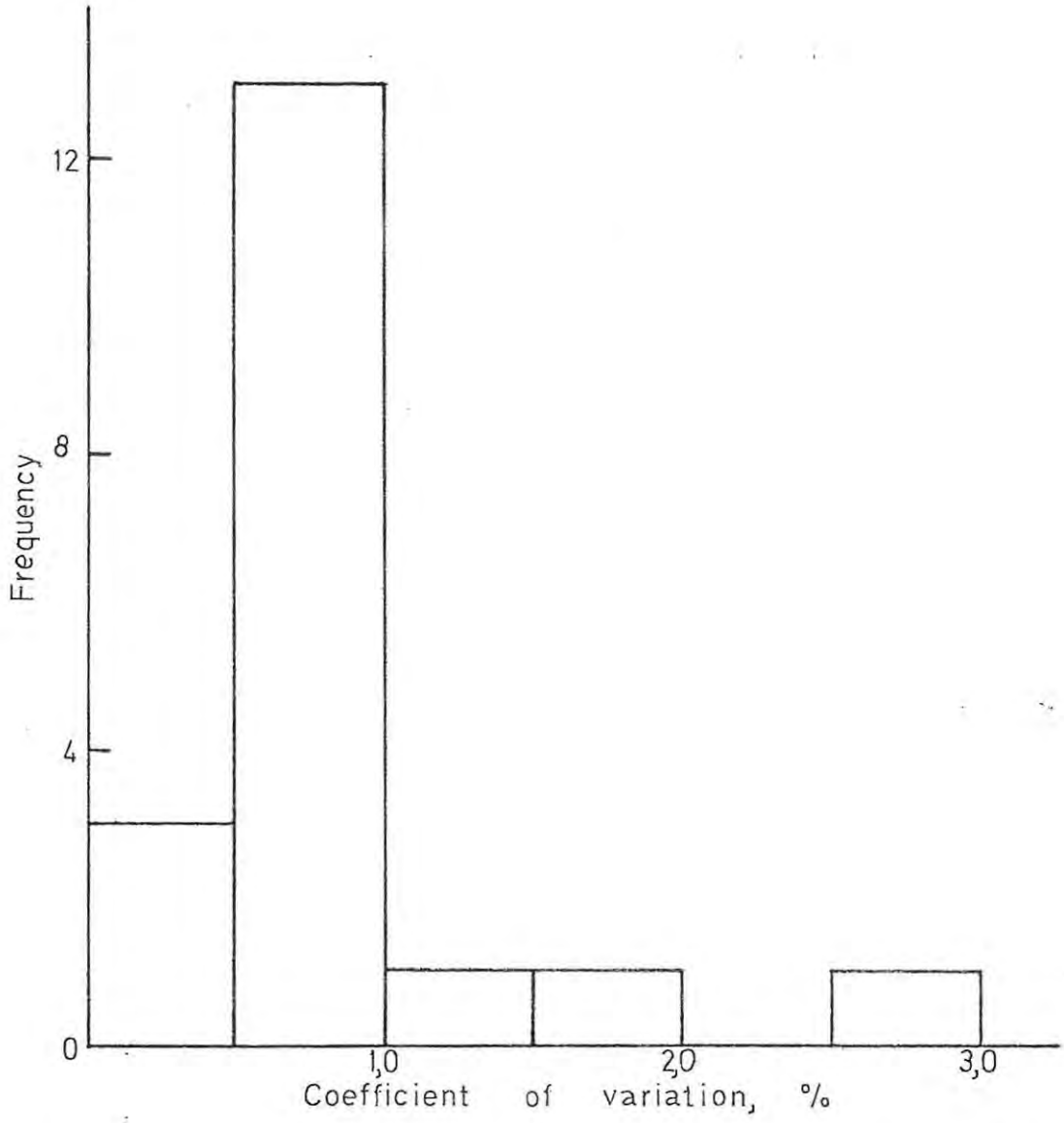

Figure 8.2. Frequency distribution for coefficients of variation.

Summary of suggestions for further work

In the course of this discussion, suggestions have been made regarding potentially fruitful areas for further research. These may be summarized briefly as follows:

(a) The volatilization of sample material in the flame. The limited amount of vapour pressure and heat transfer data has hampered investigations in this field. However, as more data become available, it should be possible to examine more complex sample systems from a theoretical as well as a practical point of view, and thus reach a clearer understanding both of the factors causing interference, and of methods for suppressing known interferences.

(b) Development of nebulizers which are capable of producing a much greater proportion of smaller droplets than do pneumatic nebulizers in current usage.

(c) The possible use, on a routine basis, of semi-shielded burners in the hope of reducing flame noise and so improving overall precision. This will require investigations into the optimum structure and geometrical arrangement of such burners, the best operating conditions for different elements in such a system, and the effect which such a burner arrangement would have on analytical sensitivity and the severity of known interferences.

REFERENCES

1. WALSH, A., Spectrochim. Acta 7, 108 (1955).

2. RUSSELL, B.J., SHELTON, J.P., and WALSH, A., Spectrochim. Acta 8, 317 (1957).

3. ALKEMADE, C.T.J., and MILATZ, J.M.W., Appl. Sci. Res. B4, 289 (1955).

4. ALKEMADE, C.T.J., and MILATZ, J.M.W., J. Opt. Soc. Amer. 45, 583 (1955).

5. INGLE, J.D., Anal. Chem. 46, 2161 (1974).

6. LANG, W., and HERRMANN, R., Optik 20, 347 (1963); Phys. Abstr. 66, 21548 (1963).

7. WINEFORDNER, J.D., and VICKERS, T.J., Anal. Chem. 36, 1939 (1964).

8. WINEFORDNER, J.D., and VICKERS, T.J., Anal. Chem. 36, 1947 (1964).

9. WINEFORDNER, J.D., and VEILLON, C., Anal. Chem. 37, 416 (1965).

10. WINEFORDNER, J.D., McCARTHY, W.J., and ST JOHN, P.A., J. Chem. Educ. 44, 80 (1967).

11. McCARTHY, W.J., and WINEFORDNER, J.D., J. Chem. Educ. 44, 136 (1967).

12. PARSONS, M.L., McCARTHY, W.J., and WINEFORDNER, J.D., J. Chem. Educ. 44, 214 (1967).

13. SLAVIN, W., "Atomic Absorption Spectroscopy", Wiley - Interscience, New York, 1968, pp 66-68.

14. RAMIREZ-MUNOZ, J., Microchem. J. 12, 196 (1967).

15. RUBESCA, I., and MOLDAN, B., "Atomic Absorption Spectrophotometry", CRC Press, Cleveland, Ohio, 1969, pp 84-85.

16. ERDEY, L., SVEHLA, G., and KOLTAI, L., Talanta 10, 531 (1963).

17. KHALIFA, H., ERDEY, L., and SVEHLA, G., Acta Chim. Hung. Tomms 41, 187 (1964).

18. KHALIFA, H., SVEHLA, G., and ERDEY, L., Talanta 12, 703 (1965).

19. WEIR, D.R., and KOFLUK, R.P., At. Absorption Newslett. 6, 24 (1967).

20. MEDDINGS, B., and KAISER, H., At. Absorption Newslett. 6, 28 (1967).

21. ROOS, J.T.H., Spectrochim. Acta 24B, 255 (1969).

22. ROOS, J.T.H., Spectrochim. Acta 25B, 539 (1970).

23. ROOS, J.T.H., Spectrochim. Acta 28B, 407 (1973).

24. HERRMANN, R., and LANG, W., Arch. Eisenhuttenw. 33, 643 (1962); Anal. Abstr. 10, 5004 (1963).

25. ZEEGERS, P.J.T., SMITH, R., and WINEFORDNER, J.D., Anal. Chem. 40 (13), 26A (1968).

26. PRICE, W.J., "Analytical Atomic Absorption Spectrometry", Heyden & Son, London, 1972, pp 50, 106-111.

27. RUBESCA, I., and SVOBODA, V., Anal. Chim. Acta 32, 235 (1965).

28. VICKERS, T.J., Anal. Chim. Acta 36, 42 (1966).

29. de GALAN, L., and SAMAEY, C.F., Spectrochim. Acta 24B, 679 (1969).

30. van GELDER, Z., Spectrochim. Acta 25B, 669 (1970).

31. BRUCE, C.F., and HANNAFORD, P., Spectrochim. Acta 26B, 207 (1971).

32. WAGENAAR, H.C., NOVOTNÝ, I., and de GALAN, L., Spectrochim. Acta 29B, 301 (1974).

33. HISKEY, C.F., Anal. Chem. 21, 1440 (1949).

34. WENDT, R.H., At. Absorption Newslett. 7, 28 (1968).

35. ROOS, J.T.H., Unpublished data.

36. LANGMYHR, F.J., and PAUS, P.E., At. Absorption Newslett. 8, 131 (1969).

37. REFERENCE 26, pp 5, 93.

38. EWING, G.W., "Instrumental Methods of Chemical Analysis", 3rd ed., McGraw-Hill, New York, 1969, pp 514-516.

39. BUTLER, L.R.P., Private communication to the author, 1974.

40. CHRISTIAN, G.D., and FELDMAN, F.J., "Atomic Absorption Spectroscopy", Wiley - Interscience, New York, 1970, p 121.

41. CRAWFORD, C.M., Chem. Eng. News 33, 5262 (1955).

42. CRAWFORD, C.M., Chem. Eng. News 34, 1075 (1956).

43. POLLARD, G.E., Anal. Chem. 27(8), 7A (1955).

44. LOTHIAN, G.F., "Absorption Spectrophotometry", Hilger and Watts, London, 1949.

45. PFEIFFER, H.G., and LIEBHAFSKY, H.A., J. Chem. Educ. 30, 450 (1953).

46. HUGHES, H.K., Appl. Optics 2, 937 (1963).

47. HISKEY, C.F., and YOUNG, I.G., Anal. Chem. 23, 1196 (1951).

48. LOTHIAN, G.F., Analyst 88, 678 (1963).

49. McBRYDE, W.A.E., Anal. Chem. 24, 1639 (1952).

50. SHIMAZU, M., and HASHIMOTO, A., Science of Light 11, 131 (1962).

51. L'VOV, B.V., Zavodsk. Lab. 28, 931 (1962).

52. BAKER, C.A., and GARTON, F.W.J., U.K. Atomic Energy Authority Report R3490, H.M. Stationery Office, London, 1960.

53. LEYTON, L., Analyst 79, 497 (1954).

54. SCHUHKNECHT, W., and SCHINKEL, H., Z. Anal. Chem. 163, 266 (1958).

55. ROOS, J.T.H., and PRICE, W.J., Spectrochim. Acta 26B, 441 (1971).

56. L'VOV, B.V., "Atomic Absorption Spectrochemical Analysis", Adam Hilger Ltd, London, 1970, pp 175-180.

57. LYKOV, A.V., Vestsi Akad. Navuk Belarusk. SSR., Ser. Fiz.-Tekhn. Navuk, 1965(1), 54; Chem. Abs. 63, 11033b (1965).

58. STUPAR, J., and DAWSON, J.B., Appl. Optics 7, 1351 (1968).

59. WILLIS, J.B., Spectrochim. Acta 23A, 811 (1967).

60. KOIRTYOHANN, S.R., and PICKETT, E.E., Anal. Chem. 38, 1087 (1966).

61. WEAST, R.C. (Editor), "Handbook of Chemistry and Physics", 51st ed., CRC Press, Cleveland, Ohio, 1970, pp D166-172.

62. KAYE, G.W.C., and LABY, T.H., "Tables of Physical and Chemical Constants", 13th ed., Longmans, London, 1966, pp 173-174.

63. MAVRODINEANU, R., and BOITEUX, H., "Flame Spectroscopy", Wiley, New York, 1965.

64. FULTON, H.A., M.Sc. Thesis, University of South Africa, 1968.

65. ROOS, J.T.H., and PRICE, W.J., Spectrochim. Acta 26B, 279 (1971).

66. RINGBOM, A., Z. Anal. Chem. 115, 332 (1939).

67. AYRES, G.H., Anal. Chem. 21, 652 (1949).

68. RAMÍREZ-MUNOZ, J., SHIFFRIN, N., and HELL, A., Microchem. J. 11, 204 (1966).

69. CHAKRABARTI, C.L., LYLES, G.R., and DOWLING, F.B., Anal. Chim. Acta 29, 489 (1963).

70. CRAWFORD, C.M., Anal. Chem. 31, 343 (1959).

71. CAHN, L., J. Opt. Soc. Amer. 45, 953 (1955).

72. BROOKS, R.R., PRESLEY, B.J., and KAPLAN, I.R., Anal. Chim. Acta 38, 321 (1967).

73. WILLIS, J.B., Anal. Chem. 34, 614 (1962).

74. SPRAGUE, S., and SLAVIN, W., At. Absorption Newslett. No. 20 (May, 1964).

75. SUNDERMAN, F.W., Amer. J. Clin. Pathol. 44, 182 (1965).

76. STRASHEIM, A., NORVAL, E., and BUTLER, L.R.P., J. S. Afr. Chem. Inst. 17, 55 (1964).

77. GROENEWALD, T., XXI CONVENTION., S. Afr. Chem. Inst., Grahamstown, 1971.

78. ELWELL, W.T., and GIDLEY, J.A.F., "Atomic-Absorption Spectrophotometry", Pergamon Press, London, 2nd ed., 1966, p 40.

79. LANGMYHR, F.J., and GRAF, P.R., Anal. Chim. Acta 21, 334 (1959).

80. PRICE, W.J., and ROOS, J.T.H., J. Sci. Fd. Agric. 20, 437 (1969).

81. "Chemical Analysis for Iron Foundries", B.C.I.R.A. Methods of Analysis Sub-Committee (Co-ord., W.E. Clarke), Allen and Unwin, London, 1967, p 121.

82. PRICE, W.J., and ROOS, J.T.H., Analyst 93, 709 (1968).

83. ROOS, J.T.H., Spectrochim. Acta 27B, 473 (1972).

84. ROOS, J.T.H., and PRICE, W.J., Analyst 94, 89 (1969).

85. CAPACHO-DELGADO, L., and MANNING, D.C., Analyst 92, 553 (1967).

86. BOULD, C., BRADFIELD, E.G., and CLARKE, G.M., J. Sci. Fd. Agric. 11, 229 (1960).

87. PRINGLE, W.J.S., Analyst 71, 490 (1946).

88. ROOS, J.T.H., Hitherto unpublished data (1963).

89. MANN, C.K., and YOE, J.H., Anal. Chem. 28, 202 (1956).

90. BRADFIELD, E.G., Analyst 82, 254 (1957).

91. VERDIER, E.T., STEYN, W.J.A., and EVE, D.J., J. Agric. Fd. Chem. 5, 354 (1957).

92. STEWART, J.A., and BARTLETT, J.C., Anal. Chem. 30, 404 (1958).

93. COOPER, M.D., Anal. Chem. 25, 411 (1953).

94. GAHLER, A.R., Anal. Chem. 26, 577 (1954).

95. COOPER, M.D., Anal. Chem. 23, 875 (1951).

96. NADKARNI, R.A.,and HALDAR, B.C., Anal. Chim. Acta 42, 279 (1968).

97. CAREY, F., ... * Cement Co., Private communication (1975).

98. STANDEN, G.W., and TENNANT, C.B., Anal. Chem. 28, 858 (1956).

99. ROUECHE, A., and MONNIER, D., Anal. Chim. Acta 31, 426 (1964)

100. BERMAN, H.A., Bull. A.S.T.M. 1959 (237), 51.

101. GERHARD, H.E., Rock Prod. 60 (2), 117 (1957).

102. ALKEMADE, C.T.J., Anal. Chem. 38, 1252 (1966).

103. WILLIS, J.B., Spectrochim. Acta 23A, 811 (1967).

104. BELCHER, C.B., KINSON, K., (and HODGES, R.J.), Anal. Chim. Acta 29, 134 (1963); 30, 64 & 483 (1964); 31, 180 (1964).

---

* Confidential information, anonymity requested